Towards An Efficient Traffic System via CAVs: Demand Management and Real-time Traffic Control

by

Huiyu Chen

A thesis submitted in partial fulfillment of the requirements for the degree of

Doctor of Philosophy

in

Transportation Engineering

Department of Civil and Environmental Engineering

University of Alberta

Abstract

With the dramatically rising traffic congestion issue, people are suffering the loss of working hours, increase in traffic accidents and pollution around the world. In Canada, drivers in the major cities were estimated to lose over 50 working hours per year in congestion during 2022, and in the US, it has cost more than 300 billion for the government to tackle the congestion issue. In recent decades, the unprecedented development in connected and automated vehicles (CAVs), coupled with the advancement of 5G and mobile edge computing (MEC), has brought profound changes to deal with the traffic congestion challenges. By enabling timely data exchange between vehicles and infrastructures, CAVs provide new possibilities for better demand management, more efficient and practical real-time traffic control.

In light of the anticipated emergence of CAVs, the research in this dissertation aims to improve the traffic system by developing intelligent traffic control strategies, real-time vehicle guidance, and appropriate demand management measures. The overarching goal is to enhance traffic efficiency to reduce congestion and improve traffic mobility, especially for the urban arterials considering the existence of traffic signals. To achieve this goal, the whole research is structured into four key components:

The first part focuses on developing a joint dynamic route guidance and signal control (DRG-SC) model for urban arterial traffic networks, which serves as a robust linkage that effectively connects demand modeling with traffic control. In this model, the real-time location and velocity data of CAVs as

well as the signal timing plan of intersections will be utilized to capture the interaction between signal control and vehicle routing. The vehicle routing plan will be optimized by considering the signal delays at each intersection, and the signal timing plans will be updated based on the real-time traffic volume resulting from routing. The joint model utilizes a closed-loop control framework, which is more effective than open-loop control and can significantly reduce travel time.

As a continuation of the first part of the research and considering that generating solutions from such a centralized model is computationally intensive, the second part of the research presented a distributed dynamic route guidance algorithm that utilizes local intersections' information only but generates globally optimized results for the whole traffic network with the support of the MEC technology. The algorithm is derived from the backpressure routing control and the result suggested that the control effectiveness was much better than the dynamic shortest path (DSP) while close to the dynamic system optimal (DSO) traffic assignment. More importantly, the algorithm was verified to be effective in reducing communication and computation cost.

In the third part, grounded on the prior research of traffic demand modeling in the first part, two strategies were proposed to better manage the CAV dedicated lane (CAV-DL) in a mixed traffic environment to improve capacity utilization. The CAV-DL is designed to physically separate the CAVs and Human Driving Vehicles (HDVs) to maximize the benefit of CAVs. However, the CAV-DL may be underutilized especially when the penetration rate of CAVs is low. To address this issue, in the first strategy, a dynamic right-of-way allocation method is adopted to allow HDVs to use the CAV-DLs when the lanes are relatively vacant. The second strategy designs tolling policies based on economic theory to explore the best demand distribution and further balance the travel time on the general lanes and CAV-DLs. Both methods

were proven to be effective in better-utilizing road capacity and improving traffic mobility.

The last part of the research focused on using CAV technology to promote electric vehicles (EVs), and a traffic environment with connected and automated electric vehicles (CAEVs) is assumed. In alignment with dual-carbon policies, encompassing carbon neutrality and carbon peaking, the promotion of EVs stands out as a prominent and transformative trend in the future of transportation. Following the similar closed-loop control logic developed in the first part, the work in this part tries to reach a trade-off between the energy consumption and the total travel time of CAEVs. By simultaneously optimizing the trajectory of the vehicles as well as the signal timing plans, the result effectively shows how CAV technology can help improve the travel and energy efficiency of EVs.

Overall, the research presented in the dissertation covers real-time traffic control and urban arterial demand management in the CAV environment. The models and algorithms presented herein can effectively improve traffic efficiency. The results in this dissertation contribute to the CAV-related studies methodologically which provide insights into realizing a sustainable and efficient traffic system in the near future.

Preface

All the contents (except Introduction, Literature Review, and Conclusion Chapters) presented in the dissertation have been published or accepted in peer-reviewed journals or presented at conferences in the areas of transportation engineering. The list of published, accepted, or presented articles related to the dissertation is as follows:

1. Refereed journal papers

- **H. Chen** and T. Qiu*: Distributed Dynamic Route Guidance and Signal Control for Mobile Edge Computing-Enhanced Connected Vehicle Environment, IEEE Transactions on Intelligent Transportation Systems, vol. 23, no. 8, pp. 12251-12262, Aug. 2022, doi: 10.1109/TITS.2021.3111855.

- **H. Chen**, F. Wu, K. Hou, and T. Qiu*: Backpressure-Based Distributed Dynamic Route Control for Connected and Automated Vehicles, IEEE Transactions on Intelligent Transportation Systems, vol. 23, no. 11, pp. 20953-20964, Nov. 2022, doi: 10.1109/TITS.2022.3170788.

- **H. Chen**, F. Wu, K. Hou, and T. Qiu*: Leveraging Dynamic Right-of-Way Allocation and Tolling Policy for CAV Dedicated Lane Management to Promote CAV and Improve Mobility, IEEE Transactions on Intelligent Transportation Systems, doi: 10.1109/TITS.2023.3347392 (Early Access).

- **H. Chen**, F. Wu, and T. Qiu*: Achieving Energy-Efficient and Travel Time-Optimized Trajectory and Signal Control for Future CAEVs, IEEE

Transactions on Intelligent Transportation Systems (Accepted and in publication).

2. Refereed conference papers

- **H. Chen** and T. Qiu*: Distributed Joint Dynamic Route Guidance and Signal Control for Mobile Edge Computing-Enhanced Connected Vehicle Environment. The Transportation Research Board (TRB) 100th Annual Meeting, 2021.

- **H. Chen**, F. Wu, K. Hou, and T. Qiu*: A Distributed Backpressure-based Dynamic Route Control Method for Connected and Autonomous Vehicles. The Transportation Research Board (TRB) 101th Annual Meeting, 2022.

Acknowledgements

I would like to thank all those who have offered me patient, enthusiastic, and selfless support throughout my Ph.D. journey.

Firstly, I would like to express my profound gratitude to my supervisor, Prof. Tony Qiu, for his invaluable guidance and unwavering support. Prof. Qiu's passion for exploring new ideas and rigorous attitude to research have inspired me a lot. His expertise and dedication have consistently pushed me to strive for excellence in my work. I am truly fortunate to have had the opportunity to learn from him and be guided by his wisdom and patience.

I would also like to extend my heartfelt appreciation to Dr. Tae J. Kown, Dr. Stephen Wong, and Dr. Amy Kim for their invaluable contributions as members of my supervisory committee. Their professional expertise and insightful suggestions have played a pivotal role in shaping the development of my dissertation. Thanks Dr. Jinfeng Liu, Dr. Ehsan Hashemi, Dr. Tae J. Kwon, and Dr. Stephen Wong for participating in my candidacy exam, and Dr. Jing (Peter) Jin, Dr. Randy Goebel, Dr. Tae J. Kown, and Dr. Stephen Wong being my defense examiners. Their meticulous review of my thesis and thoughtful feedback have been instrumental in enhancing the quality and depth of my research.

My sincere thanks also go to all the group members in the Centre for Smart Transportation and the friends I have met in class: Siqi Yan, Gary Zhang, Haibo Cui, Lucas and Mohammed Ahmed. Particularly thanks go to Fan Wu, Kaizhe Hou, Dr. Can Zhang, and Shuoyan Xu for their exceptional support and friendship. Their insightful discussions, and willingness to help have made my Ph.D. journey truly remarkable and colorful. Thanks Nicole Aubin, Dr. Sharon Harper, and Danielle Upshall for their support in enhancing

the writing quality of my research articles.

Lastly, I would like to express my deepest and sincerest gratitude to my parents, my younger brother and my beloved husband, Cheng Xue. I am truly fortunate to have such incredible individuals in my life, who have stood by my side, providing unwavering support, and reminding me of my strength and resilience. Their unconditional love and encouragement have been instrumental in shaping my journey, and I am forever grateful for their presence in my life.

Contents

List of Tables

List of Figures

List of Abbreviations

ACC	Adaptive Cruise Control
ADD	Average Departure Delay
ADAS	Advanced Driver Assistance Systems
AEC	Average Energy Consumption
AET	Algorithm Execution Time
ALT	Average Travel Length
API	Application Programming Interface
AS	Average Speed
ASC	Adaptive Signal Control
ATT	Average Travel Time
AWT	Average Waiting Time
BP	BackPressure
BPR	The Bureau of Public Roads function
BSM	Basic Safety Message
CACC	Cooperative Adaptive Cruise Control
CAEVs	Connected Automated Electric Vehicles
CAEV_SC	Connected Automated Electric Vehicle with Signal Control
CAEV_SC_TC	Connected Automated Electric Vehicle with Signal Control and Trajectory Control
CAV	Connected Automated Vehicle
CAV-DL	CAV-Dedicated Lane
CCT	Centralized Computation Time
CEVs	Connected Electric Vehicles
C-V2X	Cellular Vehicle-to-everything

CSUT	Connection Set Up Time
CTM	Cell Transmission Model
DCT	Distributed Computation Time
DRC	Dynamic Route Control
DRG	Dynamic Route Guidance
DUE	Dynamic User Equilibrium
DSRC	Dedicated Short-Range Communication
DSP	Dynamic Shortest Path
DSO	Dynamic System Optimal
DTA	Dynamic Traffic Assignment
EV	Electric Vehicle
EPA	Environmental Protection Agency
ETSI	European Telecommunications Standards Institute
FSC	Fixed Signal Control
GHG	Green House Gas
GLs	General Lanes
GSM	Golden Search Method
HDEVs	Human Driving Electric Vehicles
HDV	Human Driving Vehicle
HOT	High Occupancy Toll
HOV	High Occupancy Vehicle
IBL	Intermittent Bus Lane
IDTT	Input Data Transmission Time
I2I	Infrastructure to Infrastructure
LTE	Long-Term Evolution
MBP	Modified BackPressure
MBP+CI	Modified BackPressure with Congestion Identification
MEC	Mobile Edge Computing
MFD	Macroscopic Fundamental Diagram
MILP	Mixed-Integer Linear Programming

NEMA	National Electrical Manufacturers Association
OBU	On-Board Unit
OBP	Original BackPressure
OD	Origin and Destination
ODTT	Output Data Transmission Time
PEV	Plug-in Electric Vehicle
PR	Penetration Rate
PQ	Point Queue
RRI	Road Risk Index
RSU	Road-Side Unit
SAE	Society of Automobile Engineers
SNMS	Sensor Network with Mobile Stations
SPaT	Signal Phase, and Timing data
SOC	State of Charge
SQ	Spatial Queue
SUMO	Simulation of Urban Mobility
TEC	Total Energy Consumption
TMC	Traffic Management Center
TTT	Total Travel Time
TOP	Time for Other Process
TVN	Total Vehicle Number
VANET	Vehicular Ad hoc NETwork
VSP	Vehicle Specific Power
V2C2V	Vehicle to Cloud to Vehicle
V2V	Vehicle to Vehicle
V2I	Vehicle to Infrastructure
VT-CPEM	The Virginia Tech Comprehensive Power-based EV Energy Consumption Model
VT-CPPM	The Virginia Tech Comprehensive Power-based PHEV Model
3GPP	The 3rd Generation Partnership Project

Chapter 1

Introduction

1.1 Background

As early as 2009, IBM launched the "IBM Smarter Cities Challenge" to promote economic growth, social harmony, and sustainable development for urban cities. The goal is to provide a more convenient, efficient, and flexible lifestyle for citizens to save money and resources [1]. Nowadays, with the population explosion, urban areas all over the world have suffered severe traffic congestion which has given rise to the number of accidents, traveling costs on the road, and pollution. The United States Environmental Protection Agency (EPA) reports that transportation-related greenhouse gas (GHG) emissions currently contribute to approximately 27% of total U.S. GHG emissions, with estimates projecting a rise to 37% by 2035, making it the largest contributor to GHG emissions [2]. In Canada, the severity of congestion is also notable, leading to an estimated loss of 54 working hours per year for drivers in the major cities (INRIX 2022 Global Traffic Scorecard). These hours, which could be spent productively, are instead wasted in gridlock, affecting productivity, work-life balance, and overall quality of life.

As an essential component within the framework of a smart city, smart traffic is dedicated to enhancing the quality of people's daily commutes by mitigating congestion, prioritizing safety, and addressing environmental concerns. Over the past few decades, the remarkable advancements in internet technology and data science have ushered in profound transformations in the automotive industry. The emergence of connected and automated vehicle (CAV),

electric vehicle (EV), as well as the rapid progress in mobile edge computing (MEC) has unlocked the potential to realize the vision of smart traffic.

The pivotal challenge for the next generation of intelligent transportation systems lies in seamlessly integrating these innovative technologies into conventional transportation networks and assessing the resulting shifts in traffic patterns and behaviors. Embracing innovative technologies holds the promise of significant advancements, but their true potential can only be harnessed through astute integration. Achieving sustainable growth relies on the strategic fusion of these technologies. By designing and implementing more effective demand management and control strategies, the benefits of these new technologies can be maximized, reduce congestion-related costs, and ultimately contribute to a more prosperous and sustainable urban landscape.

1.2 Related Technologies

1.2.1 Connected and Automated Vehicle (CAV)

CAVs have been developing rapidly due to the advancements in manufacturing and information technologies [3]. Perception, communication, and computation are the three basic functions that make CAVs promising in shaping the future of travel.

In 2011, the Dedicated Short-Range Communication (DSRC) was announced by the US Department of Transportation (US DOT) to support the CAV communications. However, the low scalability is the main drawback of DSRC where the protocol is unable to provide the necessary time-probabilistic characteristics in dense traffic [4]. Moreover, the transmission distance of DSRC is relatively short and the signal is easy to be blocked by the buildings or surrounding objects.

In addition to DSRC, the Long-Term Evolution (LTE)-based technology is another promising communication solution, which can provide both low latency and high throughputs. The cellular vehicle-to-everything (i.e., C-V2X) concept was introduced by the 3rd Generation Partnership Project (3GPP) in LTE since Release 14 [5]. The C-V2X technology empowered by 5G makes

the real-time information exchange between vehicle to vehicle (V2V), vehicle to infrastructure (V2I), infrastructure to infrastructure (I2I), or any other communicating entities more rapid and effective.

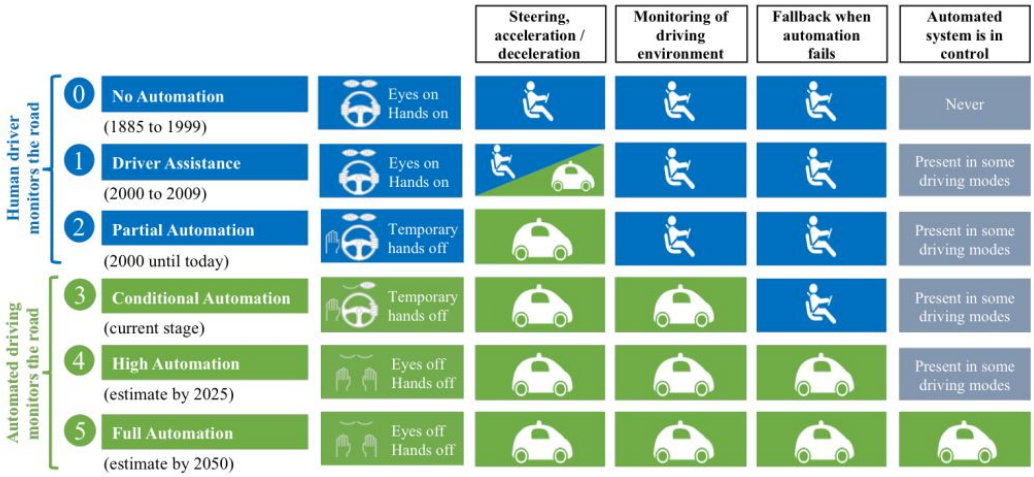

Figure 1.1: SAE classification: Levels of automation [6]

According to the SAE international classification of CAVs [6], there are six levels of automation. The highest level of CAVs can even operate and interact with traffic dynamically with little or no driver intervention or attentiveness [7]. Basic Advanced Driver Assistance Systems (ADAS) at Level 0 are commonplace in most modern vehicles. Contemporary vehicles are now equipped with a minimum of one Level 1 ADAS. Moving up the autonomy scale, Level 2 automated features have become commercially available in a variety of vehicles, including those manufactured by Audi, Tesla, GM (Cadillac), Lexus, Porsche, Daimler, BMW, and Volvo. Technically feasible Level 3 automated vehicles are also ready for deployment, pending commercialization while aligning with legislative requirements [8]. On the frontier of CAV development, the experimental programs for Levels 4 and 5 autonomy are experiencing tremendous growth, with commercial deployment becoming increasingly feasible from a technological standpoint [9]. Waymo, a leading driverless vehicle development company, has successfully introduced Level 4 self-driving taxis onto public roads. Notably, this company conducted extensive testing of its automated taxis in Arizona, covering over a year and surpassing 10 million miles. The features of these driverless taxis include the ability to safely bring the vehicle

to a stop in the event of system failures, enhancing the overall safety and reliability of CAVs. The features of the future CAVs will enable them to have great potential in reducing traffic accidents, improving safety, and mitigating traffic congestion.

1.2.2 Mobile Edge Computing (MEC)

On the other hand, the breakthrough in MEC development creates the capability of placing data storage and computation sources at the network edge, which greatly reduces end-to-end delay [10]. Fig.1.2 compares the conventional cloud-

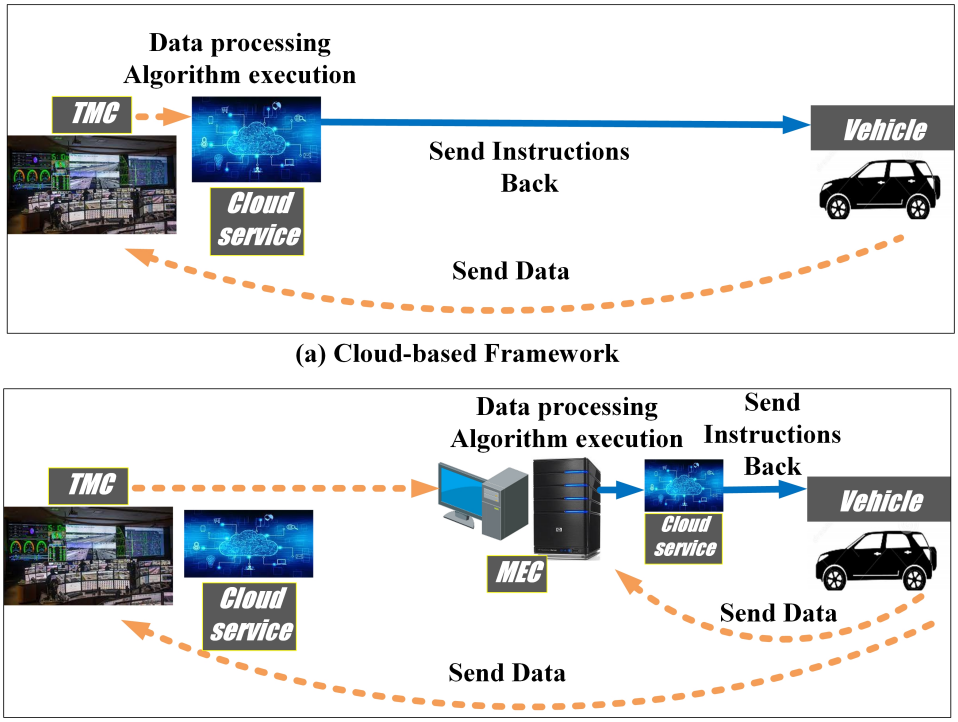

Figure 1.2: Communication and computation framework in the CAV environment (a) Cloud-based framework (b) MEC-based framework

based (Fig.1.2 [a]) and the emerging MEC-based (Fig.1.2 [b]) data-processing and control framework. In the cloud-based framework, data from CAVs was sent directly to the remote Traffic Management Center (TMC), and the cloud service at the TMC will aggregate data, solve the corresponding control problems, and forward the instructions back to vehicles. The cloud-based paradigm provides global optimal solutions and is more suitable for complex centralized

control which does not require a prompt response. On the contrary, in the MEC-based framework, part of the cloud service was moved to the network edge next to vehicles. Although not as powerful as it is in the TMC, the service at the MEC can also handle large amounts of data, execute optimization algorithms, and help CAVs make decisions. Due to the short communication distance, the timely solution from the MEC can be better applied to real-time cases that have strict requirements for response time. In addition, the MEC-based framework is flexibly scalable to support distributed control.

The detailed MEC-enabled CAV environment is drawn in Fig.1.3 which can be generally divided into three layers: vehicles as the user layer, infrastructures as the MEC layer, and the TMC as the cloud layer [11]. The V2V, V2I, and I2I

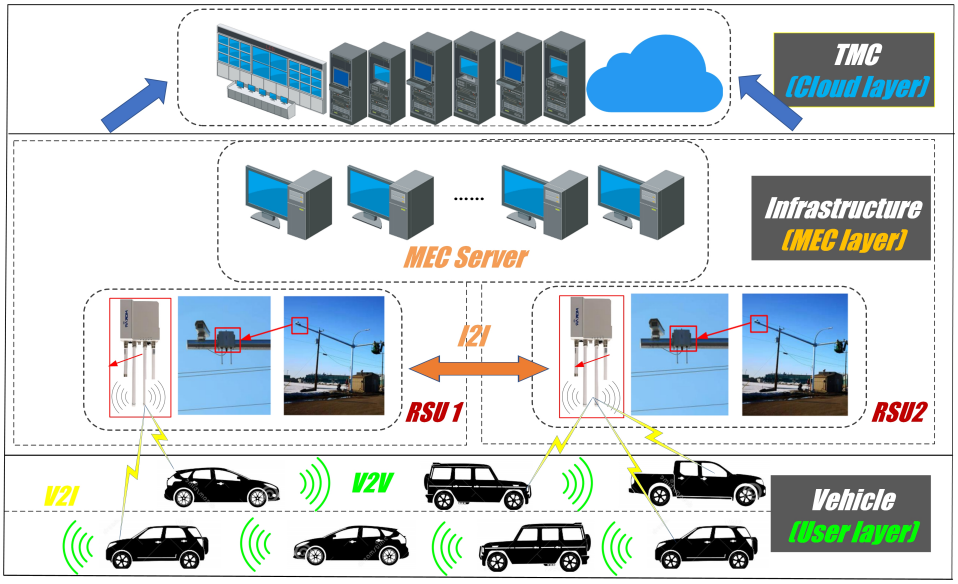

Figure 1.3: Detailed illustration of CAV environment with MEC

wireless communication technology as well as some fiber connections enable the three layers to "talk" with each other. The computational capability of vehicles is allowed by the On-Board Unit (OBU) to tackle some simple tasks. As for the MEC layer, the Road-side Unit (RSU) which is distributed along the road can act as the edge server. In addition, the edge server can also be formed by a certain demand of computation resources aggregated in a regional computer lab. Nevertheless, no matter which kind of strategies are utilized to deploy the edge servers, they are located close to vehicles. The information

from the vehicles or the edge servers can also be uploaded to the cloud layer. Accordingly, taking advantage of the three layers, diverse use cases are properly sustained in the MEC-enabled CAV environment, contributing significantly to the enhancement of CAV technology.

1.2.3 Electric Vehicles (EVs)

EVs are vehicles powered by batteries with zero operational emissions, contributing to a cleaner and greener transportation system. In recent decades, mounting concerns about the environmental repercussions of gasoline-powered vehicles and the rising cost of oil have ignited interest in EVs [12]. Beyond their environmental advantages, EVs can also result in substantial driving cost savings for individuals. According to a 2020 Consumer Report [13], EVs can help save about 60% each year on fuel costs compared to gasoline-powered vehicles.

Due to the benefits of EVs, many countries have drawn ambitious roadmaps to promote their adoption. Such as Sweden, China, and in particular, Norway. In 2021, 65% of the new private cars in Norway were EVs and this number has grown at an average annual rate of more than 60%, which is one of the fastest transition regions in the world [14]. The EV market has displayed continuous growth and is projected to maintain its rapid momentum throughout the upcoming decade.

While EVs may offer lower operational costs over time due to reduced maintenance and energy costs, the initial purchase price can be a significant deterrent for many consumers. Efforts to address this concern involve advancements in battery technology to reduce manufacturing costs and government incentives that aim to make EVs more financially appealing to consumers. Additionally, range anxiety and charge anxiety are also two main issues that hinder widespread EV adoption.

The current body of literature on EVs reflects a comprehensive exploration of various facets within the realm of electric mobility. Researchers have delved into diverse aspects, including charging infrastructure design, innovations in fast charging technologies, and the formulation of algorithms focused on min-

imizing energy consumption during EV operation. These studies collectively contribute to the understanding and advancement of electric mobility, addressing key challenges and paving the way for a more sustainable transportation future.

However, the transformative potential of CAV technology on EVs also remains an area ripe for deeper investigation and exploration. The integration of CAVs has the potential to shape the way people perceive and utilize EVs. The combined CAV technology creates possibilities to optimize energy consumption, enhance charging efficiency, and contribute to the overall integration of electric mobility into smart and connected transportation ecosystems.

1.3 Research Motivations

Amid the swift and relentless progress of these technologies, dedicated researchers and specialists have embarked on harnessing their benefits to create a greener and more efficient traffic ecosystem. This endeavor has led to the creation of an array of innovative traffic control methodologies, such as dynamic route control (DRC), adaptive cruise control (ACC), and adaptive signal control (ASC). Simultaneously, in the pursuit of propelling greener and more intelligent transportation, profound examinations into traffic management tactics and concomitant policies have taken center stage, all aimed at fostering the integration of CAVs to improve traffic efficiency. In the exploration of this area, there remain several unresolved issues and challenges, which are outlined below:

1) Limited data source for describing the traffic dynamics: Before the emergence of CAV technologies, the bedrock of traffic management and control relied heavily on data obtained from loop detectors and video cameras. However, these data sources suffered from a limited refresh rate, impeding the precise real-time tracking of vehicle locations. Despite ongoing endeavors to develop algorithms tailored to CAVs, the input data driving these algorithms still hinges on static information. Therefore, the resultant control strategies find themselves ill-equipped to flexibly accommodate the ever-evolving traffic

dynamics.

2) Overlook on the interaction between traffic control and demand management: As vehicles navigate arterial roads, the predominant component of their waiting time stems from the delays incurred while idling at red signals. These delays invariably contribute to the overall travel cost within vehicle routing. Additionally, the chosen route of vehicles significantly shapes the distribution of demand across the network, thereby exerting a pivotal influence on the parameters driving signal control inputs. Regrettably, the critical interplay between signal control dynamics and vehicle routing considerations has largely been overlooked in conventional routing strategies and signal timing plans.

3) Selfish driving behavior hinders the achievement of system optimal (SO) state: Commonplace strategies employed by popular route planning software, such as Google Maps and Waze, deliver navigation services that primarily adhere to the user-equilibrium (UE) principle, neglecting the intricate interactions with fellow vehicles. This method often leads to a scenario where vehicles sharing identical origins and destinations (OD) are consistently directed onto the same shortest route. Unfortunately, within road networks grappling with elevated demand levels, this approach can inadvertently generate an imbalanced demand distribution across the network, thereby causing emergent congestion hotspots.

4) High computation and communication cost for obtaining solutions from the centralized model: The DRC problem for a large-scale traffic network is usually formulated as complex non-linear programming models that are cost-intensive to solve. Further amplifying the complexity, these models require access to traffic information of the entire network—the data across all network links need to be continually updated to the processing center. This data, hailing from both vehicle sources and intersections, necessitates transmission to the TMC for processing. Regrettably, this mode of data processing and computation is ensnared in substantial communication latency, primarily because the TMC is often geographically distant from the vehicles. However, the CAV combined with MEC technology provides potential new

ideas for solving this issue by generating distributed solutions.

5) Low capacity utilization rate of CAV dedicated lanes (CAV-DLs) in a mixed traffic environment: In the early stages of implementing CAV technology, there should be a mixed traffic environment with both CAVs and HDVs for a long time. To make CAVs not impacted by the HDVs, the CAV-DLs were proposed to be deployed to physically separate CAVs and HDVs. However, in scenarios where the prevalence of CAVs remains modest, the optimal utilization of CAV-DLs could falter, potentially resulting in underutilized lanes and an inefficient allocation of road capacity. This particular challenge underscores the need to formulate strategies that can enhance the effective deployment and management of CAV-DLs, particularly in contexts where CAV penetration remains relatively low.

6) The trade-off between energy consumption and total travel times of EVs: While EVs boast zero emissions, it is important to note that their energy consumption tends to rise as average speeds increase. Consequently, attempts to reduce energy consumption may inadvertently result in reduced speed and longer travel time. Balancing the competing objectives of reducing energy consumption and travel time has been a topic that has received limited attention in existing studies. However, a ray of promise emerges in the form of CAVs, poised to bridge this gap. By enabling communication, the trajectory of the EVs can be controlled based on the most updated traffic information to avoid stops and reduce both energy and travel time.

1.4 Research Scopes

To address the issues mentioned above, the dissertation will specifically explore the traffic demand management and control problems with CAVs in an urban arterial network, including the DRC, ASC, trajectory control, flow, and capacity management. The research scopes are listed below:

1) This research focuses on **urban arterials**, taking into account the presence of intersections and the impact of signal timing control strategies. Traffic signals play a pivotal role in urban traffic systems, and their effective design

can significantly enhance traffic flow and mobility. Since the research specifically concentrates on urban arterials, it may not capture the full complexity of traffic dynamics in other types of roadways (e.g., local roads, and freeways).

2) The whole study models the **macroscopic-level** traffic behavior with simplified microscopic-level driving dynamics. In our traffic flow model, vehicles are considered homogeneous, with no intricate descriptions of their driving characteristics. This approach treats all vehicles equally when conducting network modeling, and it might overlook crucial individual vehicle characteristics and behaviors.

3) The primary objective of this dissertation is to **enhance traffic efficiency**, and improve traffic mobility. The investigation of traffic safety falls outside its scope. Consequently, safety-focused strategies have not been included in the dissertation. In the real-world deployment of CAVs, safety issues should be incorporated.

4) This dissertation relies on **simulation techniques** rather than real-world field testing. Analyzing traffic behavior with CAVs in actual traffic conditions poses significant complexities and inefficiencies. Additionally, the limited availability of a sufficient number of CAVs hinders the feasibility of real-world verification. It is essential to have such testing to ensure the performance of the proposed methods when the real-world CAV testing environment becomes available.

5) The information provided by CAVs was assumed to be **accurate**. The potential challenges in communication systems were not considered, such as packet loss or communication interference. Instances where CAVs may not establish reliable connections with each other should be included in future research.

1.5 Research Objectives and Tasks

Within the research scope, the overall objective of this research is to improve traffic efficiency through traffic control and demand management by leveraging the benefits of CAV technology. The specific objectives are listed below:

1) Describe the traffic dynamics in a CAV environment: Characterize the intricate traffic dynamics while formulating the DRC model, leveraging the wealth of real-time, high-resolution, and spatial-temporal data readily accessible within the CAV environment (e.g., Basic Safety Message [BSM], Signal Phase, and Timing data [SPaT]).

2) Capture the interaction between demand management and traffic control: Introduce a novel, integrated framework that melds the domains of joint demand modeling and traffic control specifically tailored for CAVs. Central to this model is its ability to capture the intricate interplay between signal control dynamics and vehicle routing decisions. The model should include real-time delay caused by signal control when computing the link cost and aggregate vehicles' routing plan to obtain the dynamic demand for adaptive signal control.

3) Achieve a system optimal traffic state: Investigate the dynamic system optimal (DSO) assignment apart from the dynamic user equilibrium (DUE) assignment and address the system performance besides the individual vehicles' benefit.

4) Reduce communication and computation cost: Develop a distributed routing strategy that only relies on local intersections' information and can be directly deployed to the MEC-enabled CAVs. The strategy should be effective in communication and computation, and the control performance is supposed to be as good as global optimization.

5) Improve capacity utilization in a mixed traffic environment: Propose appropriate CAV-DL management strategies to improve the utilization rate of the road capacity in a mixed traffic environment, and promote CAVs, especially when the penetration rate of CAVs is low.

6) Explore the benefits of CAVs on EVs: Investigate if CAV technology can help EVs balance the energy consumption and total travel time. Develop trajectory and signal control strategy to save both energy and travel time.

To attain the objectives mentioned above, four key tasks were determined:

Task 1: Model the connections between demand management and traffic

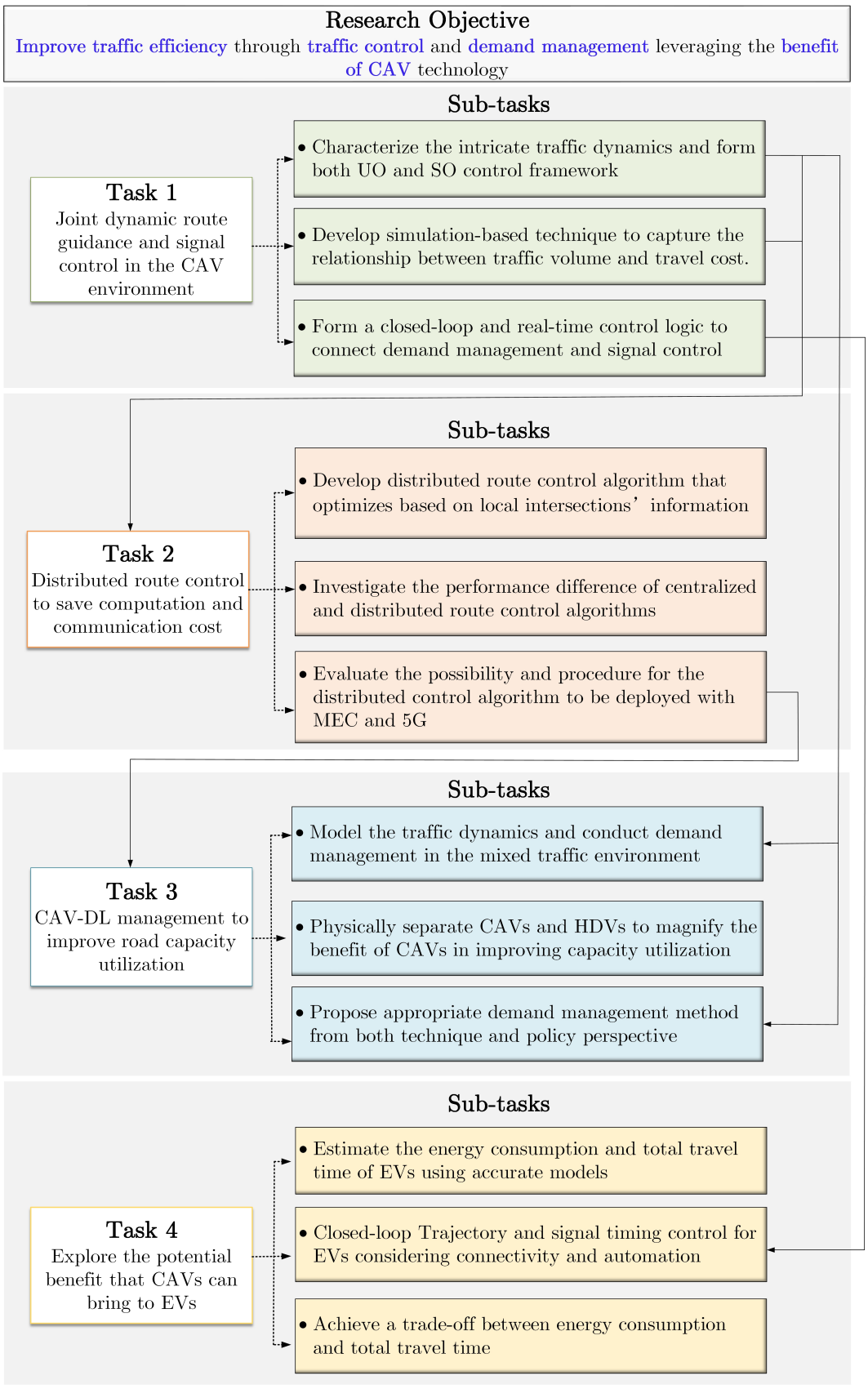

Figure 1.4: Interconnectedness of the tasks in the dissertation

control by proposing a joint route control and signal optimization model.

Task 2: Develop a distributed route control algorithm to address the issue of high computation cost in task 1.

Task 3: Propose demand management methods for CAV-DL management, and improve the utilization rate of road capacity from both technique and policy point of view.

Task 4: Leveraging the capability of CAVs to realize a compromise of energy consumption and total travel time for EVs.

The interconnection of the four tasks is visually depicted in Fig. 1.4, where subtasks within each primary task are elucidated, showcasing their intricate relationships. The closed-loop framework, initially established in Task 1, extends its relevance to Task 4, ensuring a consistent and coherent approach. Additionally, Task 2 serves as a natural extension of Task 1, introducing a distributed architectural perspective for the centralized model outlined in Task 1. As for the demand modeling introduced in Task 1, it finds practical application in Task 3, where it underpins demand management strategies. In summary, the essence of this dissertation revolves around the creation of models and algorithms, all directed toward the overarching goal of enhancing urban traffic efficiency.

1.6 Dissertation Organization

The dissertation encompasses a total of seven chapters, and Fig. 1.5 provides an overview of the whole thesis structure. Chapter 1 introduces the background and research motivations by summarizing the challenges and opportunities. This chapter also outlines the research scope and objectives. Following that, Chapter 2 provides a comprehensive literature review of related work pinpointing and summarizing the existing research lacunae. Chapters 3 and 4 are both for DRC problems of CAVs, where Chapter 3 introduces joint DRC and signal control algorithms, followed by Chapter 4's concentrated emphasis on the architecture of distributed routing strategies. The vital role of 5G and MEC is elaborated. Chapter 5 delineates strategies governing the manage-

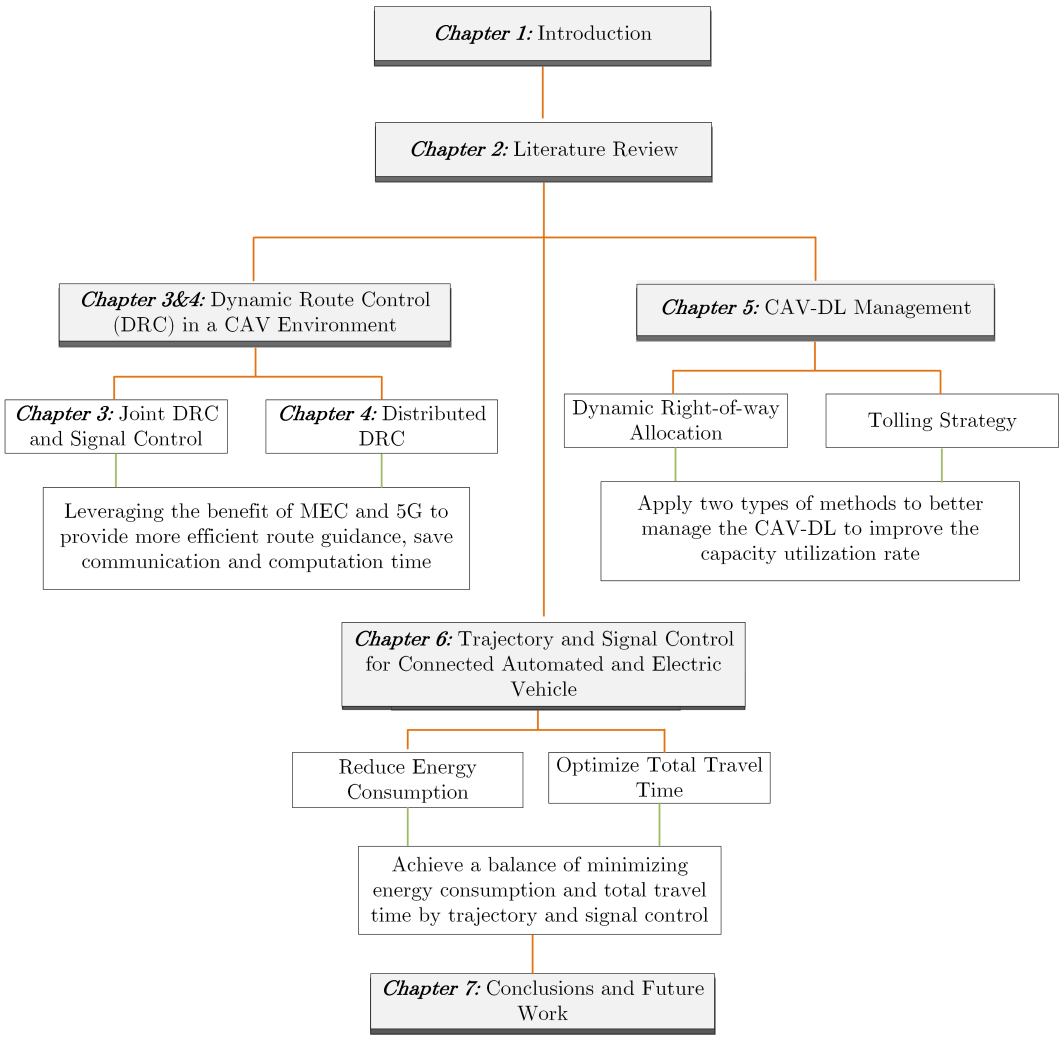

Figure 1.5: Overview of the research structure in the dissertation

ment of CAV-DLs, casting light on tolling policies as a pivotal component. Chapter 6 investigates the energy consumption problem of EVs and gives the approach of balancing energy consumption and total travel time by leveraging CAV technology. The limitations of this research and the future work are discussed in Chapter 7.

1.7 Conclusions

This chapter initiates the research by outlining the research background, motivations, scopes, objectives, and essential concepts to assist in traversing through this dissertation. The challenges and remaining issues in related re-

search fields were briefly summarized which helped to set up the research goals. In essence, this chapter functions as a linchpin, seamlessly bridging the introductory concepts with the forthcoming comprehensive elucidation of methodologies. As we delve deeper into the subsequent chapters, this connection ensures a coherent narrative flow, allowing for a smooth transition from conceptual groundwork to the practical intricacies that lie ahead.

Chapter 2

Literature Review

This chapter summarizes the existing research relevant to traffic management and control. By undertaking a comprehensive exploration of theories and empirical findings, this literature review illuminates the current state of knowledge in this dynamic field. The chapter not only synthesizes existing research but also identifies gaps, trends, and potential areas for further investigation, thereby establishing the foundation for the subsequent analyses and discussions.

The chapter commences with the DRC problem, subsequently investigating the Dynamic Traffic Assignment (DTA) models—an instrumental framework underpinning solutions to the DRC problem. This segues into an exposition on studies encompassing the intersection of dynamic routing and signal control, exploring analyses within both conventional vehicle and CAV contexts. Following that, a comprehensive synthesis of research centered on the exploration of distributed routing strategies is presented. Upon completing the introduction of DRC-related studies, attention shifts to the context of CAV-DL management in the mixed traffic environment. Additionally, the chapter expounds upon economic measures for traffic demand management, such as tolling. Subsequently, the focus broadens to research related to EVs with clarifying the control algorithms related (e.g., trajectory control, speed guidance).

2.1 Dynamic Route Control

The DRC problem has been studied extensively over the past decades and plays an important role in improving network efficiency [15]. Current DRC studies can be generally categorized into two main types.

In the first category, the distinct variations in vehicles' travel behaviors are not counted. This type of study involves aggregating vehicles that share identical Origin and Destination (OD) into a single traffic stream when formulating routing strategies. This perspective primarily aligns with the vantage point of traffic operators, with its theoretical foundation rooted in DTA [16]. Within this framework, traffic phenomena and their evolutions are incorporated through traffic flow theories, dynamically determining the traffic flow on each link. The overarching aim is to steer the network towards a state of equilibrium or system optimality.

Most of the DRC studies belong to the first category which can be traced back to early navigation systems that relied on static maps. As early as 1984, Mahmassani and Herman [17] explored the DRC problem aiming at achieving an equilibrium state of the network while considering the vehicles' departure time choice. Watling et al. [18] further extended the discourse by providing an overview of the modeling issues that need to be considered when dealing with the DRC problems. As the field progressed, studies like Nie and Wu [19] worked on the shortest path problem considering on-time arrival probability using a more detailed analytical model. There are also studies [20] on route guidance problems in large-scale networks utilizing the characteristics of the Macroscopic Fundamental Diagram (MFD) which provides an aggregated model of urban traffic dynamics linking network production and density, offers a new generation of real-time DRC strategies. More related studies will be reviewed in the following section with the summary of the DTA models.

The second category of DRC research embraces a perspective that acknowledges the inherent heterogeneity among vehicles. This paradigm recognizes the significance of personalized travel habits and distinctive requirements. These studies pivot from the standpoint of individual vehicles and prioritize fur-

nishing route guidance that not only benefits but also aligns with the unique preferences of each vehicle. In the background of burgeoning CAV technology, vehicles assume a proactive role in shaping their trips. This active participation is realized through multifaceted communication channels. Vehicles communicate their preferences directly to the TMC, allowing for the transmission of real-time road conditions—encompassing factors such as accidents, congestion, and road surface quality. These dynamic inputs empower the generation of adaptive routing strategies that fluidly respond to evolving road conditions, thereby facilitating a personalized navigation experience for each vehicle [21]–[23].

Li et al. [24] summarized multiple properties of the road and adopted the Polychromatic Sets theory for planning dynamic user-centric routes. Vehicles then select a route based on the priority level of these properties. Delling et al. [25] also considered several natural metrics including the shortest distance, walking, biking, avoid U-turns and left-turns when providing the route service. Cui et al. [26] inferred the vehicles' preferences by analyzing their historical traveling trajectory data and recommended the route based on the inferred preference. Li et al. [27] focused on safety-based route planning by exploiting the vehicle-to-cloud-to-vehicle (V2C2V) connectivity. Instead of using only travel time as the cost, they have established the time and road risk index (RRI) which further considers the number of accidents, and the weather conditions as metrics. Abdelrahman et al. [28] proposed a real-time route planning method utilizing sensing and computing capabilities in both vehicles and infrastructures. The road surface quality is collected dynamically, which together with the driver's personalized skillfulness is used in the route planning. This framework is tested and verified through a case study of a real driving scenario, which suggests that the presented framework can make a good complement to the conventional route planning systems to provide a customized routing strategy for distinguished travelers.

2.2 Dynamic Traffic Assignment

DTA is an important component within the scope of DRC, especially served as the fundation of the first category of DRC study. It is typically developed based on Wardrop's first and second principles [29], which are also famously known as the user equilibrium (UE) and system optimal (SO) principles respectively. Under the UE principle, the travel cost between the same OD is equal and minimal. In contrast, the SO principle pursues the best performance of the network through the cooperation between vehicles. The UE and SO principles are extended to dynamic user equilibrium (DUE) [17] and dynamic system optimal (DSO) [30] when the traffic dynamics are described and applied to conduct the traffic assignment. Szeto and Wong [31] provided a comprehensive review of DTA studies which classified the current research from diverse aspects and summarized current challenges and future directions for DTA studies.

Early DTA studies [32], [33] focused on traffic modeling and solution techniques. Later on, Ran and Boyce [34], Boyce. et al. [35] systematically addressed the analytical DTA formulation with a variational inequality approach. Following their studies, a series of research [36]–[38] discussed the properties of DTA and applied it in different control scenarios. Similarly, in analytical DTA models, different traffic flow models were applied in modeling vehicles' travel behavior, ranging from microscopic to the macroscopic level. Another branch of DTA studies is simulation-based DTA which emphasizes more on the traffic flow characteristics. The traffic evolution is dynamically described in corresponding simulation tools to compute optimal routing strategy and these routing strategies are applied to the simulation again to show the results of traffic assignment. Well-known simulation-based DTA tools include: TRANSIMS [39], PARAMICS [40], DYNASMART [41], DynaMIT [42], and CONTRAM [43]. Table 2.1 reviews some well-known DTA-based studies which are classified according to their belonging category, the embedded travel choice model, queueing model, flow model, and decision variable. These studies provide a comprehensive understanding of the principle of DTA models.

Table 2.1: Well-known DTA-based studies

Papers	Category	Travel choice	Queueing modeling	Embedded flow model	Decision variable
Yagar [44]	Analytical model	DUE	Physical queue	Macroscopic traffic flow model	Link flow
Szeto et al. [45]	Analytical model	DUE and Departure time choice	Physical queue	Cell-based formulation	Cell occupancy
Lo et al. [46]	Analytical model	DUE	Physical queue	Cell transmission model	Cell occupancy
Long et al. [47]	Analytical model	DUE and Departure time choice	Point queue	Link transmission model, link performance function	Link flow
Peeta et al. [48]	Simulation-based model	DUE and DSO	Physical queue	Macroscopic traffic flow model	Route flow
Tong et al. [49]	Simulation-based model	Predictive DUE	Physical queue	Macroscopic traffic flow model	Link flow
Szeto [50]	Simulation-based model	DUE	Physical queue	Lagged cell transmission model	Cell occupancy
Ben-Akiva et al. [51]	Simulation-based model	DUE-based route control; lane control	Physical queue	Microscopic traffic flow model	Link flow

2.3 Dynamic Routing Considering Signal Control

In the realm of urban arterials, the cost of travel along a given route is notably shaped by the delays incurred at intersections due to signal control. Concomitantly, the distribution of traffic flow across these routes plays a pivotal role in influencing the parameters for signal control optimization. Harnessing the gravity of this interplay, numerous scholars have passionately devoted their efforts to unveiling the intricate dynamics between traffic routing and signal controls within the context of urban arterial roads. Allsop [52], [53] appears to be the first one to focus on the dynamics between traffic signal control and

vehicle routing. Following that, Vuren et al. [54] also explored the best way to connect routing strategies and signal timing plans. However, these studies considered the signal control to be fixed and then solved the traffic assignment problem, or they used the signal control parameters as the decision variables with a fixed traffic assignment model. None of them considered the issue of optimizing traffic flow distribution and signal timing jointly. To fill this gap, later on, Yang and Yagar [55], and also Gartner [56] combined route control and signal control together, formulating a corresponding mathematical model to tackle the joint control problem. Under their scheme, an effective signal control strategy is provided to facilitate the movement of vehicles, and routes for vehicles are planned by considering the signal impacts. However, without real-time road traffic information, their model is based on experience or historical information that are static results and inconsistent with reality.

A major step forward for the joint control problem has come with the development of CAV technology. Within this context, Chai et.al, [15] proposed a dynamic shortest path (DSP) algorithm in a VANET (Vehicular Ad hoc network) based on the travel cost that is updated every second, and the signal control delay was formulated as part of the link travel cost. By combining the DSP algorithm with different signal control methods, the system's total travel time could be reduced. Another attempt comes from Li et al. [57] who formulated the joint control problem using a mixed-integer linear programming (MILP) model. A space-phase-time network is proposed to integrate both micro-level signal phasing plan and macro-level vehicle routing behavior. Although the method appropriately addressed the interaction between vehicle routing and signal control, it cannot give an intuitive description of the traffic state evolution and traffic phenomena. Other typical methods to make up for this shortcoming are based on traffic flow models, among which the Point-queue (PQ) [58], Spatial-queue (SQ) [59], and Cell transmission model (CTM) [60], [61] are the most popular approaches. Compared to the delay function and the link performance function (e.g., BPR function), the PQ, SQ, and CTM can better describe the features of different traffic states.

The PQ model assumes that the queue is formed at one point without a

specific physical length, which can simplify the model but is not consistent with reality. In the SQ model, queues are always growing up at jam density, while in CTM, queues will propagate at a shockwave speed given by the corresponding fundamental diagram [60], [61]. More variables and constraints in CTM generate more accurate results, and many papers have proved the applicability of CTM in solving traffic flow problems. Ziliaskopoulos [62] formulated the system optimal dynamic traffic assignment (SO-DTA) model based on CTM and provided linear relaxation for solving this model. Lo [63]–[65] transformed the basic CTM by adding a signal control constraint, thereby achieving the joint optimization of flow distribution and signal timing. Moreover, a CTM-based MILP model that considers enhanced signal control has been developed by Lin and Wang [66]. Wu [67] solved the route-based signal control problem by using a heuristic algorithm. However, when the path selection behavior of travelers and signal control parameters undergo significant changes, the stability of the heuristic algorithm's solution to the optimal route selection is compromised. Given the intricacies of the problem formulation and the multitude of constraints involved, resolving the joint control problem remains a formidable challenge.

2.4 Distributed Route Control

The literature discussed above adopted a centralized manner for solving the DRC problem which suffers from two intrinsic problems. First is scalability: since the models are complex, the TMC must perform intensive computation to obtain the solution, thus it is hard to be applied in large-scale networks. The second is timeliness: the global information (data for all links of a studied route) needs to be processed in the remote TMC to find the optimal route which costs a large amount of time in communication and may generate an untimely solution. Considering the drawback of the centralized methods, studies began to focus on the distributed DRC approaches, and they can be divided into three types.

The first type focused on the cooperative multi-agent-based route design

[68]–[70]. The routing strategy utilizes an agent-based distributed hierarchy where the vehicles negotiate with each other to determine the optimal departure time and route as well as to increase the chance of arriving on time. For example, Claes et al. [71] presented a decentralized approach for anticipatory vehicle routing using multi-agent systems. Vehicles' behavior is described by the ant-like agent to detect congestion and predict travel costs for re-routing. Their multi-agent routing method indicates a considerable performance gain compared to the TMC-based centralized routing strategy. Similarly, Wedde et al. [72] proposed a distributed and self-adaptive route guidance approach inspired by the honey bee foraging behavior, and the presented algorithm outperforms the dynamic shortest path in terms of travel time and congestion avoidance.

The second type of distributed routing study mainly relies on communication technologies. Guha and Chen [73] leveraged a multi-hop vehicular network to gather local information; this information will be broadcast to vehicles to determine the shortest travel route locally. Faez and Khanjary [74] developed a distributed dynamic route guidance system based on the Sensor Network with Mobile Stations (SNMS). These sensors are deployed along the street to collect local data, estimate the travel time, and send it to mobile phones or vehicles for route optimization. Pan et al. [75] designed a distributed traffic re-routing system called DIVERT which offloads a large part of re-routing computation to vehicles and the vehicles exchange messages over vehicular ad hoc networks. Although the performance of re-routing in their system is slightly inferior to the centralized model, the user's privacy is significantly increased.

The third type of research was inspired by the distributed backpressure (BP) principle. The BP algorithm was initially developed by Tassiulas and Ephremides [76] for scheduling the data packets in wireless communication networks and it was widely utilized [77]–[79] to reduce network congestion and improve throughput by pushing data packets to more vacant links. The idea of BP appropriately fits the motivation of mitigating traffic congestion using effective routing strategies. Nevertheless, it hasn't been adapted to the road traffic network until Varaiya [80], [81] first utilized it to deal with the traffic

signal control problem. Following this work, numerous researchers studied the traffic signal optimization method based on the BP mechanism [82]–[86], and it has become popular in tackling road traffic problems. Among the BP-based DRC studies, Zhang et al. [87] proposed a routing probability calculation model by defining the pressure with considering the trade-off between vehicles' satisfaction and the traffic load. Taale et al. [88] presented a weighted average pressure function that combines the pressure of the first link, the whole route, and the user preference to make re-routing decisions. Kampen [89] synoptically discussed the feasibility and challenges of applying BP to solve the DRC problem. The distributed BP-based method is verified to be effective in reducing traffic congestion. Aligned with the second task of the dissertation, the BP-based method can be appropriately applied to guide the traffic to realize an effective distributed route control. Nonetheless, the conventional BP method relies on the disparity in queue length between upstream and downstream links to determine pressure. The embedded point queue and assumption of infinite capacity, however, lack practicality. Consequently, this dissertation will rectify this limitation by introducing an enhanced BP function.

2.5 CAV Dedicated Lane Design and Management

The above sections focused on the discussion of vehicle route control. However, to alleviate traffic congestion through the implementation of CAV technology, it is crucial to go beyond merely controlling CAV behavior. In essence, CAVs have the potential to enhance road capacity utilization by minimizing the distance between vehicles through optimized car-following strategies. Nevertheless, in a mixed traffic environment, the advantage has been compromised in consideration of the driving behavior of HDVs.

Inspired by one of the most successful lane management methods: High-occupancy-vehicle (HOV) lane [90], the CAV dedicated lanes (CAV-DLs) were proposed to solve the above issue. The goal of setting CAV-DLs is to physically separate CAVs and HDVs. Meanwhile, a range of technologies including

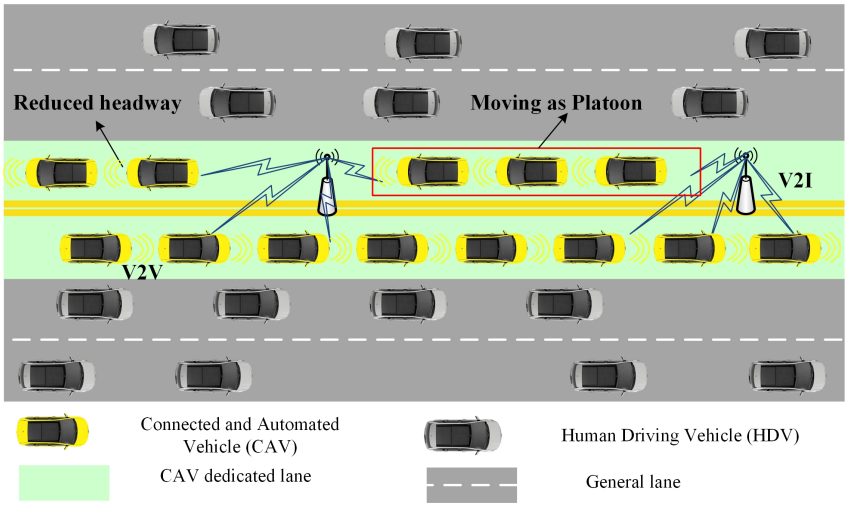

Figure 2.1: Illustration of CAV dedicated lane

cameras and sensors would enable CAVs to operate more smoothly to ultimately facilitate faster, more accessible mobility for all [91]. The CAV-DLs (as shown in Fig. 2.1) simplify the driving scenario since limited lane changing will reduce the perception and calculation tasks at both vehicle and road ends, reduce hardware costs, and as a result promote the adoption of CAVs. However, it occupies the existing road capacities and impacts the mobility of HDVs. The CAV-DLs may waste the road capacity and even worse, the overall system performance, especially in low penetration rate cases. To determine the most effective approach for deploying CAV-DLs, a series of studies focused on exploring the optimal design of the CAV-DLs over the network [92]–[96], and the benefits of separating CAVs and HDVs were properly proven.

Madadi et al. [97] formulated a bi-level network design problem based on the Amsterdam metropolitan region where the upper level finds the best infrastructure configuration and the lower level includes the travelers' response to new network topologies. The results suggested that CAV-DLs were more beneficial after 30% CAV penetration rate (PR). Hamad and Alozi [98] compared the network performance with shared and dedicated lanes, and the findings also indicated that the network improvement is more evident at higher PR. When the PR of CAV is relatively low, the road capacity would be substantially wasted, since the CAVs are not likely to fully utilize these laneways.

Furthermore, Razmi Rad et al. [99] studied the impact of CAV-DLs on the driving behavior of HDVs. Although the dedicated lane can improve efficiency by providing more possibilities for platooning, implementing such a lane will affect human drivers and significantly sacrifice HDVs' benefits.

For this reason, appropriately managing the right-of-way for CAV-DLs is critical. Some researchers suggested activating the CAV-DLs flexibly by allowing them to operate as general lanes (GLs) during non-peak hours [100]. This is a good way to reduce the waste of underutilized road capacity. However, Chan and Shaheen [101] demonstrated that even if the dedicated lane was only available in peak hours, the capacity is still typically not reached. Later on, in the dedicated bus lane management, Viegas and Lu [102] proposed the Intermittent Bus Lane (IBL) to dynamically adjust the right-of-way for dedicated lanes according to the real-time arrival of buses. If there is no bus occupying the dedicated lane, it will be available to the general traffic. The IBL scheme can significantly improve the utilization rate of the dedicated bus lane and ultimately improve the mobility of the whole traffic network. Founded on this, Eichler and Daganzo [103] improved the concept of IBL and further formulated this problem to optimize roadway capacity utilization. Similarly, the CAV-DL management can draw on the experience of such an approach. Indeed, effectively managing CAV-DLs involves the fundamental task of overseeing and controlling traffic flow, a domain inherently encapsulated within the realm of traffic demand management. Inspired by the exisiting dedicated lane management strategies, the dissertation will propose a realistic dynamic right-of-way allocation method based on real-time traffic prediction to address the above issues.

2.6 Economic Measure-based Traffic Demand Management

The economic measure-based traffic demand management serves as an effective way to regulate traffic flow and mitigate traffic congestion. The principle of economic measure-based traffic demand management is to treat the road space

as a common commodity, and travelers use it by paying toll or trading with each other. Existing popular economic measure-based policies include price instruments and quantity instruments [104].

Among those instruments, road pricing has received far more attention than quantity control in both theory and practice, which has already been deployed in cities such as Singapore, London, and California, and has proven to be effective in alleviating traffic congestion. There are also many studies focused on congestion price [105]–[107], where vehicles using the congested road links will pay a toll to achieve the best system performance, and the toll is usually calculated based on the marginal travel cost. Congestion pricing is commonly structured as either a zone or cordon system, and alternatively, it can be applied based on the distance traveled within a designated area. However, a significant challenge arises as this approach tends to disproportionately burden certain drivers, particularly those lacking access to dependable public transit or alternative modes of transportation.

The plate-number-based rationing strategy is one of the typical quantity instruments, which restrict vehicles' access to the road according to their plate number [108], [109]. Nevertheless, this policy was proven to lead to an increase in vehicle numbers and induced a change towards older and cheaper vehicles which bring more pollution and safety concerns [110].

The limitations of congestion price and plate-number-based rationing strategy stimulated the idea of a tradable credit scheme, which has been extensively studied in recent decades [104], [111]–[114]. The tradable credit scheme distributes a certain number of credits to vehicles for free and predetermines the charge of credits for each roadway link. Each credit has a price, and these credits can be traded freely between travelers. In this case, travelers can have a better balance between travel time and money, and the benefit of different types of vehicles can be guaranteed.

In the realm of CAVs, a range of economic-measure-based management approaches can be implemented. These methods serve the purpose of incentivizing CAV adoption, shaping policies, and enhancing the management of CAV technology. For the CAV-DLs management, these economic-measure-based

approaches are appropriate and have the potential to improve the utilization rate of road capacity. As such, the dissertation will look specifically at using economic measures to regulate traffic considering the existence of CAV-DLs.

2.7 Electric Vehicle Technology and Control

The above studies focused on improving traffic efficiency considering the existence of traditional gasoline-based vehicles. Recently, given the pressing concerns of the greenhouse effect and global warming, the electrification of transportation stands as a pivotal element within the realm of smart transportation. It plays a vital role in fostering environmentally friendly transportation and contributing to the development of sustainable, green cities. In the coming years, EVs may have a very important role in Smart cities, along with shared mobility, public transport, etc. EVs have various advantages over traditional cars, such as [115]:

(1) Zero emissions: EVs stand out as vehicles with zero operational emissions, making them an environmentally conscious choice. Additionally, their manufacturing processes prioritize environmental sustainability.

(2) Cost: EVs offer economic benefits in multiple ways. Their streamlined design results in fewer engine components, translating to lower maintenance costs. Moreover, the operational expenses of EVs are notably lower than those of traditional gasoline vehicles. Additionally, the cost per kilometer for energy is significantly reduced with EVs.

(3) Simplicity: EVs feature simplified and compact engine designs. These engines operate without the need for a cooling circuit, and they eliminate the necessity for components like gearshifts and clutches that contribute to engine noise. This streamlined design enhances efficiency and minimizes unnecessary complexities.

(4) Comfort: Choosing EVs ensures a more comfortable travel experience, thanks to the absence of vibrations and engine noise. This creates a serene environment for passengers, promoting a more enjoyable and peaceful journey.

Due to the potential of EVs to improve energy security and protect the

environment, countries all over the world are actively promoting the adoption of them using various incentive programs [116]. These programs are proven to be effective in some countries (e.g., Norway and China), and the growing adoption of EVs illustrates a trend of future greener and cleaner traffic systems.

Addressing traffic control challenges associated with EVs, various studies have delved into regulating EV car-following behavior to enhance energy efficiency. For instance, Yang [117] developed an optimal velocity model that not only reduces energy consumption but also stabilizes the flow of vehicles. Li et al. [118] introduced a sophisticated vehicle-following driving model and proposed periodic control measures to minimize fuel consumption effectively. Additionally, researchers have proposed energy control strategies for automated car-following scenarios [119]. Determining the appropriate velocity, as well as optimizing acceleration and deceleration patterns, has emerged as a critical aspect of EV control [120]. Interestingly, a report on EVs [121], highlights that EV drivers tend to prefer driving at lower speeds in urban arterials to conserve energy. However, it's important to note that maintaining a consistently low driving speed can lead to increased travel time, potentially conflicting with the primary goal of efficient travel. Balancing these factors is essential when developing traffic control strategies for EVs.

The current trend in the transportation system showcases a swift transition towards the adoption of CAVs. Among these, the Connected Automated Electric Vehicles (CAEVs) are poised to be pivotal in the burgeoning revolution towards sustainable, low-carbon mobility. Their potential to achieve substantial reductions in GHG emissions positions them at the forefront of this rapid transformation in transportation. CAEVs hold significant promise for operating with enhanced vehicle efficiency, particularly when charged using renewable energy sources. This strategic approach not only contributes significantly to reducing emissions but also diminishes our reliance on fossil fuels, marking a critical step towards a more sustainable future. In such a circumstance, utilizing the CAEV technology is a potential solution to realize the trade-off between energy consumption and travel time for EVs, and the dissertation will explore more efficient strategies to address the mentioned

research gaps.

2.8 Conclusions

This chapter embarks on a comprehensive exploration of various research domains encompassing the intricate landscape of DRC, DTA, joint route and signal control, CAV-DLs, CAEVs, and the relentless evolution of transportation systems.

A thorough review of state-of-the-art studies reveals a compelling need for more efficient and pragmatic DRC strategies, despite the substantial body of work in recent years. In the context of joint routing and signal control, it is evident that most studies have employed simplified signal timing plans, overlooking the nuanced aspects of realistic phase sequences and duration constraints. The dissertation aims to rectify this by integrating simulation-based DTA models to capture the intricacies of traffic dynamics.

Additionally, within the realm of distributed DRC, it becomes apparent that prior studies lack comprehensive insights into the algorithmic processes and fail to present the exact computational costs involved. The dissertation aims to shed light on the performance of distributed DRC, evaluating its efficacy and computational complexity, particularly in its applicability within the MEC-enhanced CAV environment.

In the context of traffic demand management based on economic measures, a key challenge lies in designing the optimal toll structure, especially in mixed traffic scenarios comprising both CAVs and HDVs. Considering the research gap in capacity and demand management in traffic environments involving CAVs, the research will place a special emphasis on traffic networks featuring CAV-DLs, and design-related lane management approaches and policies.

Lastly, based on the literature review on the behavior of CAEVs, a critical gap exists in formulating a refined driving strategy that strikes a balance between reducing energy consumption and total travel time. Studies trying to regulate the CAEVs' behavior with respect to the existence of CAV technology are lacking. The dissertation will endeavor to enhance this aspect and develop

better trajectory and signal control strategies. In the upcoming chapters, each of these research topics will be meticulously examined, unveiling innovative models and algorithms in a comprehensive manner.

Chapter 3

Joint Dynamic Route Guidance and Signal Control for CAVs

3.1 Introduction

The space-time diagram is one of the most intuitive methods to describe vehicles' travel information (e.g., route, departure time, arrival time, delay, and speed). In a dynamically changing traffic network, travel plans based on experienced travel time are usually more efficient than those based on instantaneous travel time. Fig. 3.1(a) is a 2 by 2 road network and Fig. 3.1(b) displays the trajectories of four vehicles (indicated by different colors) running in this network. The red line and light green line represent two vehicles starting from node 1 and going to node 8. Their departure time is the same but they choose two different routes and arrive at their destination at different times. The blue line and the dark green line describe two vehicles going from node 3 to node 7. They are selecting the same route. Due to the different departure times, the traffic conditions they have encountered are varied; the delay for the blue vehicle at the intersection is much longer than that of the dark green. Consequently, despite the blue vehicle departures earlier, they arrive at the destination at the same time. (Here, d, d_d, d_a, d_w represents total delay, deceleration delay, acceleration delay, and waiting delay respectively). Notably, an equitable route control strategy considering the real-time road and traffic signal control information is pivotal in aiding vehicles to make efficient travel decisions.

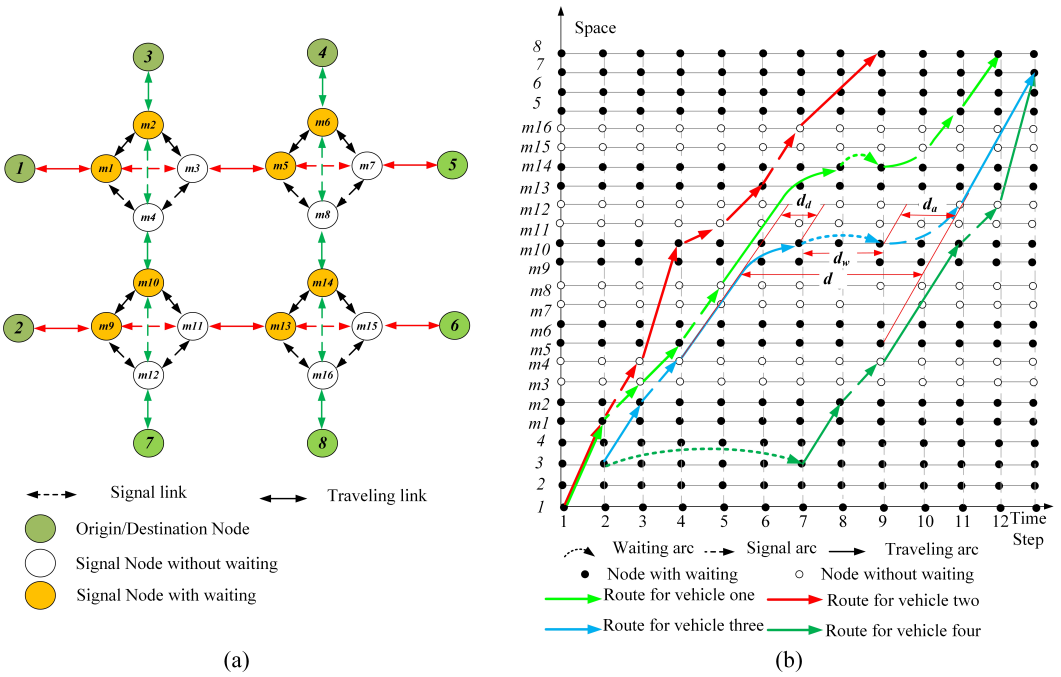

Figure 3.1: (a) 2 by 2 Road network (b) Space-time diagram illustrating different route strategies

Inspired by the importance of joint dynamic route guidance and signal control (DRG-SC), Karoonsoontawong and Waller [122], Chen and Hu[123] solved route guidance and signal optimization using a complex centralized mathematical bi-level model. Ceylan and Bell [124], Teklu et al. [125], and Sun et al.[126] also adopted the centralized mode to simultaneously solve the DRG-SC problem. These studies, although, with varying mathematical formations, the model is usually non-convex and the solution is obtained using heuristic algorithms, the resulting computation cost is pretty high even with a powerful computer server. Other centralized analyses [127] for the DRG-SC problem are also limited to a small network, the real-time application in the larger networks stays unsolved.

The most distinguished feature between CAVs and conventional cars is that the operation of CAVs is highly dependent on real-time, accurate instructions from traffic control or management centers. For that reason, the weakness of the centralized framework in dealing with such a complex problem is in plain sight. Benefiting from the 5G and MEC technology, it becomes increasingly practicable to build a distributed control framework to deal with the DRG-SC

problem for CAVs.

Many studies channeled their efforts towards single distributed SC [128]–[131] or distributed DRG [71], [72], [132], [133], but there remains space for exploring efficient approaches for distributed DRG-SC in large traffic networks. In these limited studies, Yu et al. [134] tested the performance of a route guidance strategy integrated with several signal control methods, using a simulation-based model developed in the traffic software PARAMICS. Chai et al. [15] also simulated a CV environment using SUMO [135] and OMNET++ [136] to combine the shortest path algorithm with adaptive signal control. Li et al. [137] developed a mathematical optimization model by using a space-time diagram to find the time-dependent solution for simultaneous routing and signal control. Although they stated that the proposed method can be applied to a distributed framework, the detailed processing flow was not adequately described. Moreover, the role of MEC in such a distributed framework needs further investigation.

Additionally, before a sufficiently developed CAV environment can be made available in reality, testing the related algorithms in a similar simulation environment is essential. In recent decades, simulation techniques have been extensively adopted to evaluate and compare the operational performance of new alternative strategies [134], [138]–[140]. The simulation-based methods are realistic since they stress the prevailing situations and are able to describe the dynamically changing traffic conditions. Thus, the result can always shed some light on how a specific control measure performs in the real world. For that reason, the study in this dissertation revolves around simulation-based techniques. In general, this chapter has investigated all of the research gaps mentioned above with the following contributions:

I. A complete distributed data processing, information communication, and transmission procedure for conducting DRG-SC in the MEC-enabled CAV environment is designed: To the best of our knowledge, this is the first time the exact tasks of vehicles, infrastructures, and TMC are presented towards solving a DRG-SC problem. The pivotal position of MEC is particularly explained and hence generates fresh insight into how it will promote the CAVs' intelligent

operation and control.

II. A novel DRG-SC model that aims at improving network efficiency is developed: Different from the conventional methods that formulate the DRG-SC problem into a mathematical model and then solve it by optimization algorithms, the route strategy in our paper is distributed at the level of individual vehicles and the signal control is distributed at the level of intersections. Vehicles select the user-optimal (UO) or system-optimal (SO) targeted route first, and subsequently enhance the network performance by cooperating with other vehicles. When computing travel time for routes, the proposed model addresses the crucial impact of intersection delay caused by signal control on vehicles' routing plans which is not specifically deliberated even in the most popular route planner, Google Maps [141]. Moreover, the relationship between travel time and traffic volume is identified by a simulation manner rather than a simplified link performance function. The proposed signal control strategy also keeps vehicles' routing plan and waiting time in view so that the timing plan is more accurate and effectual.

III. The study has probed into the computation time for the proposed method and verified its benefit in ameliorating computation efficiency in the case study. Since the presented method allows to be implemented in a parallel manner, which can further accelerate the distributed process. A preliminary test was conducted using different numbers of computer server cores with adopting the parallel computing technique. The result demonstrated the potential of the developed method to be applied in real-world cases.

3.2 Methodology

This section elaborates the method for conducting the DRG-SC with presenting the detailed route and signal control strategies. Table 3.1 lists the notations for all parameters, sets and variables used in this chapter.

Table 3.1: Notations

Parameters			
τ	Step size (Time duration for each step)	k	Index of time step
t	Index of time interval ($k = t/\tau$)	f	Index of vehicles
L_a	Length of link a	i	Index of current intersection
m	Index of upstream intersection of intersection i	n	Index of downstream intersections of intersection i
$l_i(m,n)$	Link serving vehicles coming from intersection m, arrives at intersection i and goes to intersection n	$N_i(m,n)$	Number of vehicles on link $l_i(m,n)$
G_{min}	Minimum green time for each phase	G_{max}	Maximum green time for each phase
$T_{p_i^t}$	Time duration for phase p of intersection i at time interval t	T_f	Total study time horizon
Sets			
R	Set of routes for OD pair od	A	Set of all travel links
O	Set of all origins	D	Set of all destinations
N	Set of all nodes	I	Set of all intersections
F	Set of all vehicles	Ωi	Set of all phases of intersection i
Variables			
T_a^t	Experienced travel time on link a at time interval t	x_a^t	Time dependent vehicle number on link a at time interval t
$f_{od}^{r,t}$	Time dependent traffic flow on route r of the OD pair od at time interval t	f_{od}^t	Time dependent traffic demand of OD pair od at time interval t
δ_{od}^a	Link-route incidence (0-1 variable)	x_a^{t-1}	Time dependent vehicle number on link a at time interval $t-1$
e_a^{t-1}	Time dependent vehicle number entering link a at time interval $t-1$	l_a^{t-1}	Time dependent vehicle number leaving link a at time interval $t-1$
$\overline{v}_a^t$	Space mean speed of link a during time interval t	$T_a^{r,t}$	Time-dependent average travel time on link a during time interval t
$\varphi_{a,i}^t$	Delay of intersection i on link a in time interval t	$T_{o,d}^t$	Shortest route travel time of OD pair od in time interval t
p_i^t	Current phase for time interval t of intersection i	$G_{p_i^t}$	Green split of phase p at intersection i in time interval t

3.2.1 Overall Framework and Data Flow

The complete data communication, processing, and computing procedure for the proposed DRG-SC framework are shown in Fig. 3.2. The basic data is the immediately accessible fixed data set, while some flexible data is acquired by further processing or computing. From the vehicle unit, we can obtain BSM data that includes real-time vehicle speed and location information. This data will be sent to the infrastructure and, based on real-time speed data, the RSU installed within the infrastructure will compute the average travel

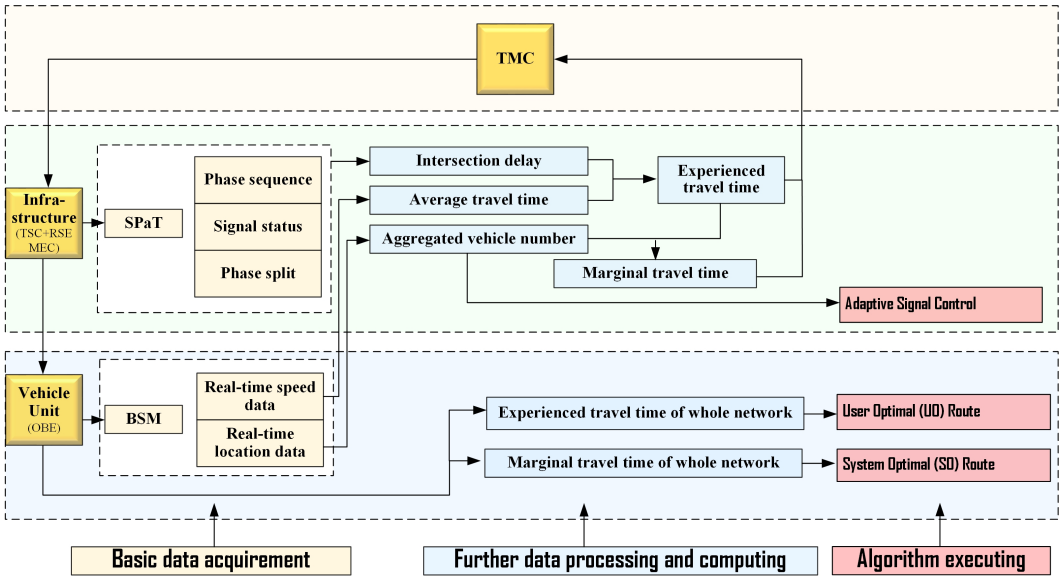

Figure 3.2: Data communication, processing, and computing procedure for DRG-SC

time for links. Also, it can aggregate and predict the number of vehicles using location data. In terms of the infrastructure, the basic data that can be obtained from the RSU is SPaT data, used to compute intersection delay. The experienced travel time is then calculated at the infrastructure by adding intersection delay and average travel time on links. Further, the marginal travel time can be computed when combining the experienced travel time with vehicle count information. After that, all RSUs will send both experienced travel time and marginal travel time information to the TMC, the TMC will gradually depict and gather the information for the whole network and send it back to the RSU, and then the RSU will broadcast it to every vehicle within its communication range. After these steps, the information on the whole network will be now available in TMC, RSU, and vehicle units. With the required data ready, the RSU will perform the ASC algorithm, and each vehicle unit will perform re-routing algorithms. With such a data processing flow, the TMC, RSU, and vehicle unit each need only tackle a relatively small piece of the work.

3.2.2 Joint Dynamic Route Guidance and Signal Control Formulation

The DRG strategy can be given by solving the DTA based model. The well-known DTA models include UO-DTA and SO-DTA, which can be formulated as follows. The corresponding objective function is described by Eq. (3.1) and Eq. (3.2) with corresponding constraints in Eq. (3.3)-Eq. (3.7). Eq. (3.3) requires the summation of all time-dependent route flow of the OD pair equals to the OD demand, Eq. (3.4) gives the relationship between time-dependent route flow $f_{od}^{r,t}$ and link flow x_a^t through the 0-1 variable δ_{od}^a, Eq. (3.5) states that the time-dependent travel time on link a is a function of the time-dependent traffic flow, Eq. (3.6) ensures the conservation law, and Eq. (3.7) guarantees the non-negative characteristics.

$$\min\ Z(X) = \sum_{a \in A} \int_0^{x_a^t} T_a^t(w)dw \quad (UO-DTA) \tag{3.1}$$

$$\min\ Z(X) = \sum_{a \in A} \sum_{t \in T_f} x_a^t T_a^t(x_a^t) \quad (SO-DTA) \tag{3.2}$$

$$\sum\nolimits_r \sum f_{od}^{r,t} = f_{od}^t,\ \forall r \in R, o \in O, d \in D, t = 1, 2, ..., T_f \tag{3.3}$$

$$\begin{aligned} \textstyle\sum_o \sum_d \sum_r \delta_{od}^{r,a} \cdot f_{od}^{r,t} = & x_a^t,\ \forall r \in R, o \in O, \\ & d \in D, a \in A, t = 1, 2, ..., T_f \end{aligned} \tag{3.4}$$

$$T_a^t(x_a^t) = F(x_a^t), \quad \forall a \in A, t = 1, 2, ..., T_f \tag{3.5}$$

$$x_a^t = x_a^{t-1} + e_a^{t-1} - l_a^{t-1}, \quad \forall a \in A, t = 1, 2, ..., T_f \tag{3.6}$$

$$f_{od}^{r,t}, x_a^t, T_a^t \geq 0, \ \ \forall a \in A, t = 1, 2, ..., T_f \tag{3.7}$$

Analytical DTA models are difficult to be solved and converged when applied in large traffic networks. Moreover, Eq. (3.5) is usually approximated using simplified link performance functions (e.g. The Bureau of Public Roads (BPR) function) that are impractical and often lead to unrealistic results. Therefore, this study develops a simulation-based method that can acquire the accurate travel time and vehicle number on links directly from the simulation instead of using the empirical link performance function. When the network reaches a UO condition, all vehicles should be on the shortest travel

time route and no vehicle can make improvement by switching to another route. Similarly, when all vehicles are on the shortest marginal travel time route, the network will reach an SO condition. In the proposed simulation-based model, vehicles will first select the minimum time-dependent travel time route or marginal travel time route and then cooperate to reach either a UO or SO state.

To find the shortest route, the first step is to calculate the experienced travel time. Here, the intersection delay was addressed as a portion of the travel time. Then, it consists of three parts: free flow travel time, delay caused by congestion, and intersection delay caused by the signal control. In the CAV environment, the vehicle speed information is updated at a high frequency; thus, the calculation for real-time space mean speed on links is straightforward. When using the real-time speed information to calculate average travel time, the delay caused by congestion has already been included. So, the experienced travel time in the CAV environment only consists of two parts: average travel time computed by space mean speed and the intersection delay.

The time-dependent space mean speed as the average of the mean speed of all CAVs over the link at an instant of time k within a time interval t can be calculated by Eq. (3.8). The average travel time is then computed (Eq. (3.9)) using the length of a link divided by the time-dependent space mean speed. The experienced time-dependent travel time T_a^t is the summation of average travel time $T_a^{r,t}$ on the link and the delay $\varphi_{a,i}^t$ of the downstream intersection, decided by the exact signal control strategies (Eq. (3.10)). With these equations, the experienced dynamic shortest route travel time between an OD pair at time interval t is sought using Eq. (3.11) where g is the successor node of origin node, and the predecessor node of h.

$$\overline{v}_a^t = \frac{\sum\limits_{t/\tau}\left(\frac{\sum_{f=1}^{x_a^k} v_{f,a}^k}{x_a^k}\right)}{t/\tau} \quad \forall f \in F; a \in A; k = 1, ..., t/\tau; t = 1, 2, ..., T_f \tag{3.8}$$

$$T_a^{r,t} = L_a/\overline{v}_a^t, \quad \forall a \in A; r \in R; t = 1, 2, ..., T_f \tag{3.9}$$

$$T_a^t = T_a^{r,t} + \varphi_{a,i}^t, \quad \forall a \in A; r \in R; i \in I; t = 1, 2, ..., T_f \tag{3.10}$$

$$T^t_{O,D} = \min \sum_{a \in A} \sum_{t=1}^{T_f} T^t_a = \min\{T^t_{O,g} + \sum_{h=1}^{D} \sum_{t=1}^{T_f} T^t_{g,h}\}, \quad \forall a \in A; g, h \in N; t = 1, 2, ..., T_f \tag{3.11}$$

The route marginal travel time refers to the change on route travel time with a unit change of the number of vehicles. It is calculated by taking the deviation of travel time over vehicle numbers as shown in Eq. (3.12). Here, $T^t_a(x^t_a) + x^t_a \cdot (\partial T^t_a(x^t_a)/\partial x^t_a)$ represents the link marginal travel time. In this equation, in order to compute $\partial T^t_a(x^t_a)/\partial x^t_a$, the relationship of link flow and link travel time needs to be known in advance. However, there's no known adequately accurate analytical function to capture the relationship. When the vehicle number is lower than link occupancy, the value of $\partial T^t_a(x^t_a)/\partial x^t_a$ is 0 and the marginal travel time equals the free flow travel time. In congestion cases, the time-dependence of the derivative is assumed to be caused by 'time-varying' link performance function, and this link performance function changes over time. The travel time can be significantly different, although the vehicle number on link is the same because it depends on the real-time queuing condition.

$$\begin{aligned} \frac{\partial Z(X)}{\partial f^{r,t}_{od}} &= \sum \frac{\partial Z}{\partial x^t_a} \frac{\partial x^t_a}{\partial f^{r,t}_{od}} = \sum \frac{\partial}{\partial x^t_a} [\sum_a x^t_a \cdot T^t_a(x^t_a)] \cdot \delta^{a,r}_{od} \\ &= [T^t_a(x^t_a) + x^t_a \cdot \frac{\partial T^t_a(x^t_a)}{\partial x^t_a}] \cdot \delta^{a,r}_{od} \end{aligned} \tag{3.12}$$

$$T^t_a(x^t_a) = \alpha \cdot (x^t_a)^2 + \beta \cdot (x^t_a) + \gamma \tag{3.13}$$

In the proposed simulation-based model, an approximation approach is used which assumes that during a small-time interval, three consecutive points are on the same link performance curve (as shown in Fig. 3.3). Thereby, a quadratic fitting (Eq. (3.13)), where α, β, γ are corresponding coefficients) is utilized to capture the relationship between travel time and vehicle number. In adopting this approach, we need to pay attention to the selection of time interval. If the time interval chosen is too small, the curve is not stable; if it is too large, the interval cannot describe the current time-dependent relationship accurately. Peeta and Mahmassani [48] have analyzed how to choose the time interval to solve the stability problem in detail. Interested readers are referred to their work.

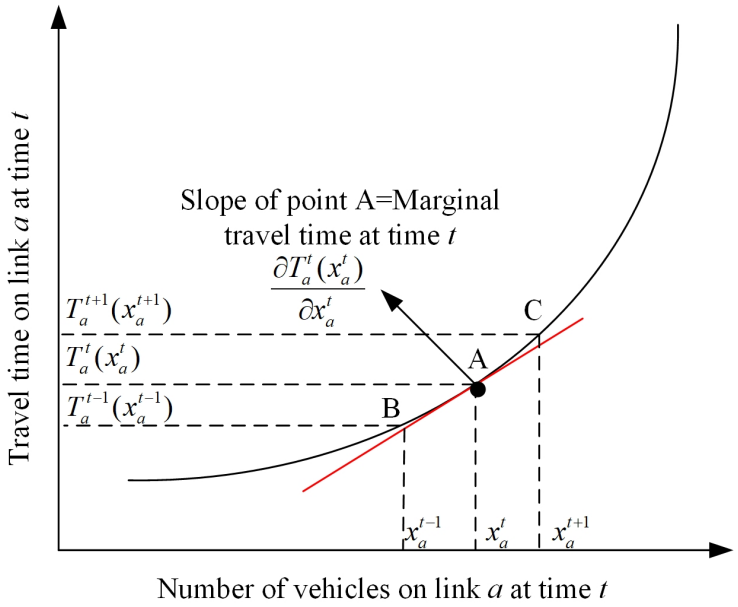

Figure 3.3: Quadratic fitting of derivative for link marginal time .

3.2.3 Embedded Signal Control Strategy

An ASC strategy that considers the influence of vehicles' waiting time and routing plan is developed for this study. For the ASC, the number of vehicles on links for the upcoming time interval is the most critical input. Accordingly, the method to predict the vehicle number will be explained first.

Define $l_i(m,n)$ to represent the link serving vehicles coming from intersection m, arriving at intersection i, and going to intersection n. $N_i(m,n)$ represents the corresponding number of vehicles on link $l_i(m,n)$. Then, the number of vehicles that will arrive at intersection i before the start of next time interval $t+1$ can be computed in four parts (Eq. (3.14)).

1) $N_i[(m,n),t]$: Number of vehicles already arrived at intersection i on the link $l_i(m,n)$ at the start of the time interval t (obtained via V2I communication by analyzing the real-time location of vehicles);

2) $N_{ri}[(m,n),t]$: Number of vehicles running on the link $l_i(m,n)$ at the start of the time interval t and will arrive intersection i before $t+1$ (relying on V2I communication by analyzing the real-time vehicle speed and location);

3) $N_{ci}[(m,n),t]$: Number of vehicles from neighboring intersections within time interval t and arrive intersection i before $t+1$ (based on I2I communica-

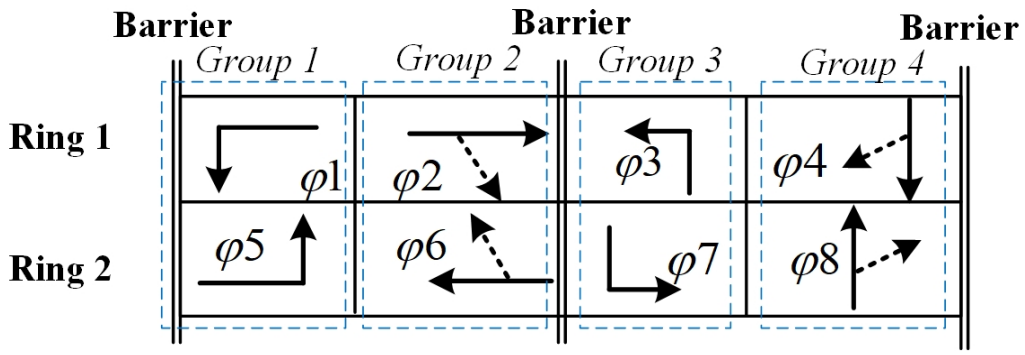

Figure 3.4: A four-phase diagram.

tion to get vehicle number from adjacent intersections and also from vehicles' routing plan to determine vehicles' next travel link);

4) $N_{di}[(m,n),t]$: Number of vehicles leaving from intersection i through the link $l_i(m,n)$ within time interval t (depend on V2I communication by analyzing real-time vehicle speed and location; also relies on signal control strategies).

$$\begin{aligned} N_i[(m,n),t+1] = N_i[(m,n),t] + N_{ri}[(m,n),t] \\ + N_{ci}[(m,n),t] - N_{di}[(m,n),t] \end{aligned} \tag{3.14}$$

A four-phase, eight-movement phase plan is utilized in this study. The National Electrical Manufacturers Association (NEMA) phase sequence is adopted to label the eight movements that are divided to four groups, each corresponding to one phase (Fig. 3.4). The detailed explanation for the signal control variables is as follows:

Offset: As signal coordination is not the focus of this study, so it hasn't been defined as a variable but is included with a predefined fixed value;

Cycle length: Different from the traditional cycle length definition, the cycle length in this study has no fixed value and changes flexibly to the phase split;

Phase sequence: The movement with the longest vehicle waiting time or the highest predicted number of vehicles will be chosen as the next phase. To be more specifically, in Eq. (3.15), $p_{i,max}^{t,WT}$ implies the phase serving vehicles with the longest waiting time in intersection i, at time interval t, and $MAXWT$ means the predefined maximum waiting time. In order to ensure vehicles on

links with relatively low volume are passable, it is necessary to first record vehicles' waiting times on all links (right-turn not included) and then compare to find the one with the longest waiting time. If the longest vehicle waiting time is larger than the pre-defined threshold ($MAXWT$), the phase serving these vehicles should be selected as next phase. Otherwise, movement with the highest predicted number of vehicles $p_{i,max}^{t,N_i}$ will be set as next phase.

$$p_i^{t+1} = \begin{cases} p_{i,max}^{t,WT}, if\ longest\ waiting\ time \geq MAX\ WT \\ p_{i,max}^{t,N_i}, if\ longest\ waiting\ time < MAX\ WT \end{cases} \tag{3.15}$$

Phase split: Phase split depends on the chosen time interval. It is also different from the traditional split definition that equals to the summation of the time interval from the 'green to red' phase status, as shown in Eq. (3.16). Also, the green time for each phase is constrained by the minimum and maximum green (Eq. (3.17)).

$$G_{p_i^t} = \sum_{t \in T_{p_i^t}} t \tag{3.16}$$

$$G_{min}^t \leq G_{p_i^t} \leq G_{max}^t \tag{3.17}$$

3.2.4 Algorithm Solving Procedure

The detailed problem-solving procedure is shown in Table 3.2. First, SUMO simulates the traffic to generate vehicle trajectories with the initial information. Then, Python can compute the experienced travel time and marginal travel time for vehicles to seek their optimal route using the Dijkstra algorithm [142]. Moreover, the traffic signal controller combines the newly updated traffic information to adjust the signal timing plan. At this step, the travel time is also renovated. Subsequently, the classical Golden Search Method (GSM) [143] is applied to do several iterations until the algorithm converges to an equilibrium state.

Table 3.2: Problem solving procedure

Step	**Initial Input**: Signal Timing Plan (Cycle length, phase sequence, split); Network Parameters (Topology, free flow speed, capacity); OD information (Demand, origin and destination)
1	**SUMO** simulator: Generate vehicle trajectories
	For all intersection i, link a and vehicle f:
2	**Compute**: $\overline{v}_a^t$, $T_a^{r,t}$, $\varphi_{a,i}^t$
3	Then, **calculate** experience travel time T_a^t
4	**Aggregate** all vehicles' routing plan;
	Predict vehicle number of next step:
	$N_i[(m,n),t+1] = N_i[(m,n),t]+N_{ri}[(m,n),t]+N_{ci}[(m,n),t]-N_{di}[(m,n),t]$
5	**Quadratic** fitting to derivative and compute link marginal time
	$T_a^t(x_a^t) = \alpha \cdot (x_a^t)^2 + \beta \cdot (x_a^t) + \gamma$
6	**Search** the shortest route by Dijsktra
7	Vehicles **Re-route** to corresponding route
8	**Update** link occupancy x_a^t
	If vehicle's longest waiting time $\geq MAXWT$:
	$p_i^t = p_{i,max}^{t,WT}$
	Else:
	$p_i^t = \underset{p_i^t \in \Omega_i, G_{min}^t \leq t \leq G_{max}^t}{\arg\max} \{N_i[(m,n),t+1]\}$
	End:
9	**Update** p_i^{t+1}, $G_{p_i^{t+1}}$
10	**Recompute** T_a^{t+1}, yield auxiliary variable link flow: y_a^{t+1}
11	**Apply** GSM, Set $x_a^{t+1} = (1-\theta)x_a^t + \theta y_a^t$, θ= 0.618
12	**Test convergence**, $\left\|x_a^t - x_a^{t-1}\right\| / x_a^{t-1} \leq \varepsilon$, otherwise, go to step 2
	End

3.3 Case Study

3.3.1 Simulation Settings

This section evaluates the effect of the proposed method via a case study on a signalized three-by-four traffic network (Fig. 3.5). This network is effective as all the intersections are signalized and it provides sufficient alternative routes for dynamic routing. The other detailed simulation settings are illustrated in Table 3.3.

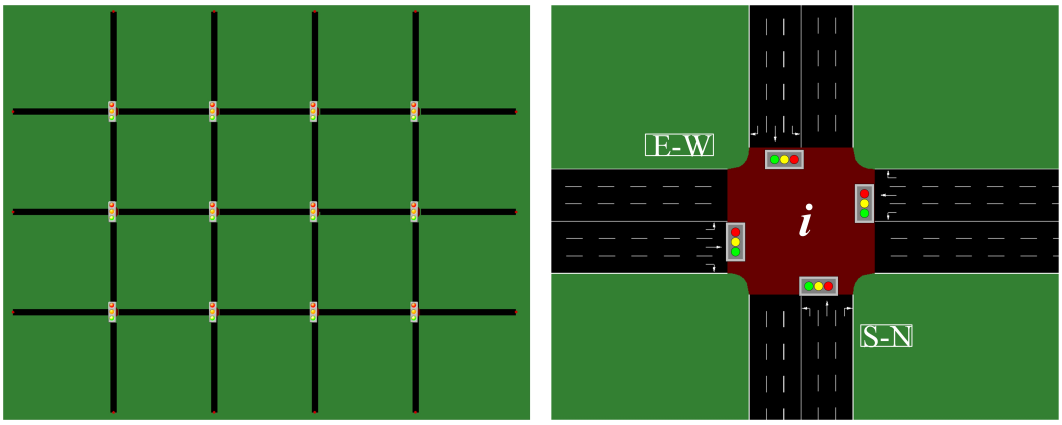

Figure 3.5: Simulation network.

The microscopic traffic simulation tool SUMO [135] was used to simulate the traffic. Python was integrated to implement the proposed model and control strategies. The online interaction between SUMO and Python was realized by the SUMO application programming interface (API) TraCI which allows the real-time data exchange and implementation of an up-to-date control strategy.

In the simulation, the demand loading pattern is a key factor influencing the results. In this study, two kinds of loading profiles were considered (Fig. 3.6): one loaded uniformly and the other loaded with a peak period. Vehicles were loaded every five minutes with the first five minutes as the start-up time to ensure the network was reasonably occupied. Although the testing network was symmetric, the OD distribution was asymmetric to ensure different flow patterns on links. What's more, three different levels of demand (Free flow: 600 tagged vehicles, Moderately congested: 2400 tagged vehicles, and

Table 3.3: Simulation settings

Network information (3*4 grid network; 12 intersections; 26 nodes, 62 links)	
Number of lanes	Each approach has 3 lanes (one LT, one Through, one RT, 186 in total)
Length of each link	300m
Maximum speed (free flow speed)	14m/s(50km/h)
Simulation Parameters	
Simulation time step	1s
Signal timing updating interval	every 10 s
Vehicle re-routing interval	Every 180s (3minutes)
Total simulation time horizon	4500s (ensure all vehicles leave the network)
Maximum waiting time	36s
Signal Control Parameters	
Min/Max Green for each phase	6s/30s

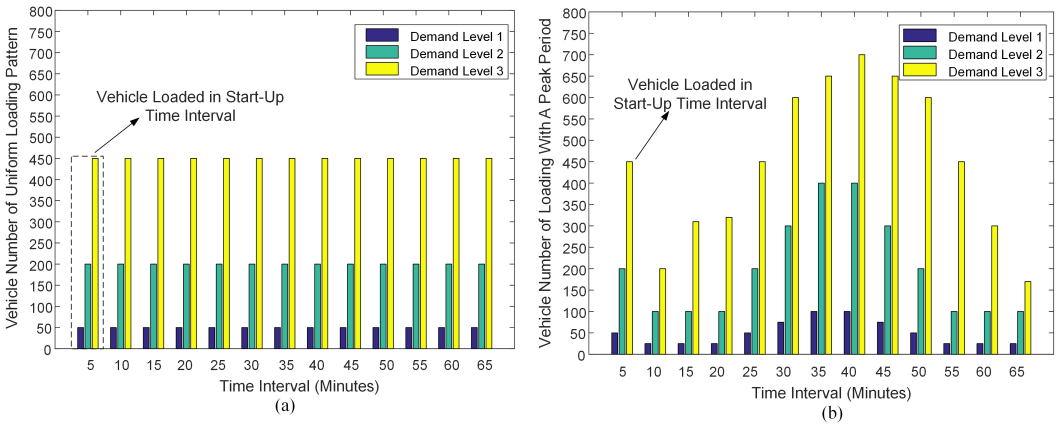

Figure 3.6: Demand loading profile (a) Loading uniformly (b) Loading with a peak period.

Congested: 5400 tagged vehicles) were tested. Five different control scenarios were considered in this study. FSC-Only used a simple FSC strategy without considering re-routing possibilities, and this was used as a comparison benchmark to test the performance of other control strategies. The FSC timing plan was estimated according to the simulated volume with a cycle length set to be 90s. For left-turn movements, the green time was 15s, and through movements were 24s, followed by a clearance time of 3s for each phase. UO and SO targeted re-routing were combined with FSC and ASC (that are: UO-FSC, SO-FSC, UO-ASC, and SO-ASC).

3.3.2 Overall Control Performance

The results of different control strategies are illustrated in Fig. 3.7. Four performance metrics (average departure delay, average travel speed, average waiting time, and average travel time) were calculated respectively. In general,

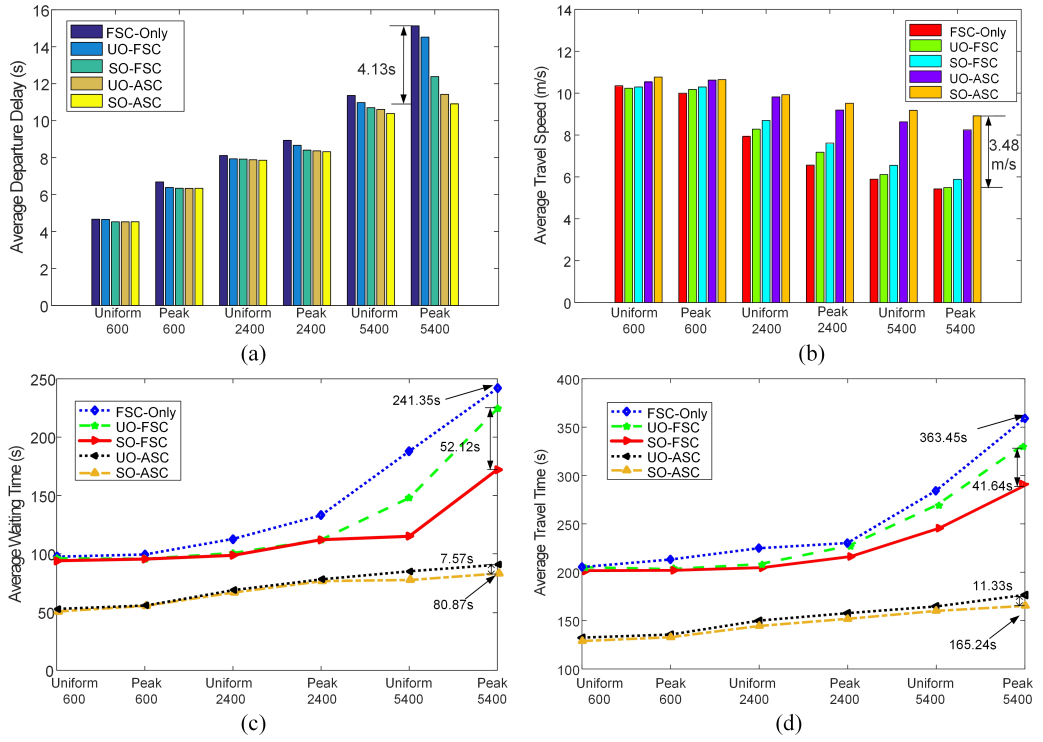

Figure 3.7: Performance of different control strategies: (a) Average departure delay (b)Average travel speed (c) Average waiting time (d)Average travel time

SO-ASC outperformed other control strategies in all performance metrics. The

benefits are especially prominent in high-demand cases. (e.g., in the Peak 5400 demand, the average waiting time for SO-ASC was 80.87s, only about 33% of the 241.35s for FSC-Only control).

Effect of demand loading pattern:

For the two kinds of demand loading patterns, the performance was inferior when loading vehicles with a peak period, despite loading the same number of vehicles. Because when there is a peak period, the congestion level can become very high in a short period.

Effect of signal control strategies:

We can see that ASC consistently had lower departure delay, waiting time, travel time, and higher travel speed than FSC (by comparing the performance of UO-ASC to UO-FSC or SO-ASC to SO-FSC), because when the demand level is low, the corresponding congestion level will be low, and the FSC strategy may cause unnecessary waiting time. While in higher demand level conditions, the FSC cannot provide enough green time for the required traffic movement, thus causing longer queues.

Effect of route guidance strategies:

By comparing the results of UO-FSC to SO-FSC or UO-ASC to SO-ASC, it is apparent that the SO-based route guidance strategy demonstrated better system performance than the UO-based strategy. In low demand level (600 vehicles), UO- and SO-based strategies performed similarly, because when the congestion level was low, the travel time on the link approximately equaled free-flow travel time, and the resulting optimal route was the initial shortest static route. Along with the increased demand level, the benefit of SO re-routing became evident since it may have guided some vehicles towards longer routes, thereby reducing congestion.

There is also another interesting discovery, see Fig. 3.7 (c), the waiting time reduction brought by adopting SO re-routing over UO re-routing is more evident in the FSC control scenario than that of the ASC control scenario. (e.g., in peak5400 demand level, the relative improvement is 52.12s and 7.57s respectively). A similar phenomenon can be noticed in the average travel time shown in Fig. 3.7 (d). This phenomenon can be explained because when

utilizing ASC strategy, the congestion has already been mitigated to some extent by signal control, and the travel time difference between alternative routes is smaller than in the FSC case. This discovery also indicates that the innovative signal control has a latent force in leading the network to the SO state.

3.3.3 Specific Signal Control Analysis

To show the superiority of the proposed ASC over the FSC strategy, Fig. 3.8 has drawn the number of vehicles on all the lanes during the whole simulation for peak600, peak2400, and peak5400 demand level respectively (the results of loading uniformly gives a similar conclusion). The number of vehicles on

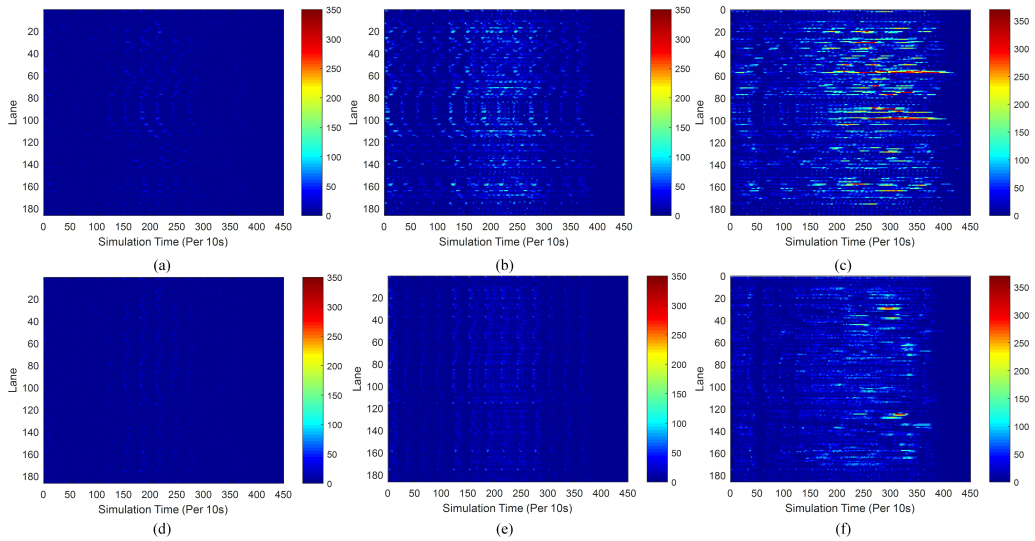

Figure 3.8: Number of vehicles on lanes: (a) FSC-only in peak600 (b) FSC-only in peak2400 (c) FSC-only in peak5400 (d) ASC in peak600 (e) ASC in peak2400 (f) ASC in peak5400

the lane was aggregated by 10s. If the vehicle cannot leave the lane within the first 10s interval, as a result, it will be counted repeatedly in the next 10s interval. Therefore, the higher the number is, the longer the delay it will reflect. Fig. 3.8(a), (b), and (c) indicate the FSC-only case, while (d), (e), and (f) refer to the ASC case. At a low demand level (i.e., peak 600), there is no significant difference between FSC-only and ASC. However, the number of vehicles is much lower with the ASC strategy when the demand level increases, especially at the peak 5400 demand level.

To specifically analyze the effectiveness of ASC, Fig. 3.9 gives the trajectories of vehicles on one of the most congested lanes during the peak period for peak 5400 demand level. For the FSC case, the dissipation of vehicles strictly follows the fixed 'red' to 'green' change, which usually leads to long queues in high-demand cases. In contrast, the proposed ASC strategy could more flexibly adjust the green split and change the phase sequence to the approach with heavier traffic demand. Thus, it's obvious that trajectories in ASC are more dispersed than those in FSC because once a certain number of vehicles are accumulated on the line, they will be served at once instead of waiting for the fixed green to come. This phenomenon also demonstrates the considerable capability of the proposed ASC strategy in reducing delays in congestion cases.

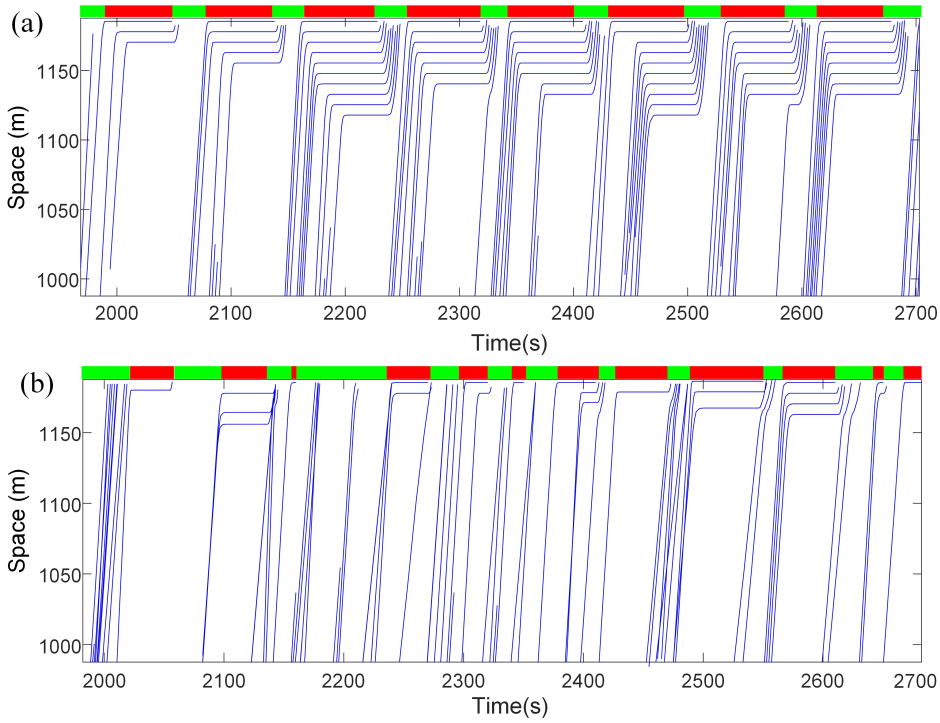

Figure 3.9: Trajectories on one congested lane as an example: (a)FSC case (b)ASC case

3.3.4 Re-routing Analysis

Vehicles were rerouted during the simulation time horizon. Fig. 3.10(a) shows the distribution of vehicles' re-routing frequency under the SO-ASC control strategy. For some vehicles, the optimal route is always the initial route, so

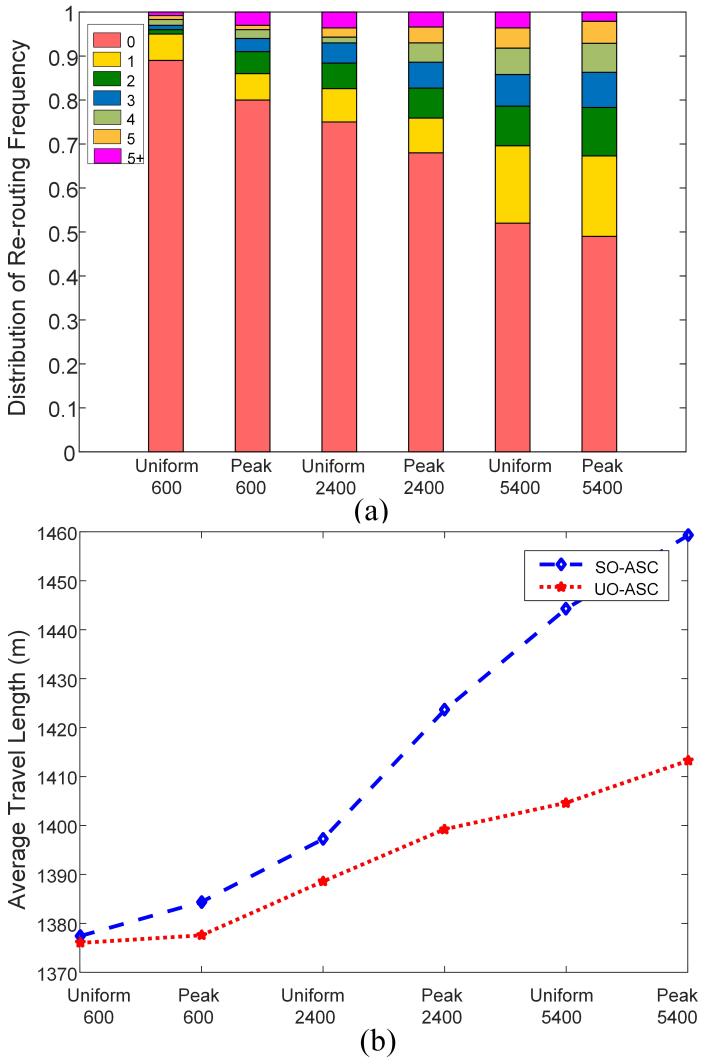

Figure 3.10: (a) Distribution of re-routing frequency under SO-ASC (b) Average travel length comparison of UO-ASC and SO-ASC

they have never re-routed. However, this percentage decreased from almost 90% in demand Uniform 600 to around 50% in demand Peak 5400. With the increase in demand level, the proportion of vehicles re-routed more than once began to increase, allowing higher utilization of the roadway capacity in more congested cases. Fig. 3.10(b) compares the average travel length of UO-ASC and SO-ASC control strategies. The average travel length rose with the increase in demand. In addition, the average travel length under the SO route guidance strategy was longer than UO because more vehicles were guided to longer routes to reduce the system's total travel time.

In a real CAV environment, if the compliance rate of vehicles to the provided route strategy is 100%, there is a greater possibility of realizing the SO condition. However, individual vehicles usually prefer switching to the shortest route without considering the behavior of other vehicles. This is more consistent with the UO-based re-routing. Thus, the study hereby define the compliance rate for vehicles' re-routing behaviors as the percentage of vehicles adopting the SO-targeted strategy. For instance, when the compliance rate equaled 20%, then 20% of vehicles adopted the shortest marginal travel time route. The remaining 80% followed the shortest travel time route. Then, the results of a complete UO or SO strategy are more like providing a lower and upper boundary. Table 3.4 compares the network performance by calculating the total travel time (TTT) of the whole network with respect to the compliance rate as it increased from 0% to 100%. The embedded signal control strategy was ASC.

Table 3.4: System TTT of different compliance rate

Compliance Rate	0%(h)	20%(h)	40%(h)	60%(h)	80%(h)	100%(h)
Uniform 600	22.08	22.12	22.06	22.06	21.88	21.82
Peak 600	22.60	22.54	22.33	22.29	22.27	22.24
Uniform 2400	100.03	99.83	98.12	97.64	97.09	96.31
Peak 2400	105.18	104.27	103.68	102.45	101.66	101.26
Uniform 5400	247.04	243.88	242.95	240.97	240.65	240.04
Peak 5400	264.86	261.93	258.04	253.43	248.69	247.86

In low demand levels (600 vehicles), it seems the change in compliance rate did not make a significant difference to TTT, due to UO and SO equivalence when congestion levels are low. However, in higher demand levels (2400 vehicles and especially with 5400 vehicles), the benefit of the SO re-routing, coupled with the increase of vehicles' compliance rate, in reducing TTT was observable. There was a significant improvement when the compliance rate increased from 40% to 60% in Peak 5400 demand level, while the improvement from 80% to 100% when the compliance rate reached 80% is relatively smaller.

3.3.5 Computation Time Analysis

In this section, the computational cost of the proposed distributed method in dealing with the SO-ASC control under different demand levels were presented. The experiment was carried out on a laptop computer with an Intel 2.80 GHz CPU and 16GB memory. First, the result was compared with several state-of-the-art studies (See Table 3.5) to highlight the effectiveness of the method in saving computation time. Second, since the proposed method allows to be implemented in a parallel manner, which can further reduce the computation time, we also performed a preliminary test using multiprocessing-based parallelism with different number of computer server cores (shown in Table 3.6).

Table 3.5: Computation time comparison of distributed and centralized method

Network size	Simulation Method	CCT(s)	DCT(s)	Δ CT	Reference
56 intersections, 194 links	Cell Transmission Model	13,320	1,980	85%	Adacher and Tiriolo [144]
2 intersections, 7 links	Cell Transmission Model	334 (10 iterations)	11	97%	Mehrabipour and Hajbabaie [145]
		N/A (150 iterations)	195	>100%	
15 intersections, 36 links	link-node model	500	300	40%	Chow et al .[146]

*CCT is for Centralized Computation Time, DCT is for Distributed Computation Time, ΔCT=(CCT-DCT)/CCT which represents for percentage that has been improved with the distributed method, N/A means Not Available to find the optimal solution.

For the literature listed in Table 3.5, all of the distributed methods outperform the centralized methods significantly in computation time, including Chow et al. [146] who conducted their study on a network with 15 signalized intersections, comparable to our case study network size (12 intersections). Their centralized method required 500s and the distributed method required 300s. There is no doubt that if we utilized a centralized model to conduct our study, the computation time would exceed 500s. After all, Chow et al. [146] only dealt with signal parameters optimization while we further coped with the more complex dynamic route guidance. However, our method only takes

Table 3.6: Time cost for parallel computing in Python

Number of Cores	Computation Time(s)					
	Peak 600	Uniform 600	Peak 2400	Uniform 2400	Peak 5400	Uniform 5400
1	131.81	131.64	181.41	166.67	343.35	267.28
2	105.68	104.23	136.77	117.46	301.27	224.67
3	89.39	92.39	112.63	95.38	238.76	177.24
4	53.44	50.44	108.35	85.13	196.37	129.03
			Percentage			
1	100.00%	100.00%	100.00%	100.00%	100.00%	100.00%
2	80.17%	79.18%	75.39%	70.47%	87.74%	84.06%
3	67.82%	70.18%	62.09%	57.23%	69.54%	66.31%
4	40.54%	38.32%	59.73%	51.08%	57.19%	48.28%

343.35s even in the highest simulated demand level (See Table 3.6 in peak5400 case when number of cores=1). What is more, the computation time for the whole distributed process indeed decreases in tandem with an increase in the number of cores, as is illustrated in Table 3.6. It can also be inferred that when a computer server with more powerful computing capability is adopted, more time will be saved.

3.4 Conclusions

The study in this chapter contributed to the overall state-of-art by proposing a simulation-based DRG-SC method. Unlike the single centralized control system applied in most of the literature, the computational efficiency gained is more favorable and practically suitable in the application of large traffic networks. The developed model captured the natural relationship between DRG and SC, which has been overlooked in previous research. More importantly, the division and cooperation of work for the vehicle unit, infrastructure, and TMC described in this chapter can be easily transferred to similar distributed control problems. The overall study clarifies how MEC technology can make progress on the traffic operation and control problems for CAVs.

Firstly, for dynamic routing, the UO and SO targeted strategy were inves-

tigated that represented the system's achievable long-term performance and upper bound best performance respectively. The model looked into the delay caused by signal control to compute the travel time more precisely. From the case study, vehicles were noticed to re-route more frequently under higher demand cases. Moreover, the 'compliance rate' was defined to discuss the system performance, and as expected, it surpassed when more vehicles selected the SO-based routes; Secondly, since the proposed ASC strategy considered both vehicles' maximum waiting time and routing plans to decide the exact phase split and sequence, it was particularly effective in reducing delay and improving throughput. Finally, according to the computation time testing result, the capabilities of the distributed framework in enhancing computation efficiency is notable, which yet confirmed the necessity of disposing MEC in a CAV environment.

Looking ahead, an essential component to be considered is travel time prediction. With predicted travel time information, vehicles can avoid congestion by responding in advance, thereby improving system performance cooperatively instead of reactively on real-time information only.

Chapter 4

Distributed Back-Pressure Routing for CAVs

4.1 Introduction

As introduced in Chapter 3, Existing DRC solutions usually derive from a DUE or DSO model. DUE focuses on benefiting individual vehicles by guiding them to the shortest route using the Dynamic Shortest Path (DSP) algorithm. In practice, the DSP is widely utilized in popular route planners such as Google Maps and Waze. In research, the DSP is also applied in extensive papers for designing effective DRC strategies [15], [147], [148]. For instance, Chai et al. [15] proposed a dynamic traffic routing algorithm for CAVs that seeks the shortest path by looking up a real-time updating cost table. The researchers consider the impact of signal control, and their algorithm significantly reduces the average delay when tested in a simulated network. Mahajan et al. [149] designed a user equilibrium-routing strategy for CAVs by conducting a multi-agent control. Individual vehicles are smart enough to 'talk' with each other, anticipate future traffic dynamics, and make decisions. This study predicts travel time using neural networks, and vehicles choose the most beneficial route based on the predicted travel time. Since these studies characterize CAVs as selfish travelers without considering the behavior of others, they direct all vehicles with the same OD to the same shortest route. As a result, the solution based on DSP often results in unbalanced density over the network which may instead cause new congestion, especially in higher-demand cases.

Different from the DUE-based principle, the DSO assigns vehicles to routes that can achieve the best performance of the whole system where some vehicles may sacrifice to go to longer routes. This benefit of the DSO's better system performance is entirely achievable by CAVs when they travel cooperatively and follow strictly the given instructions, thus attracting the interest of traffic management and control agencies. Research inspired by the idea of DSO [150]–[152] is supported by the postulation that all CAVs will adopt the DRC strategy given by the system to achieve the best network performance. With this potential, Bagloee et al. [150] formulated a mathematical DRC model for mixed-traffic conditions where the non-CAVs travel along the shortest route and all CAVs follow the system's optimal route. Their model outperforms the single DUE-based model with respect to vehicles' average travel time. Du et al. [132] also proposed a coordinated online in-vehicle routing mechanism that balances DUE and DSO by information perturbation. Both systems and individual vehicles can benefit from the strategy even when vehicles make selfish route choices. Despite achieving excellent network performance, the problem in these DSO-based studies is formulated as complex non-linear programming models that are complicated to solve and costly to converge. For this reason, the DSO-based model has not been broadly applied in real-time CAV control cases so far.

As a matter of fact, both the DUE and the DSO models are solved in a centralized manner. In other words, the real-time information of all links over the network is required to update the travel cost for the studied route. That real-time data gathered from CAVs and intersections is sent to the cloud (i.e., TMC) to be processed, and the TMC is generally located far away from vehicles. Therefore, this type of centralized data processing framework costs significant amounts of communication time [153], which compromises the performance of the real-time route control.

The potential problems of centralized methods motivated the emergence of distributed DRC approaches. The MEC architecture introduced by the European Telecommunications Standards Institute (ETSI) has undoubtedly given rise to the possibility of a more efficient distributed DRC algorithm [154].

With increasing data storage, privacy concerns, and the need to reduce end-to-end delay and improve control performance, distributed DRC supported by the MEC framework is increasingly considered the better choice for CAVs.

However, despite the aforementioned advantages, the computational capability of the MEC is not as powerful as that of the TMC [141]. And, unlike the TMC which maintains global information of the whole network, only local information is available at the MEC. Considering such circumstances, a distributed DRC method that possesses low computational complexity and exploits only local information should be developed. Coincidently, the back-pressure (BP)-based principle appropriately fits the needs.

As introduced in chapter 2, the BP algorithm was initially developed by Tassiulas and Ephremides [76] for scheduling the data packets in wireless communication networks and it was widely utilized in the packet routing control [155], [156] to reduce the network congestion and improve throughput. The principle of BP is to define a function to measure the degree of occupation and direct data packets to those more vacant links. The algorithm incorporates the features of both distributed and feedback control, simple but flexible, making it also popular to be applied in many control systems (e.g., Piping systems and road traffic systems).

For the road traffic system, the BP has also gained attention in vehicle routing [87], joint signal control and routing problems [86], [89]. Representative studies applying the BP principle were summarized in Table 4.1, where the embedded network model, BP function, control effectiveness, and drawbacks were presented.

From the Table, most of the existing BP-based studies defined the BP function based on queue length. As a result, issues arise as the queues at each node need to be separated for different turning movements, and the embedded point queue model assumes an unrealistically infinite capacity of links. Thus, queue length-based BP application although can maximize the network throughput and stabilize the queue, may lead to traffic conservation failures and congestion propagation. To avoid the infinite queue length assumption, researchers further proposed travel time, virtual queue length, etc. as BP

Table 4.1: Comparison of BP utilized in different applications

Control objective	**Embedded model**	**BP function**	**Effectiveness (Y) and drawback (N)**	**Paper**
Packet routing control	Graph-based network model	Packet queue length	(Y)Maximizes throughput and stabilizes queues (N)Point queue assumption and the queuing system requires to be synchronized	Tassiulas and Ephremides [76]
Packet routing control	Graph-based network model	Packet queue length	(Y)Minimizes path length between origin and destination (N)Point queue assumption and increased delay under light traffic	Ying et al. [155]
Packet routing control	Graph-based network model	Link transmission rates	(Y)Reduces average packet delay especially for heavy traffic (N)Increases delay under light traffic	Gao et al. [156]
Signal timing control	Store-and-Forward Model	Queue length	(Y)Maximizes network throughput, stablizes queues (N) Unrealistic infinite capacity assumption	Varaiya [80] Kouvelas et al. [83]
Signal timing control	Cell-based flow model	Estimted queue length	(Y)Better than adaptive control even with only 10% penetration rate of CVs (N)Performance is limited by the control frequency	Li et al. [157]
Signal timing control	VISSIM-based simulation model	Cyclic and non-cyclic based queue length	(Y)Outperforms the actuated signal control (N)Point queue assumption	Sun and Yin [84]
Signal timing control	AIMSUN-based simulation model	Travel time	(Y)More effective than queue length-based BP control, especially for avoiding spillback phenomena (N)Lead to reduced average speed	Mercader et al. [158]
Signal timing control with adaptive routing	VISSIM-based simulation model	Virtual queue length	(Y)Shows good control performance in congested case (N)Point queue assumption and poor performance in light traffic	Zaidi et al. [86]
Signal timing control with adaptive routing	DSMART-based simulation model	Queue length and Travel time	(Y)Combined link and route pressure for signal control and routing respectively (N)Poor performance in light traffic	Kampen [89]
Vehicle route control	Discrete traffic flow model	Queue length	(Y)Considering individual satisfaction while aiming to achieve better system performance (N)Limited demand profiles were tested	Zhang et al. [87]

functions (Mercader et al. [158], Zaidi et al. [86], Kampen [89]), and the results turned out to be more effective and realistic when compared with those using queue length only. These BP functions can help to evenly distribute the demand among the links and improve network mobility. However, most of them were only effective in congested cases while showing poor performance in light traffic cases. To address the above issues, this chapter contributed in the following aspects:

I. A novel BP-based routing algorithm was proposed to deliver scalable and responsive DRC strategies: The proposed algorithm only relies on the real-time upstream and downstream traffic information as input so that it can be solved at the network edges without the data transmitted to the cloud. The communication latency and computing cost were significantly reduced, which is highly suitable for the MEC-enabled CAV controls.

II. Different from most BP-based applications, in the proposed algorithm, a new BP function was defined to avoid the unrealistic point queue assumption: Instead of using queue length, the ratio between real-time link density and jam density was utilized to calculate the BP. Furthermore, the proposed method pre-identifies the congestion degree of the network to determine whether re-routing is necessary which helps to improve the control effectiveness of the algorithm in low-demand cases.

III. The proposed algorithm performs better than DSP and can even compete with DSO in congested cases but the computational cost is far below the DSO: Verified by case studies, the presented algorithm outperforms DSP in average travel time, waiting time, etc. while can get a close performance of the system optimal state generated by the centralized DSO control. The developed algorithm is not intricate but effective, which is of great practical significance.

Table 4.2: Notations

N	Set of all nodes
L	Set of all links
R	Set of all routes
F	Set of all vehicles
I	Set of all signalized intersections
Ω_q	Set of all traffic streams
M	Set of all movements
τ	Time duration of each time interval
T	Maximum time horizon
Γ_{ij}^{-1}	Set of predecessor links of link ij
Γ_{ij}	Set of successor links of link ij
q_{ij}^t	Flow on link ij during time interval t
ρ_{ij}^t	Density on link ij during time interval t
v_{ij}^t	Average Speed on link ij during time interval t
L_{ij}	Length of link ij
${q_{in,ij}}^t$	Inflow of link ij during time interval t
${q_{out,ij}}^t$	Outflow of link ij during time interval t
${\gamma_{mi}}^t$	Turning ratios in the predecessor intersection m of intersection i
${Q_{ij}}^{q,t}$	The queue length for flow q on the upstream link ij within the time interval t
${Q_{jl}}^{q,t}$	The queue length for flow q on the downstream link jl within the time interval t
${BP_{[ij,jl]}}^{q,t}$	Backpressure of flow q going from ij to jl in time interval t
$q_{[ij,jl]}^{t*}$	Traffic stream with the highest backpressure
$w_{[ij,jl]}^t$	The weight of movement going from link ij to link jl in time interval t
r_f^{t*}	The optimal route (link set) for vehicle f in time interval t
${\rho_{ij}}^{jam}$	Jam density of link ij
$P_{[ij,jl]}^t$	Routing probability for movement from ij to jl in time interval t
ξ_{ij}^t	Binary variable, describing whether re-routing is conducted for vehicles on link ij in time interval t
x_{ij}^t	Real-time vehicle number on link ij in time interval t
$x_{\max,ij}$	The maximum vehicle number the link ij can bear
α	The proportion of the link to be occupied, $\alpha \in [0, 1]$

4.2 Methodology

4.2.1 Network Model

Define an arterial traffic network as a directed graph $G = (N, L)$, where N is the set of nodes and L is the set of directed links. A directed link from node i to node j is represented by ($ij \in L$); vehicles with the same OD constitute a traffic flow q, and the OD pair of flow q is denoted by $(o(q), d(q))$, where $o(q), d(q) \in N$. Eq. (4.1) describes the fundamental flow-density-speed relationship which ensures the flow ${q_{ij}}^t$ on a particular link ij during time interval t equals the product of time-dependent density ${\rho_{ij}}^t$ and speed ${v_{ij}}^t$ on link ij (t=1,2,.....,T. T is the maximum time horizon). Eq. (4.2) describes the flow conservation law, where L_{ij} is the length of link ij. $L_{ij}{\rho_{ij}}^t$ represents the total vehicle number on the lane during time interval t. It is an iterative variable which equals the summation of the number of vehicles on the lane during the last time interval $t-1$ and the difference between inflow and outflow accumulated during the time duration τ of each interval. In addition, the inflow should be part of the flow from its upstream links as shown in Eq. (4.3) where ${\gamma_{mi}}^t$ is the turning ratios in the predecessor intersections, and m is the index of the predecessor node of node i. The notations used in this section were given in Table 4.2.

$$ {q_{ij}}^t = {\rho_{ij}}^t \cdot {v_{ij}}^t, \quad \forall ij \in L; t = 1, 2, ..., T \tag{4.1} $$

$$ \begin{aligned} L_{ij}{\rho_{ij}}^t = L_{ij}{\rho_{ij}}^{t-1} + [{q_{in,ij}}^t - {q_{out,ij}}^t] \cdot \tau, \\ \forall ij \in L; t = 1, 2, ..., T \end{aligned} \tag{4.2} $$

$$ {q_{in,ij}}^t = {\gamma_{mi}}^t \sum_{mi \in \Gamma_{ij}^{-1}} {q_{out,mi}}^t, \quad \forall ij \in L, t = 1, 2, ..., T \tag{4.3} $$

4.2.2 Original Back-Pressure (OBP) Routing Algorithm

To explain the OBP routing algorithm, let ${Q_{ij}}^{q,t}$ be the queue length for flow q on the link ij within the time interval t, and ${Q_{jl}}^{q,t}$ be the queue length for the same flow q on its downstream link jl within the time interval t. From Athanasopoulou's work [77], the original back pressure of movement from link

ij to link jl is defined as (Eq. (4.4)):

$$BP_{[ij,jl]}{}^{q,t} = Q_{ij}{}^{q,t} - Q_{jl}{}^{q,t}, \quad \forall ij, jl \in L; t = 1, 2, ..., T \tag{4.4}$$

Use $q^{t^*}_{[ij,jl]}$ to denote the traffic stream with the highest backpressure, where Ω_q is the set of all traffic streams:

$$\begin{aligned} q^{t^*}_{[ij,jl]} = \arg\max_{q \in \Omega_q} \{Q_{ij}{}^{q,t} - Q_{jl}{}^{q,t}\}, \\ \forall ij, jl \in L; t = 1, 2, ..., T \end{aligned} \tag{4.5}$$

Then, the weight assigned for this stream $q^{t^*}_{[ij,jl]}$ is:

$$\begin{aligned} w_{[ij,jl]}{}^{t} = \max\{[Q_{ij}{}^{q^t_{[ij,jl]}{}^*,t} - Q_{jl}{}^{q^t_{[ij,jl]}{}^*,t}], 0\}, \\ \forall ij, jl \in L; t = 1, 2, ..., T \end{aligned} \tag{4.6}$$

A route is composed by a set of links that can be activated simultaneously. The optimal route (link set) for vehicle f during time interval t, $r^{t^*}_f$ is derived from the following equation, where R is the set of all candidate routes.

$$\begin{aligned} r^{t^*}_f = \arg\max_{r \in R} \sum_{(ij,jl) \in r} w_{[ij,jl],f}{}^{t}, \\ \forall ij, jl \in L; f \in F; t = 1, 2, ..., T \end{aligned} \tag{4.7}$$

4.2.3 Modified Back-Pressure Routing Algorithm (MBP)

Considering the disadvantages of the OBP based on queue length, the study proposed to define BP using the difference of the squared ratio of density and jam density of two adjacent links (Eq. (4.8)). This ratio can appropriately describe the degree of occupation for links and the square puts additional weight on links near jam conditions.

$$\begin{aligned} BP_{[ij,jl]}{}^{t} = \left[\frac{\rho_{ij}{}^{t}}{\rho_{ij}{}^{jam}}\right]^2 - \left[\frac{\rho_{jl}{}^{t}}{\rho_{jl}{}^{jam}}\right]^2, \\ \forall ij, jl \in L; t = 1, 2, ..., T \end{aligned} \tag{4.8}$$

Then, the weight of the traffic flow going from link ij to link jl changed accordingly:

$$\begin{aligned} w_{[ij,jl]}{}^{t} = \max\left\{\left[\frac{\rho_{ij}{}^{t}}{\rho_{ij}{}^{jam}}\right]^2 - \left[\frac{\rho_{jl}{}^{t}}{\rho_{jl}{}^{jam}}\right]^2, 0\right\}, \\ \forall ij, jl \in L; t = 1, 2, ..., T \end{aligned} \tag{4.9}$$

Additionally, the routing probability is adaptively updated by the multinomial logit model (Eq. (4.10)) rather than allowing all the vehicles to choose the

link with the highest BP.

$$P_{[ij,jl]}{}^{t} = \frac{e^{w_{[ij,jl]}{}^{t}}}{\sum_{[ij,jl]\in M} e^{w_{[ij,jl]}{}^{t}}}, \forall ij, jl \in L; t = 1, 2, ..., T \tag{4.10}$$

4.2.4 Modified Back-Pressure Routing Algorithm with Congestion Identification (MBP+CI)

According to the calculation above, the probability of vehicles being routed to links with higher pressure is always greater than those with lower pressure. When the link congestion level is low, the algorithm may cause unnecessarily longer routes. In fact, the best route for vehicles should initially be the static shortest route during cases without congestion. For that reason, a binary variable $\xi_{ij}{}^{t}$ is adopted to determine whether to carry out the MBP re-routing control. At every time interval, the real-time traffic state is acquired and, only when the obtained number of vehicles on the link exceeds a particular threshold, the re-routing process is conducted. Here, the threshold was defined as α multiplied by $x_{\max,ij}$, the maximum vehicle number the link can bear, as shown in Eq. (4.12), where the value of α ranges from 0 to 1, representing the proportion of the link to be occupied.

$$\xi_{ij}{}^{t} = \begin{cases} 0, & x_{ij}{}^{t} < x_{threshold,ij} \\ 1, & x_{ij}{}^{t} \geq x_{threshold,ij} \end{cases}, \quad \forall ij \in L; t = 1, 2, ..., T \tag{4.11}$$

$$x_{threshold,ij} = \alpha \cdot x_{\max,ij}, \alpha \in [0, 1]; ij \in L; \tag{4.12}$$

The procedure of the MBP+CI algorithm is summarized in Table 4.3.

4.2.5 Dynamic Shortest Path (DSP) and Dynamic System Optimal Assignment (DSO)

The DSP and DSO control serve as comparison benchmarks. In this chapter, the average travel time on links is calculated using the link length divided by the real-time mean speed. Additionally, apart from the average travel time on links, the delay at intersections caused by the signal control was particularly considered. Then, the route with the shortest travel time for a traffic

Table 4.3: Procedure for the MBP+CI algorithm

Input	Network topology, demand, signal control parameters; The number of vehicles on adjacent links of intersection i; The set of all candidate routes of each specific vehicle f;
Output	The routing probability ${P_{[ij,jl]}}^t$
Step 1	Get the set of downstream links of the current link ij, Γ_{ij}
Step 2	Get the subset of Γ_{ij} as $S\Gamma_{ij}$, where the candidate routes of vehicle f are included;
	For $jl \in S\Gamma_{ij}$:
Step 3	Get the real-time vehicle number ${x_{ij}}^t$, the density ${\rho_{ij}}^t$, ${\rho_{jl}}^t$ on links;
	If ${\xi_{ij}}^t = 0$, ${x_{ij}}^t \leq x_{threshold}$:
Step 4	Keep the original route of vehicles;
	Else:
Step 5	Calculate the pressure ${BP_{[ij,jl]}}^t$ between link ij and link jl;
Step 6	Determine the weights: $${w_{[ij,jl]}}^t = \max\left\{\left[\frac{{\rho_{ij}}^t}{{\rho_{ij}}^{jam}}\right]^2 - \left[\frac{{\rho_{jl}}^t}{{\rho_{jl}}^{jam}}\right]^2, 0\right\}$$
Step 7	Calculate the routing probability ${P_{[ij,jl]}}^t$;
Step 8	Choose the next link based on ${P_{[ij,jl]}}^t$;
	End
	End

stream can be searched by the Dijkstra algorithm. The analytical DSO model is hard to solve, and in our study, the DSO was formulated and solved in a simulation-based manner. A quadratic fitting was utilized to find the relationship between travel time and traffic volume, and the shortest marginal travel time was derived based on this relationship as introduced in chapter 3. After that, the shortest marginal travel time route is searched for solving the DSO. Details for the formulation and solution of both DSP and DSO can be found in [37], [38].

4.3 Case Study

The algorithm was tested in SUMO and during the simulation, the re-routing policies were updated every 90s. During each interval, Python acquired the real-time data from SUMO to process and solve the corresponding DRC model to find the next optimal link to go. The solution was conversely imposed on the vehicles to change their route, and this procedure was repeated until all vehicles left the network.

4.3.1 Testing Network

Two networks were simulated to evaluate the effectiveness of the proposed algorithm.

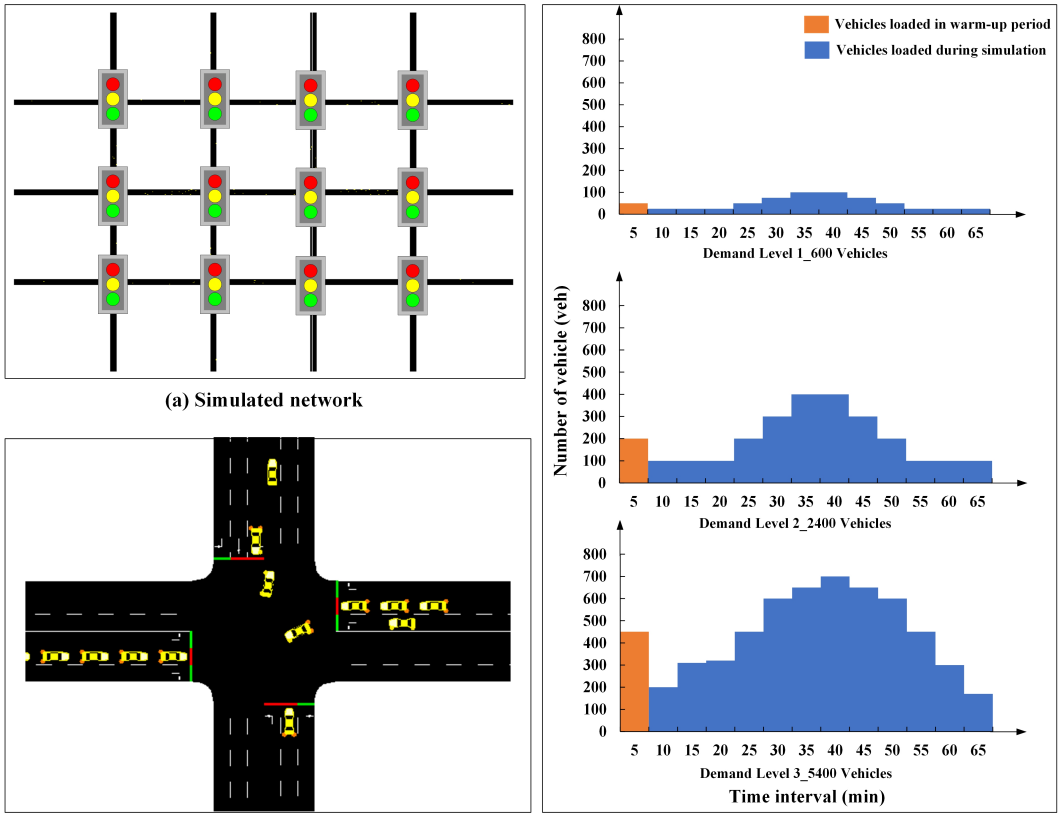

Figure 4.1: Testing network 1 and demand profile

1) Testing network 1: A three-by-four grid network (Fig. 4.1 (a)) with 12 signalized intersections (as illustrated in Fig. 4.1 (b)) served as testing network

1. There were 62 links in total, with a speed limit of 50km/h and each link was 300 meters long. Moreover, each link had three lanes for left-turn, through and right-turn movements, respectively. The signal timing plan was fixed and determined in advance according to the demand.

Three different demand levels were tested, as outlined in Fig. 4.1(c). The demand was loaded in the first simulation hour, during which the vehicles were generated every five minutes. What is more, there was a five-minute warm-up duration before the start, and a particular demand of vehicles was fed to the simulation so that the network could be reasonably occupied. Then, 600, 2,400, and 5,400 tagged vehicles were loaded for demand levels 1, 2, and 3 corresponding to free flow, moderately occupied and congested road traffic conditions. The distribution of the OD demand was asymmetrically generated over the network so that the flow patterns were different for distinguished links.

2) Testing network 2: The larger and more complex downtown area of Edmonton, Canada was utilized as the testing network 2 (as shown in Fig. 4.2) which provides enough routing possibilities for further verifying the algorithm performance. The detailed information (e.g., number of lanes, lane length, speed limit, type of control for intersections) was built according to the field condition. Most of the link length is less than 150 meters and there are 234 links and 79 nodes in total where 43 nodes were controlled by a signal. Similarly, three demand levels were tested still correspond to free-flow, moderately occupied, and congested networks with 3,000 vehicles, 9,000 vehicles, and 12, 000 vehicles loaded for demand levels 1, 2, and 3. The demand loading pattern and re-route settings were similar to that in testing network 1.

4.3.2 Overall Performance

In the simulation, four different control strategies (i.e., the DSP, DSO, MBP and MBP+CI) were compared, and the corresponding results were discussed. For the MBP+CI control, the α was set to 0.5, and the sensitivity analysis of the α value will be given at the end of this Section. As outlined in Table 4.4, four performance metrics, including vehicles' Average Waiting Time (AWT),

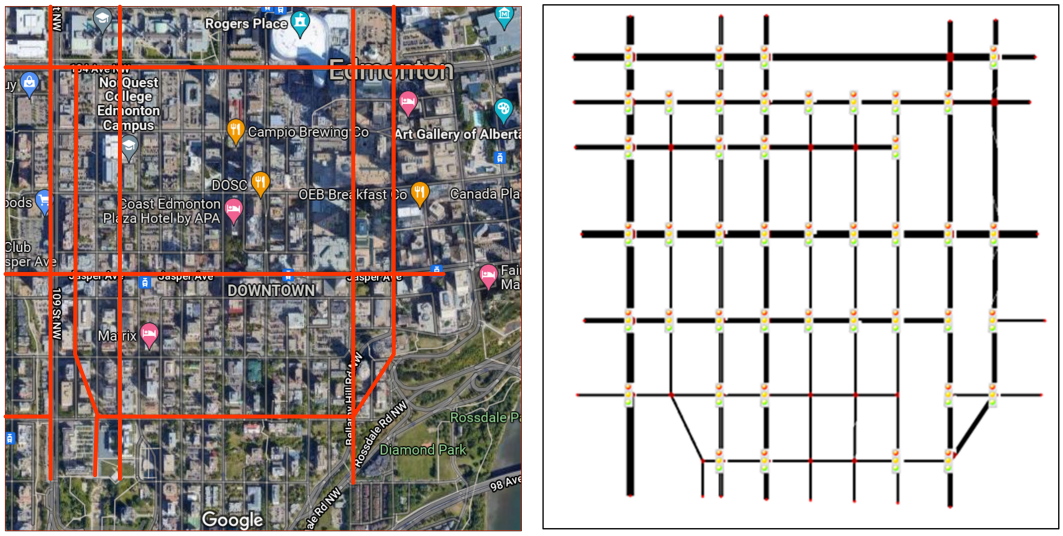

(a) Edmonton downtown area in Google Map

(b) Edmonton downtown aera simulated in SUMO

Figure 4.2: Testing network 2-Edmonton downtown area

Average Travel Time (ATT), Average Departure Delay (ADD) and Average Speed (AS), were adopted to measure the effectiveness of these methods. AWT and ATT were defined as standard, while ADD represented the time difference between the vehicle's scheduled departure time and its real departure time. AS only counted the speed values larger than zero. As expected, when the network was less congested, the value of AWT, ATT and ADD would decrease while the value of AS would increase.

In Table 4.4, the effectiveness of the control methods was represented by the number of stars, with one being the worst and five being the best. No matter for testing network 1 or network 2, in demand level 1, the performances of the DSO and DSP are close in value since, in free-flow cases, the dynamic shortest path or dynamic marginal shortest path is the same as the static shortest path. However, the performance deteriorated when the MBP was applied. All four metrics worsened compared to those with DSP control. Basically, the MBP algorithm is a greedy searching algorithm because it only considers the first link of the route when computing the BP. In free-flow conditions, the network performance can be good enough when vehicles follow the pre-defined static shortest path, and almost no congested links can be further improved by re-routing. In this case, applying the MBP algorithm may in-

Table 4.4: Performance of different control strategies

			AWT (s)	ATT (s)	ADD (s)	AS (km/h)	Effectiveness
Testing Network 1	Demand Level 1 (Free flow)	DSP	92.11	226.15	6.17	36.79	****
		MBP	127.93	297.17	6.19	36.54	*
		MBP+CI	92.15	229.42	6.18	36.65	**
		DSO	89.36	207.77	6.17	36.82	*****
	Demand Level 2 (Moderately Occupied)	DSP	169.54	325.67	14.28	29.77	*
		MBP	159.21	309.32	14.22	30.68	**
		MBP+CI	121.40	253.29	14.15	33.49	***
		DSO	100.48	214.93	14.06	35.11	*****
	Demand Level 3 (Congested)	DSP	530.45	736.07	24.62	19.84	*
		MBP	305.82	458.57	21.74	26.71	***
		MBP+CI	163.82	300.67	21.08	29.84	****
		DSO	149.34	271.00	21.34	33.34	*****
Testing Network 2	Demand Level 1 (Free flow)	DSP	65.42	188.25	4.56	36.84	****
		MBP	77.64	198.59	6.37	36.16	*
		MBP+CI	72.42	191.23	5.48	36.46	**
		DSO	60.73	177.75	4.25	36.91	*****
	Demand Level 2 (Moderately Occupied)	DSP	275.81	443.78	13.37	30.04	*
		MBP	206.59	331.95	11.38	31.85	**
		MBP+CI	164.72	298.66	10.92	32.74	***
		DSO	112.04	222.49	8.77	33.15	*****
	Demand Level 3 (Congested)	DSP	623.59	802.89	22.74	20.12	*
		MBP	347.13	548.95	15.22	21.49	***
		MBP+CI	329.26	502.37	14.47	23.06	****
		DSO	265.64	398.20	13.53	24.33	*****

stead guide some vehicles to unnecessarily longer routes and result in inferior network performance. Thus, although the proposed MBP+CI algorithm still demonstrated poorer performance than the DSP, it performed better than the MBP because the added constraint that only when the link was identified as congested, the re-routing process was conducted.

The situation has changed in higher demand cases (demand level 2 and especially demand level 3). The DSP algorithm was no longer as effective as it was in free-flow conditions. Both MBP and MBP+CI outperformed the DSP. In demand level 3, when the whole network is congested, the superiority of the MBP+CI is more pronounced, with significant improvement on all performance metrics, becoming even comparable to the DSO. This level of performance also indicates the potential of the proposed method to achieve system optimal with local information.

To further explore the algorithm performance, the Macroscopic Fundamental Diagram (MFD) analysis and the Queuing analysis were also conducted where the testing network 1 was chosen as an example.

4.3.3 MFD Analysis

The MFD was initially formalized by Daganzo [159] describing the relationship between the aggregated flow along all the links in the network (i.e., production or flow) and the total number of vehicles in the network (i.e., accumulation or density). The MFD can considerably relieve the understanding of complex traffic phenomena and is thus widely adopted to analyze diverse traffic control measures [160]. Fig. 4.3 draws the relationship between the network production and accumulation for different demand levels and control scenarios. From the scatter plot of demand level 1 in Fig. 4.3(a), although these dots

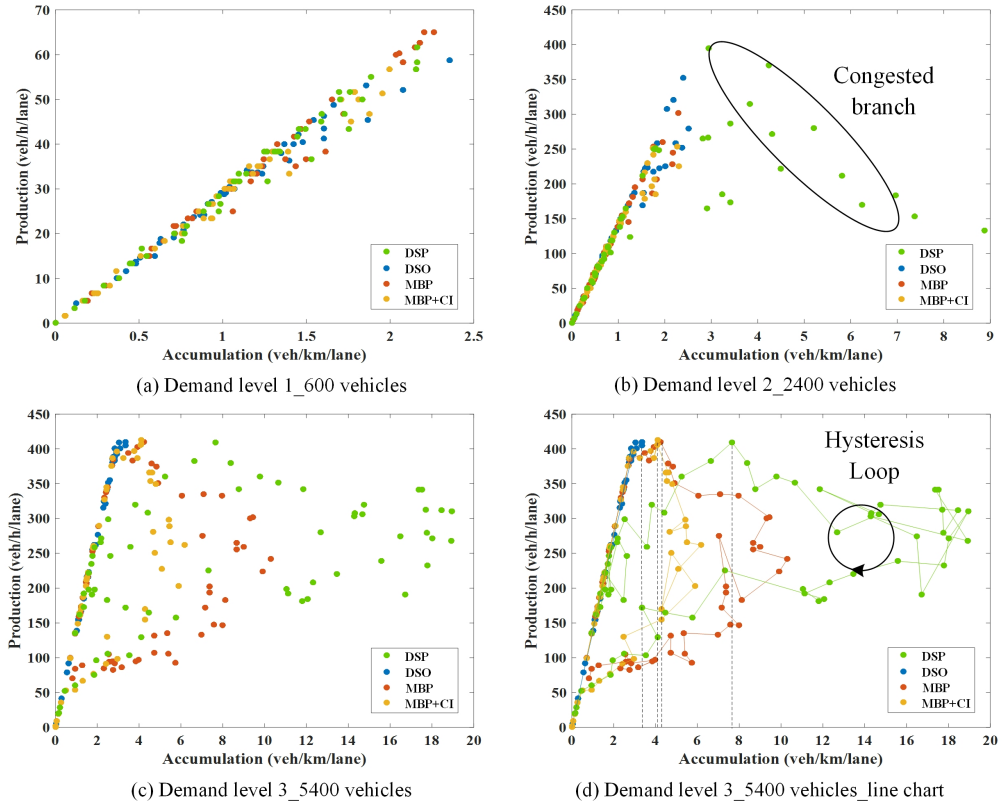

(a) Demand level 1_600 vehicles

(b) Demand level 2_2400 vehicles

(c) Demand level 3_5400 vehicles

(d) Demand level 3_5400 vehicles_line chart

Figure 4.3: Relationship between network production and accumulation

are spread out within a certain region, they are sparse in higher-density places while dense in lower-density regions. There is little difference between the MFD of different control methods, and none of them has a congested branch. However, in demand level 2, an inverse-U shape of MFD was obtained; A congested branch appeared when the DSP control was applied but disappeared

for the other three control strategies. Furthermore, the performance of the other three methods also seems similar.

In demand level 3, in addition to the scatter plot, the line chart was also given in Fig. 4.3(d) to better illustrate the MFD patterns. Under this demand level, the other three control methods possessed a congested branch other than for the DSO control. Moreover, the network production was consistently higher during the onset of congestion than during the dissipation of congestion. In other words, the relationship between network production and accumulation exhibits prominent clockwise hysteresis loops. This phenomenon is caused by the uneven demand distribution and the naturally occurring instabilities when the network is congested [161]. Yet, the critical density evidently moves to the left (i.e., lower value) region when the MBP and MBP+CI methods were applied compared to the DSP, demonstrating a decrease of congestion on the links. As for the network outflow, the critical point for demand levels 2 and 3 had a comparable value at around 400 veh/h/lane. However, it is noted that the value in demand level 1 was much lower than the other two demand levels which is caused by the under-utilization of the road capacity in free-flow conditions.

4.3.4 Queueing Analysis and Congestion Pattern Visualization

Fig. 4.4 illustrates the evolution of average queue length and congestion heatmap under different control methods. In all three demand levels, the queue length value changed principally according to the demand loading profile. However, the figures demonstrate a periodic increase and decrease trend with the drastic ups and downs for demand levels 1 and 2. This phenomenon is because most of the queues that accumulated during the red signal can be discharged during the following green, and new vehicles can enter the lane in the next time interval. Nonetheless, the line becomes smoother in demand level 3 since only a few queued vehicles can be served within each time interval.

The congestion pattern of the network under demand level 3 with different control methods was also visualized in Fig. 4.4(d). The average volume under

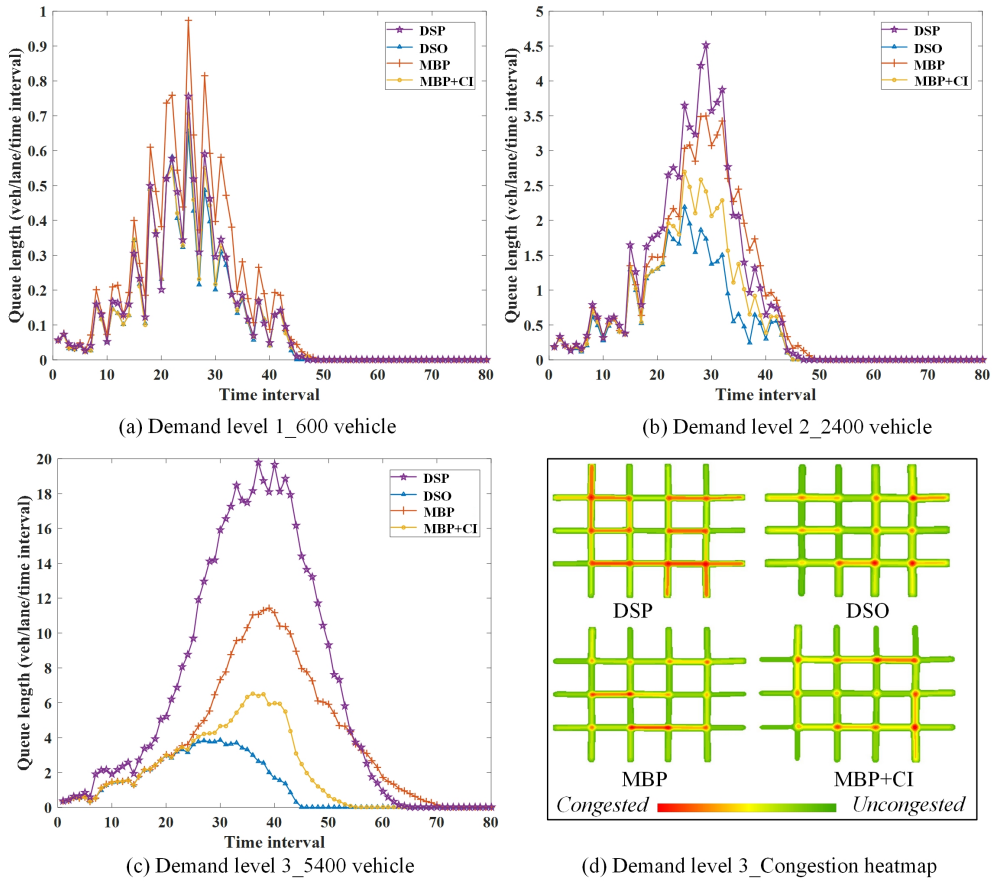

Figure 4.4: Vehicle queueing for different demand levels and congestion heatmap under different control

each control strategy was adopted as weight to draw the congestion heatmap. The network under the DSO routing strategy is unimpeded. Moreover, since the proposed MBP and MBP+CI routing algorithm can not only push vehicles toward less congested links but also keep vehicles from moving to those congested links, the traffic flow under the BP-based methods demonstrates a more uniform pattern than under the DSP control.

4.3.5 Sensitivity Analysis of Parameter α

As stated in Section 4.2, the drawback of the MBP algorithm is that some vehicles may be guided to unnecessarily longer routes especially when they are traveling on uncongested links. Hence, the improvement of the MBP+CI algorithm over the MBP algorithm is clarified here, i.e., the MBP algorithm

will only be applied provided that the number of vehicles on the link exceeds the threshold. In Eq. (4.12), the MBP+CI algorithm is equivalent to the MBP when $\alpha = 0$, since the number of vehicles on links will always be larger than or equal to 0 (${x_{ij}}^t \geq 0$ always holds). Along with the increase of α , the MBP algorithm will be specifically applied to links with a certain number of vehicles that exceeds the threshold, while for those with a vehicle number lower than the threshold, the re-routing process will not be applied, and consequently, the vehicles will obey the initially static shortest path.

To investigate the impact of α on the control performance, the ATT was calculated in testing network 1 under MBP+CI control using different α values. The results were compared with the other three control methods and illustrated in Fig. 4.5.

In demand level 1 (Fig. 4.5(a)), the free flow case, the MBP, and MBP+CI control were worse than the DSP and DSO control. Essentially, since there's no congestion happening, the static shortest path is sufficient for achieving the best system performance. In this case, the static shortest path, the DSP, or even the DSO shows comparable control effectiveness. However, when applying MBP+CI, with the increase of α , the ATT was reduced compared with MBP because many unnecessary re-routing has been avoided. That is why we can see a decreasing trend of the ATT in Fig. 4.5(a) from $\alpha = 0$ to $\alpha = 0.6$. When $\alpha > 0.6$, since only very few links can reach the re-routing threshold, most of the vehicles will not be re-routed but just obey the static shortest path, resulting in a very close ATT value with the DSP control.

For the moderately occupied case in demand level 2 (Fig. 4.5(b)), when the value of α is relatively low (≤ 0.5), the MBP+CI can also reduce the ATT compared with the MBP control. However, when $\alpha \geq 0.6$, the ATT begins to increase since the high threshold limited many vehicles to be re-routed. When $\alpha \geq 0.8$, the performance was even worse than the DSP control since most of the vehicles hadn't been re-routed. This is different from the free flow case. When the network is moderately occupied, if no re-routing was conducted, vehicles obeying the static shortest path will fail to adapt to the real-time traffic condition and lead to higher travel time.

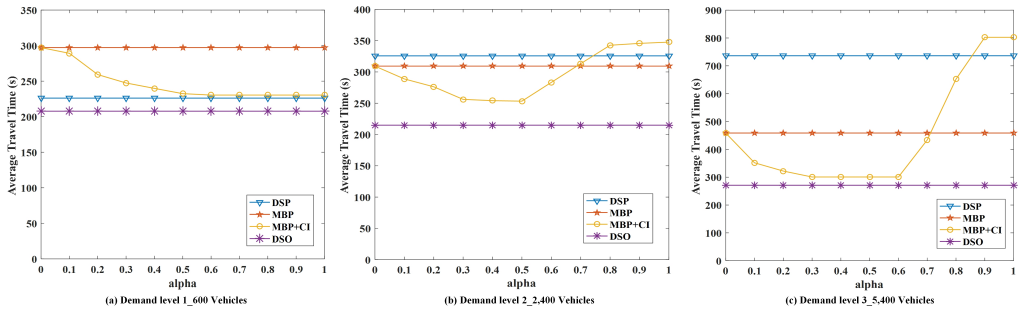

Figure 4.5: Average travel time with different values (a) Demand level 1-600 Vehicles (b) Demand level 2-2,400 Vehicles (c) Demand level 3-5,400 Vehicles

In demand level 3 (Fig. 4.5(c)), the congested case, the overall trend is similar to that in demand level 2. Nevertheless, in such a congested case, the performance of the MBP+CI is better than the DSP until $\alpha \geq 0.9$. That is because most of the links were occupied to a higher extent, when $\alpha = 0.7$ or $\alpha = 0.8$, a majority of the vehicles can still be effectively re-routed.

Overall, to guarantee the MBP+CI control performance, the value of α cannot be too small or too large. Although in different demand cases, the best value of α is different ($\alpha \geq 0.5$ for demand level 1; $0.3 \leq \alpha \leq 0.5$ in demand level 2; $0.3 \leq \alpha \leq 0.6$ in demand level 3), a value of 0.5 or 0.6 is generally a good choice. In specifc networks, the best value of α can be designed according to the exact demand level and demand loading patterns. With an appropriate design of the α value, the proposed algorithm can always generate a good control performance using local information to compete with the DSO control.

4.3.6 Communication and Computation Cost

Having presented the performance of the proposed method in mitigating traffic congestion and improving efficiency, this Section discusses the related communication and computation costs of these methods to determine the feasibility of applying the proposed approach to the MEC-enabled CAV environment.

First, the Time-Complexity, which describes the computer time it takes to run the algorithm, was analyzed for all methods. The complexity of DSP is $O(N^2, F, T)$, where N is the number of nodes over the network, F is the

number of vehicles and T is the total number of control intervals. The DSO is more complex than the DSP since it considers the converged case. The complexity of the DSO is $O(N^2, F, T, I)$, where I represents the number of iterations. It is apparent that when the traffic demand (F) becomes higher and the network becomes larger (N), the computation complexity of both the DSP and DSO would increase exponentially and be difficult to solve within a polynomial-time range. For the MBP and MBP+CI, on the other hand, the corresponding algorithm complexity is $O(N, F, T)$, which is a linear operation and can be solved rapidly even in large networks. Table 4.5 illustrated the algorithm execution time of different methods. It is obvious that the MBP and MBP+CI outperformed the other two algorithms.

Table 4.5: Execution time of different algorithms

		DSP[s]	DSO[s]	MBP[s]	MBP+CI[s]
Testing network 1	Demand level 1	13.77	18.58	12.40	12.57
	Demand level 2	42.02	95.29	22.32	26.97
	Demand level 3	143.74	511.59	34.72	42.47
Testing network 2	Demand level 1	155.76	170.72	149.12	153.46
	Demand level 2	428.11	569.22	198.77	216.83
	Demand level 3	635.58	1467.04	237.03	244.68

In a real CAV environment, a successful control process includes model calculation and solution communication. The radar chart in Fig. 4.6 compares the total time cost for a complete process using the four different control methods. The time is divided into five parts:

1) Connection set up time (CSUT): CSUT is the preparation time before control commences ensuring all the necessary utilities are successfully connected. This time cost is low, and it is the same for all the control methods.

2) Input data transmission time (IDTT): IDTT represents the time to transfer the original data precepted by the CAVs to the computing server. The DSP and the DSO require the data for the whole network to search for the optimal route. Thus, data from all CAVs must be sent to the TMC for processing, with a significantly high time cost. The MBP and MBP+CI require

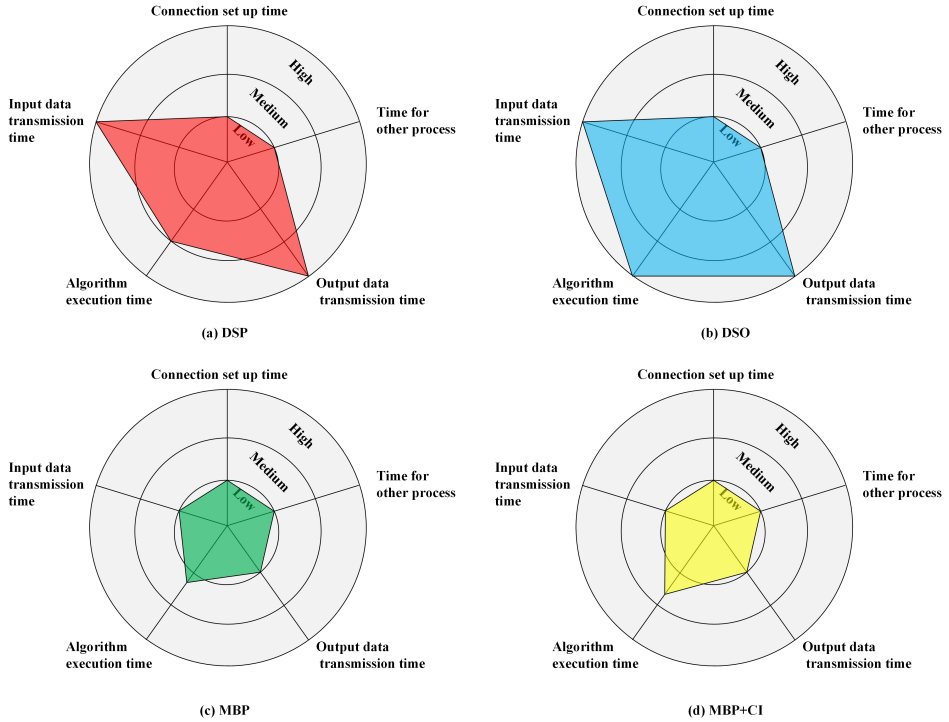

Figure 4.6: Time cost comparison of different DRC strategies to be applied in a real CAV environment

only upstream and downstream information, and the MEC manages the input data. The resulting IDTT for the MBP and MBP+CI would be notably lower than the DSP and DSO.

3) Algorithm execution time (AET): AET represents the time needed to execute the corresponding algorithms that generate output when the input data is ready. This is the time illustrated in Table 4.5. It is worth noting that since the MBP and MBP+CI algorithms are designed in a distributed manner, the computation tasks can be divided and run in parallel by several servers similar to the comparision in the last Chapter, which can further reduce the AET for MBP and MBP+CI.

4) Output data transmission time (ODTT): ODTT is similar to IDTT, which is the time to communicate the output DRC strategy to CAVs. The MBP and MBP+CI that are solved at the MEC are still dominant for the ODTT.

5) Time for other processes (TOP): TOP is the time for any other necessary processes. This time cost is also low and the same for all the control methods.

4.3.7 Scalability

In general, the scalability of a control method is determined by the input data collection and the algorithm solving manner. For centralized DRC methods, the input data of the entire network needs to be sent to the TMC, and the algorithm can only be executed with all these data ready. In addition, as analyzed above, the computational cost has an exponential relationship with the vehicle number and the network scale. As a result, they cannot even find a feasible solution within a polynomial-time range when applied to a large network. In this case, the scalability is very low.

Different from the centralized DRC approaches, the proposed method in this Chapter applied a distributed manner for both collecting data and solving the DRC problem, and the distributed control manner is inherently scalable. The scalability of our method mainly depends on the definition of the BP function. To analyze from Eq. (4.8), the calculation of the BP only related to the real-time density of the studied intersection and its downstream intersections, and the routing strategy was directly determined by the BP value. In other words, the solution of the routing strategy can be independently obtained from the MEC server at each intersection with the data from neighboring intersections. Therefore, the data processing and computation are independent of the network scale, and the scalability of the proposed method is in plain sight.

4.4 Conclusions

This chapter developed a novel distributed DRC algorithm that can be appropriately applied to the MEC-enhanced CAV environment based on the idea of BP routing. The algorithm aims to provide CAVs with reliable and prompt routing advice to achieve more efficient traffic circulation. Unlike the traditional DSP or DSO routing strategies, the algorithm relies on local information only. It identifies congestion and computes the routing probability according to the pressure calculated by real-time traffic density.

The study investigated the performance of the proposed algorithm through case studies conducted in SUMO. The proposed algorithm outperformed the

DSP for improving traffic efficiency, especially in higher demand cases. The MFD was applied to analyze and help understand the network performance under different control strategies. The result demonstrated that the proposed algorithm can effectively mitigate congestion, as illustrated by the dots in the MFD moving from the high-density region to the low-density region. Although the performance of the proposed distributed algorithm is not as good as the centralized method, the gap between the MBP+CI and the DSO is relatively small. However, the proposed method's reduced communication and computation cost over the DSO more than compensates. Overall, the proposed distributed DRC method turns a global routing decision into a set of local decisions, and the whole research work showcases the potential of distributed DRC algorithms to be deployed within a real MEC environment.

Chapter 5

Leveraging Dynamic Right-of-Way Allocation and Tolling Policy for CAV Dedicated Lane Management

5.1 Introduction

As mentioned in Chapter 2, the technology of CAV has achieved remarkable milestones [162]. The CAV technology has gained strong momentum due to its potential benefits in improving traffic safety and efficiency [163]. The reliable wireless communication between CAVs enables them to operate safely with a shorter headway among two consecutive vehicles, thus increasing average speed, saving energy, and reducing emissions.

A great number of publications have studied the impact of CAVs on the road or intersection capacity using either analytical or simulation models [164]–[166]. Among these, Levin and Boyles [166] have developed a multi-class car-following model that has been widely utilized in the studies of road capacity analysis under a mixed traffic environment. Based on their model, the fundamental diagram under different CAV penetration rate (PR) cases is drawn and illustrated in Fig. 5.1. The figure has demonstrated that the road capacity and wave speed can be significantly enhanced along with the increase of CAV PR.

The potential benefits of CAV have attracted researchers not only in the

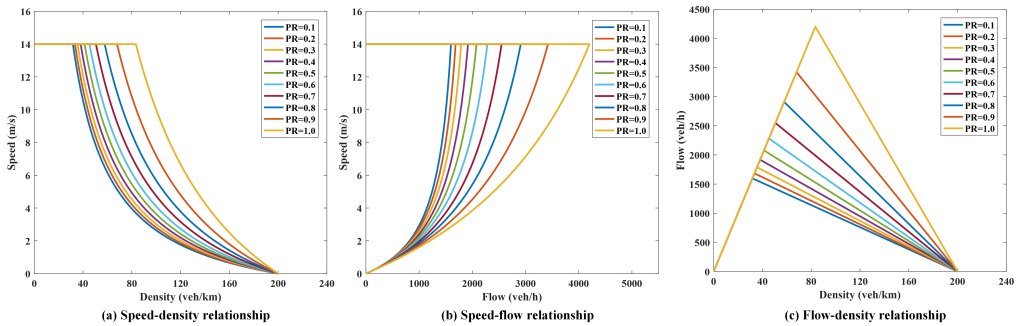

Figure 5.1: Fundamental diagram in a mixed traffic environment under different PR cases (**Parameter settings: Free flow speed is 14 m/s, vehicle length is 5 meters, reaction time of CAVs and HDVs are 0.5s and 1.0s respectively).

academy but also in industry. Several internet enterprises and automakers (e.g., Google, Baidu, Audi, Ford, etc.) have been actively launching and testing their CAV prototypes. Furthermore, many countries all over the world have legalized the testing of CAVs on public roads. However, in the early stage of the CAV deployment, the CAV, and HDVs will coexist for a long time [167]. This mixed traffic environment in the transition period makes it hard for CAVs to give full play to their advantages. The reduced headway of CAVs is usually limited by the longer reaction time of HDVs which is a knotty but inevitable problem.

As introduced in Chapter 2, the CAV dedicated lanes (CAV-DLs) were proposed to solve the above issue which tries to physically separate CAVs and HDVs and achieve the goal of improving the road capacity utilization. However, according to the literature review, most existing research on CAV-DLs' management stays more at the theoretical level, and only a few of them have presented a detailed control strategy.

Jiang and Shang [168] proposed a dynamic CAV-DLs allocation method with the joint optimization of signal timing and vehicle trajectory. The CAV-DLs will be utilized as GLs when they are vacant, and the GLs can also be turned into CAV-DLs when there are fewer HDVs but more CAVs. The idea is innovative but hard to implement since the operation of CAV-DLs requires support from specific communication and computation equipment that may not be installed in the GLs. Shao et al. [169] developed a more sophisticated

CAV-DLs control model that optimized the utilization of the CAV-DLs. The control strategy was highly dependent on the accurate monitoring of the lane occupancy rate. Although their simulation results appropriately demonstrated the effectiveness of their control model, the real-time prediction of the CAV occupancy on the dedicated lanes was not sufficiently described.

As a matter of fact, to improve efficiency and promote the adoption of CAVs, efforts on both the technical level and policy levels are of critical importance. Another efficient lane management approach is invigorated from the economics, which maximizes the network performance through road pricing policy. In general, the first type of pricing strategy was developed upon the fundamental economic principle of marginal cost, where the tolling rate on the road would be equal to the marginal travel cost caused by the new unit of traffic flow [170], [171]. The second type of tolling method charges travelers only on some restricted links or zones to realize certain objectives [172] (e.g., ensure equity [91], minimize emission [173], maximize revenue [174]). The second type of tolling policy was more practical and easier to deploy. Principally, the toll policy for mixed traffic with CAV-DLs is to grant free access to CAVs for traveling on the dedicated lanes while allowing HDVs to use the dedicated lanes by paying a toll. These tolls can serve as revenue and be split between companies and the city. In this regard, the tolls will aid in funding the infrastructures and incentivizing users to shift to CAVs which should eventually help to reduce emissions and improve mobility.

The idea of CAV toll lanes is derived from the HOV and HOT (High-occupancy-toll) lanes [175]–[177]. Motivated by this concept, Liu and Song [163] established a bi-level optimization model for the CAV toll lane deployment and solved the optimal toll value for HDVs on each dedicated lane. The results based on two simulated networks illustrated that the system's performance can be significantly improved through the deployment of a CAV toll lane. Based on the CAV toll lane proposed by Liu and Song [163], Wang et al. [178] further designed the optimal toll rate for HDV flows with an improved mixed traffic flow model. Although the analytical model developed in their study captures the elasticity of the traffic demand for vehicles in response to

the tolls, the optimization process is far from practical application due to its high complexity.

To briefly summarize, although the CAV-DLs management strategy has attracted many researchers, the fine-grained prediction of real-time CAV occupancy on the dedicated lane was not well addressed in the state-of-art literature. Accurate prediction of the capacity utilization on the CAV-DLs is necessary to further improve the effectiveness of the dynamic allocation algorithm. Moreover, for the CAV-DLs tolling policy, the toll rate stays the same for each dedicated lane whenever the HDVs enter, which cannot be flexibly adjusted according to the real-time congestion conditions. Furthermore, a systematic analysis and comparison of the advantages and disadvantages of different lane management strategies as well as their implementation rules were lacking. As such, this chapter contributes in threefold:

I. A dynamic right-of-way allocation approach is proposed to improve the capacity utilization rate of the CAV-DLs. The traffic flow on the dedicated lane during each cycle is predicted by a Kalman Filter-based [179]–[181] method, which can help better determine the lane occupancy in the next time interval and further enhance the control effectiveness.

II. A dynamic tolling strategy has been designed to allow HDVs to use the CAV-DLs. Different from existing tolling schemes, the toll rate here is calculated in real-time and changes accordingly with the travel time difference between the CAV-DLs and the GLs. The tolling rule is more realistic and straightforward to implement.

III. The two proposed lane management strategies can tremendously improve traffic efficiency, especially in low PR cases, and they can be easily applied to any other network. The strengths and weaknesses of the two schemes are comprehensively compared and analyzed, with suggestions given from both the technical and policy implementation points of view. The contents presented herein can benefit both traffic policymakers and practitioners in promoting the adoption of CAVs.

5.2 Methodology

5.2.1 Problem Formulation

This section introduces the mathematical formulation of the proposed CAV-DLs management problem, with the primary objective of minimizing the total travel time through optimized traffic flow on both CAV-DLs and GLs. To reach the goal, two specific strategies were elaborated: Dynamic Right-of-Way Allocation and Tolling. The Dynamic Right-of-Way Allocation method is initially presented, starting with an explanation of its fundamental rules. Subsequently, a Kalman-filter-based estimation model is described, which plays a crucial role in predicting traffic flow to determine the right-of-way. The second strategy, Tolling, is then elaborated upon. The procedures for computing the tolling are outlined, providing insights into how this approach complements the overall management strategy. Related notations used in this chapter were given in Table 5.1.

To present the model, firstly, an arterial traffic network was defined as $G = (N, A)$, where N is the set of nodes and A is the set of directed links. A directed link is formed by CAV-DLs and GLs, where the set of CAV-DLs is denoted as $\overline{A}$, and the set of GLs is defined as $\widetilde{A}$, satisfying $\overline{A} + \widetilde{A} = A$; Vehicles with the same OD constitute a traffic flow q, and the OD pair w of flow q is represented by $q^w(w \in W)$. The objective function is formulated in Eq. (5.1), which equals the summation of travel time on both CAV-DLs and GLs.

$$\min F(X) = \sum_{\overline{a} \in \overline{A}} t_{\overline{a}}(x_{\overline{a}}) x_{\overline{a}} + \sum_{\widetilde{a} \in \widetilde{A}} t_{\widetilde{a}}(x_{\widetilde{a}}) x_{\widetilde{a}} \,, (\overline{a} \in \overline{A}, \widetilde{a} \in \widetilde{A}) \tag{5.1}$$

Eq. (5.2) denotes the travel cost on lane a. VOT_m represents the value of time for different types of vehicles, m is the vehicle type, t_a is the travel time on lane a which is a function of the lane flow x_a, and $\tau_{m,a}$ is the toll on the CAV-DLs. By multiplying the VOT_m with the travel time, the unit of travel time and toll are converted to both be in dollars. This allows them to have the same unit and order of magnitude, enabling straightforward addition. For CAVs,

Table 5.1: Notations

N	Set of all nodes
A	Set of all links
W	Set of all OD pairs
$\overline{A}$	Set of CAV-DLs
$\widetilde{A}$	Set of GLs
R	Set of all routes
T_k	Set of study time intervals
q	Flow index
w	OD pair index
a	Lane index
m	Vehicle type index
r	Route index
$\tau_{m,a}$	The toll for vehicle type m on lane a
x_a	Traffic flow on lane a
$t_a(x_a)$	Travel time on lane a
δ_a^r	Binary variable, describing whether link a is on route r
$f_m^{r,w}$	Path flow on a specific route r for the OD pair w, vehicle type m
$C_m^{r,w}$	Minimum travel cost for a specific route r for the OD pair w, vehicle type m
q^w	The flow of OD pair w
$x_{a,m}^w$	Flow from OD pair w for vehicle type m on lane a
$p_{\overline{a}}^k$	The effective utilization rate of the green time on CAV-DL $\overline{a}$ at the k^{th} cycle
$q_{\overline{a}}^k$	Traffic flow on the dedicated lane $\overline{a}$ at the k^{th} cycle
$h_{\overline{a}}^k$	Saturated headway of lane $\overline{a}$ at the k^{th} cycle
$g_{\overline{a}}^k$	The green time of the phase corresponds to lane $\overline{a}$ in the k^{th} cycle
$AI_{\overline{a}}^k$	CAV-DL right-of-way allocation index
α^k	Kalman filter modeling parameter
ω^k	White observation noise at time interval k
φ^{k-1}	White modeling noise at time interval $k-1$
$\mathbf{X}^k$	State vector at time interval k
$\mathbf{Q}^k$	State transition matrix at time interval k
$\mathbf{Z}^k$	Observational vector at time interval k
$\mathbf{H}^k$	Relevance matrix at time interval k
$\widehat{\mathbf{X}}^k$	Predicted value of $\mathbf{X}^k$
$\widehat{\mathbf{P}}^k$	Predicted error matrix at time interval k
$\mathbf{D}^k$	Process noise covariance at time interval k
$\mathbf{K}^k$	The Kalman gain at time interval k
$\mathbf{R}^k$	Measurement noise covariance at time interval k
$t_{\overline{a}}$	Travel time on CAV-DLs
$t_{\widetilde{a}}$	Travel time on GLs
$\tau_{\overline{a},\widetilde{v}}(n)$	The toll for vehicle $\widetilde{v}$ using CAV-DL

the value of $\tau_{m,a}$ would be 0, and for HDVs, the value would be determined dynamically using the method introduced in the following sections. In Eq. (5.3), δ_a^r is a 0-1 variable, representing the relationship between route and lane. If the lane is included in the route, the value of δ_a^r will be 1, otherwise, the value will be 0. $C_m^{r,w}$ means the minimum travel cost, and $f_m^{r,w}$ denotes the route flow on a specific route r for the OD pair w. Eq. (5.3) represents the user equilibrium condition, and means that all vehicles from OD pair w, with type m using the path r will have the same and minimum travel cost $C_m^{r,w}$. For paths with higher travel costs, the flow will be zero.

$$\begin{aligned} &C = VOT_m \cdot t_a(x_a) + \tau_{m,a} \\ &(m = CAVs, HDVs; a \in A, \forall r \in R, w \in W) \end{aligned} \tag{5.2}$$

$$\begin{aligned} &\begin{cases} \sum\limits_{a \in A} ((VOT_m \cdot t_a(x_a) + \tau_{m,a}) \cdot \delta_a^r) = C_m^{r,w}, f_m^{r,w} > 0 \\ f_m^{r,w} = 0, \left\{ \sum\limits_{a \in A} ((VOT_m \cdot t_a(x_a) + \tau_{m,a}) \cdot \delta_a^r) - C_m^{r,w} \right\} > 0 \end{cases} \\ &(m = CAVs, HDVs; a \in A, \forall r \in R, w \in W) \end{aligned} \tag{5.3}$$

Eq. (5.4) is the flow conservation constraint, ensuring the summation of all path flow is equal to the total demand. Eq. (5.5) is the path and link flow incident relationship, and Eq. (5.6) makes sure the summation of lane flow equals link flow. Eq. (5.7) guarantees the flow of the two types of vehicles equal to the link flow and Eq. (5.8) is the non-negative constraint for these variables.

$$\sum_r f_m^{r,w} = q_m^w, (m = CAVs, HDVs; r \in R, w \in W) \tag{5.4}$$

$$\sum_{r,w} f_m^{r,w} \delta_a^r = x_{a,m}^w, (m = CAVs, HDVs; r \in R, w \in W) \tag{5.5}$$

$$\begin{aligned} &x_{\overline{a},m}^w + x_{\widetilde{a},m}^w = x_{a,m}^w, \\ &(\overline{a} \in \overline{A}, \widetilde{a} \in \widetilde{A}, a \in A, m = CAVs, HDVs; w \in W) \end{aligned} \tag{5.6}$$

$$\sum_m x_{a,m}^w = x_a^w, (m = CAVs, HDVs; w \in W) \tag{5.7}$$

$$\begin{aligned} &f_m^{r,w}, x_a^w, x_{a,m}^w, x_{\overline{a},m}^w, x_{\widetilde{a},m}^w \geq 0, \\ &(\overline{a} \in \overline{A}, \widetilde{a} \in \widetilde{A}, a \in A,\ m = CAVs, HDVs; r \in R, w \in W) \end{aligned} \tag{5.8}$$

5.2.2 Dynamic Right-of-way Allocation

Basic Rules

To achieve the objective of minimizing travel time and determine the traffic flow of different vehicle types on the CAV-DLs and GLs, the first method is to dynamically allocate the right-of-way on the CAV-DLs. In this approach, the effective utilization rate of the CAV-DLs should be determined first which is equivalent to the effective utilization rate of the green time on that lane [168]. It is calculated in Eq. (5.9), where $q_{\overline{a}}^k(\overline{a} \in \overline{A}, k \in [1, T_k])$ is the traffic flow on the dedicated lane $\overline{a}$ at the k^{th} cycle, $h_{\overline{a}}^k$ is the saturated headway of lane $\overline{a}$, and $g_{\overline{a}}^k$ is the green time of the phase corresponds to the dedicated lane in the k^{th} cycle.

$$p_{\overline{a}}^k = q_{\overline{a}}^k h_{\overline{a}}^k / g_{\overline{a}}^k \tag{5.9}$$

Then, the dedicated lane Allocation Index ($AI_{\overline{a}}^k$) can be expressed as Eq. (5.10):

$$AI_{\overline{a}}^k = \begin{cases} \text{GLs}, \ if \ p_{\overline{a}}^k \in [0, \varepsilon] \\ \text{CAV} - \text{DLs}, otherwise \end{cases} \tag{5.10}$$

From the literature [182], the lanes are determined to be not fully utilized if the saturation occupancy is lower than 0.6. Therefore, it is rational to set $\varepsilon = 0.6$ because the effective utilization rate of the green time is equivalent to the saturation occupancy. If $p_{\overline{a}}^k \in [0, 0.6]$, it is necessary to grant access to HDVs to the CAV-DLs, and the traffic flow will be redistributed according to the traffic assignment model (Eq. (5.11)).

$$f_{\substack{HDV \\ \forall r \in CAV-DLs}}^{r,w} = \begin{cases} By \ assignment \ model, if \ AI_{\overline{a}}^k = GLs, \\ 0, otherwise \end{cases} \tag{5.11}$$

Kalman Filter-based traffic flow prediction

The traffic flow $q_{\overline{a}}^k(\overline{a} \in \overline{A})$ on the lane is important for predicting the effective utilization rate of the green time on CAV-DLs. It changes constantly over time but is not a strict function of time, so the prediction of $q_{\overline{a}}^k$ is a typical time series analysis problem. The Kalman Filter can be selected here to properly and effectively handle the short-term time-series traffic flow prediction [133]. Based on the modeling equation and estimation objective, the state function

can be flexibly developed to achieve the optimum prediction of the required information with guaranteed accuracy under the unknown statistical noise and other inaccuracies [183]. In the study, the value of $q_{\overline{a}}^{k}$ is calculated by a linear function of the set of traffic volumes on the lane as shown in Eq. (5.12), which concisely describes the system behavior with fairly good performance.

$$q_{\overline{a}}^{k+1} = \alpha_0^k x_{\overline{a}}^k + \alpha_1^{k-1} x_{\overline{a}}^{k-1} + \omega^k \tag{5.12}$$

$x_{\overline{a}}^{k}$, $x_{\overline{a}}^{k-1}$ represents the traffic flow on the lane $\overline{a}$ at time interval k and $k-1$. α_0^k and α_1^{k-1} are corresponding parameters, ω^k is the white observation noise. To convert Eq. (5.12) to the standard form of Kalman Filter, Let $\mathbf{X}^k = (\alpha_0^k, \alpha_1^{k-1})^T$, $\mathbf{H}^k = (x_a^k, x_a^{k-1})$, $\mathbf{Z}^k = q_a^{k+1}$ so that Eq. (5.12) be transformed into Eq. (5.13) and (5.14):

$$\mathbf{X}^k = \mathbf{Q}^k \mathbf{X}^{k-1} + \varphi^{k-1} \tag{5.13}$$

$$\mathbf{Z}^k = \mathbf{H}^k \mathbf{X}^k + \omega^k \tag{5.14}$$

where $\mathbf{X}^k$ is a state vector at time k, and $\mathbf{Q}^k$ is a state transition matrix. $\mathbf{Z}^k$, $\mathbf{H}^k$, φ^{k-1} is the observational vector, the relevance matrix and the white modeling noise respectively.

Based on the converted form of the equation, the predicted value $\widehat{\mathbf{X}}^k$ can be calculated by Eq. (5.15), and the auto-covariance matrix for the predictive state variables $\widehat{\mathbf{P}}^k$ can be calculated by Eq. (5.16), where $\mathbf{D}^{k-1}$ is the auto-covariance matrix for modeling bias.

$$\widehat{\mathbf{X}}^k = \mathbf{Q}^k \mathbf{X}^{k-1} \tag{5.15}$$

$$\widehat{\mathbf{P}}^k = \mathbf{Q}^{k-1} \widehat{\mathbf{P}}^{k-1} (\mathbf{Q}^{k-1})^T + \mathbf{D}^{k-1} \tag{5.16}$$

Then, the optimal Kalman gain $\mathbf{K}^k$ is determined by Eq. (5.17), and the optimal filtering estimate vector $\mathbf{X}^k$ can be obtained by Eq. (5.18), where $\mathbf{R}^k$ is auto-covariance matrix for measurement noise.

$$\mathbf{K}^k = \widehat{\mathbf{P}}^k (\mathbf{H}^k)^T [\mathbf{H}^k \mathbf{P}^k (\widehat{\mathbf{H}}^k)^T + \mathbf{R}^k]^{-1} \tag{5.17}$$

$$\mathbf{X}^k = \widehat{\mathbf{X}}^k + \mathbf{K}^k (\mathbf{Z}^k - \mathbf{H}^k \widehat{\mathbf{X}}^k) \tag{5.18}$$

To apply the Kalman Filter for prediction, the first step is to initialize all necessary variables. Typically, a larger $\mathbf{R}^k$ and $\mathbf{D}^k$ imply a stronger variation due to measurement noise and modeling mismatch respectively. In our case study, the initial value of $\mathbf{R}^k$, $\mathbf{D}^k$ and $\mathbf{P}^0$ can be set as diagonal matrixes, where $\mathbf{R}^k = \text{diag}(0.001, 0.001)$, $\mathbf{D}^k$= $\text{diag}(0.001, 0.001)$, $\mathbf{P}^0 = \text{diag}(0.001, 0.001)$, and $\mathbf{X}^0$ was set as a zero vector. These settings are able to make sure the convergence of the estimation process is asymptotically stable [184], i.e., the eigenvalues of the closed-loop estimation matrix are all within the discrete z-domain [185]. After that, the filter error $\mathbf{P}^k$ is updated by Eq. (5.19), and $\widehat{q}_{\overline{a}}^{k+1}$ can be predicted by Eq. (5.20).

$$\mathbf{P}^k = (\mathbf{I} - \mathbf{K}^k\mathbf{H}^k)\widehat{\mathbf{P}}^k \tag{5.19}$$

$$\widehat{q}_{\overline{a}}^{k+1} = \mathbf{H}^k\mathbf{X}^k \tag{5.20}$$

5.2.3 Tolling

The second strategy is tolling which allows HDVs to reduce their travel time by paying money. When the travel time of CAV-DLs is lower than the GLs, HDVs are possible to change to the CAV-DLs. Based on the user equilibrium theory, after the HDVs used the CAV-DLs, the travel time difference between the GLs and the CAV-DLs will be afforded by the HDVs. In this way, the total travel costs (including travel time and toll) on the CAV-DL and its paired GL will be identical, which makes sure all vehicles are on the shortest travel cost route and the network is in an equilibrium state. This strategy can not only reduce the travel time of HDVs but also improve the capacity utilization rate of the CAV-DLs. The step-by-step procedures for conducting the tolling are described below:

Step 1: At each time step n, acquire the travel time $t_{\overline{a}}(n)$ ($\overline{a} \in \overline{A}$), $t_{\widetilde{a}}(n)$ ($\widetilde{a} \in \widetilde{A}$), as well as the set of vehicle ID (V_{CAV}, V_{HDV}) on the CAV-DLs and GLs.

Step 2: At the time step when HDVs enter the intersection, compare $t_{\overline{a}}(n)$ and $t_{\widetilde{a}}(n)$, if: $t_{\widetilde{a}}(n) > t_{\overline{a}}(n)$ and $t_{\widetilde{a}}(n) - t_{\overline{a}}(n) \geq \sigma$ (σ is set to be 5 seconds

in this study, since the lane-changing durations are on average of 5 seconds [186]), HDVs are allowed to use the CAV-DLs.

Step 3: Run the simulation and let the HDV ($\widetilde{v} \in V_{HDV}$) change its traveling lane from GLs to CAV-DLs.

Step 4: Calculate the toll for HDV traveling on the CAV-DLs using Eq. (5.21).

$$\tau_{\widetilde{a},\widetilde{v}}(n) = VOT_{HDV}[t_{\widetilde{a}}(n) - t_{\overline{a}}(n+1)] \tag{5.21}$$

Step 5: Update the travel time on all lanes and compare $t_{\widetilde{a}}(n)$ with $t_{\overline{a}}(n)$.

Step 6: If $t_{\widetilde{a}}(n) \leq t_{\overline{a}}(n)$ or $t_{\widetilde{a}}(n) - t_{\overline{a}}(n) < \sigma$, Stop. Otherwise, repeat **Step 1** to **Step 3**.

5.3 Case Study

The performance of the proposed methods was evaluated by conducting a case study. Although the phased deployment of CAV technology is already in progress, building new CAV-DLs has many technical issues and economic concerns. Converting the existing lanes (e.g., Bus dedicated lane, HOV lane, GLs) into the CAV-DLs is more practical. In addition, in the early stages, instead of deploying the CAV-DLs all over the network, it is more realistic to implement them in some selected corridors. The likely setup will consist of sensors and roadside units (RSUs) along the corridor to track which vehicles are using the laneway. There will also be some sort of mobile edge computing (MEC) platform to enable monitoring and coordination of the vehicles and signal controllers. The RSUs collect CAVs' real-time travel information by communicating with the onboard units (OBUs), and the information will be further processed at the local MEC. Subsequently, the MEC will solve the optimization model, generate corresponding control strategies, and give feedback to the RSUs and OBUs.

5.3.1 Simulation Design

The network of the downtown area of the City of Edmonton, Canada (Fig. 5.2(a)) was simulated (Fig. 5.2(b)) in the discrete-event traffic simulation tool

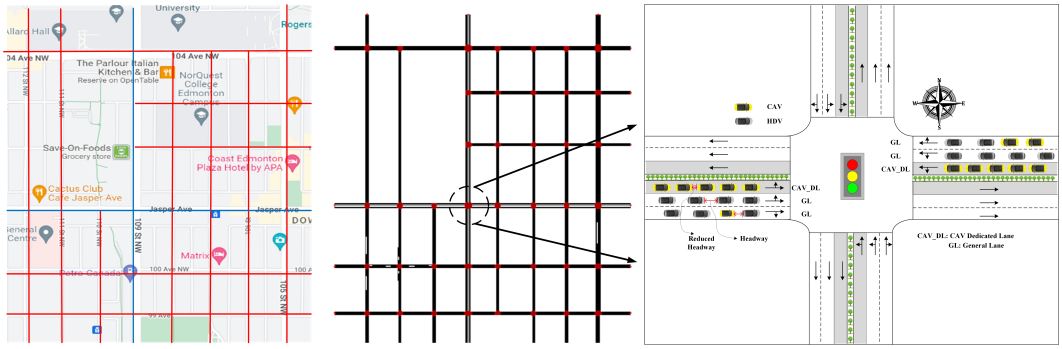

Figure 5.2: Testing network and intersection layout.

- SUMO [135] to assess the effectiveness of the proposed strategies. As stated, two corridors are selected to deploy the CAV-DLs, that are 109 Street and Jasper Avenue (represented by blue lines in Fig. 5.2(a)) since they are the two main corridors with the busiest traffic within the network. The detailed simulation parameters were given in Table 5.2. The geometry, including the

Table 5.2: Simulation parameter settings

Parameters	**Value**
Total simulation time horizon (s)	5,400
Number of CAV-DLs	32
Number of intersections	41
Simulation time step (s)	1
Traffic flow prediction time interval (s)	Each cycle
Lane length (m)	100/200/600
Maximum Speed (m/s)	13.89
Average vehicle length (m)	5
Saturation headway between CAV and CAV (s)	0.5
Saturation headway between HDV and CAV (s)	1.0
Saturation headway between HDV and HDV (s)	2.0
Cycle length (varying in intersections) (s)	90/110
Green time duration (varying in intersections) (s)	Field/optimized

number of lanes, lane length as well as speed limit for the network were set according to the field conditions, and the rest of the important parameters were defined according to the relevant literature [187], [188]. Fig. 5.2(c) illustrates the detailed layout of the simulated intersection. For each direction, there are three lanes in total. The lane on the far left was designed as a CAV-DL, it allows both left turn and through CAVs, and the lane in the middle also allows left turn and through movement but for HDVs. For those CAVs that need a

right turn, they will share the right turn lane with the HDVs.

Two time periods of traffic demand, including peak and non-peak hours were tested, with the CAV PR ranging from 0.1 to 1.0. The peak-hour and non-peak hour volumes were obtained from the City of Edmonton using the turning movement data of each intersection (see examples in Fig. 5.3). For the signal control strategy, CAVs on the CAV-DLs are given precedence over HDVs to avoid conflict. That is, the West-East left-turn and going straight CAVs on the CAV-DLs share the first phase to go through the intersection, followed by left-turn and going straight HDVs on the GLs, and the right-turn and going straight HDVs will leave at last. After vehicles in the west-east direction complete their movement, the vehicles in the North-South direction will start to move.

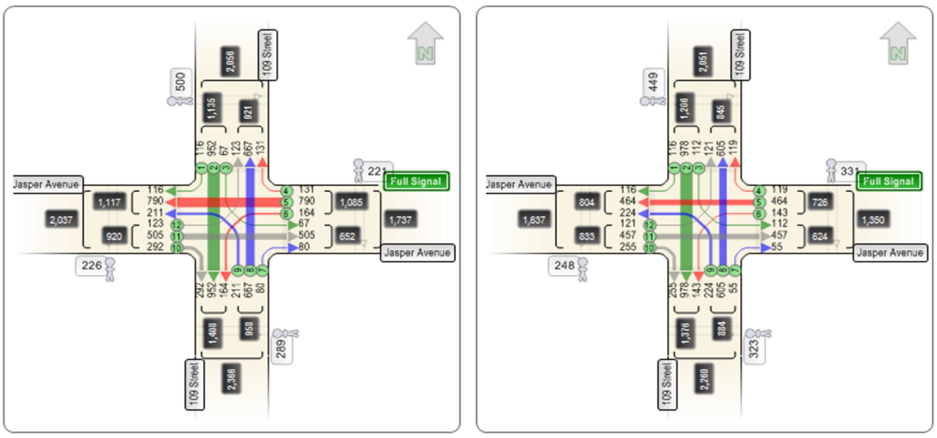

(a)Peak-hour turning movement data for 109 St@Jasper Ave

(b)Nonpeak-hour turning movement data for 109 St@Jasper Ave

Figure 5.3: Examples of the turning movement data (a)Peak hour and (b)non-peak hour.

5.3.2 The Performance of Deploying CAV-DLs

Similarly, the real-time traffic scenario is simulated in SUMO according to the given demand, and Python was integrated to deal with the control algorithms. The information exchange and control strategy implementation between SUMO and Python was executed by the SUMO application programming interface (API) TraCI [189]. Python acquired the real-time data from SUMO at every simulation time step, and the traffic flow prediction on the

CAV-DLs was performed for each cycle, based on which the dynamic allocation of the right-of-way was conducted. The right-of-way for the dedicated lanes can be changed in SUMO with the optimized results from Python. Likewise, the toll is calculated in Python, following which the tolling strategy will be imposed on vehicles by SUMO. These procedures were repeated until all vehicles leave the network.

Before evaluating the effectiveness of the proposed methods, the performance of deploying the CAV-DLs was assessed. Fig. 5.4 demonstrates the network performance with and without CAV-DLs in peak and non-peak hours respectively following the rules below:

Only CAVs are permitted to utilize the CAV-DLs while HDVs can only use GLs. CAVs with right movements can use GLs, otherwise use CAV-DLs.

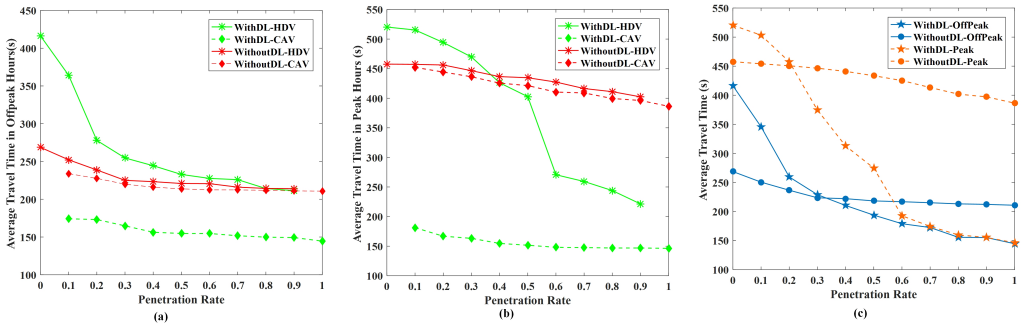

Figure 5.4: ATT of the network with and without CAV-DLs (a) ATT of CAVs and HDVs separately in non-peak hour (b) ATT of CAVs and HDVs separately in peak hour (c) ATT of all vehicles

Fig. 5.4(a) presents the average travel time (ATT) for CAVs and HDVs separately, although the ATT of CAVs is slightly lower than HDVs, they have not shown a significant difference if there is no dedicated lane. However, the ATT of CAVs is much lower than HDVs when the dedicated lane was implemented. Similar trends can be observed in the peak-hour scenarios in Fig. 5.4(b). This distinguished difference between the ATT of CAVs and HDVs will potentially attract more HDVs to upgrade to CAVs. Fig. 5.4(c) demonstrates the ATT for all vehicles. For the case in peak hour and PR is lower than 0.3, the dedicated lane resulted in higher travel time, while in non-peak hour, the network performance is worse even when the PR reaches 0.4. This phenomenon

also suggested the necessity of imposing an effective control strategy to manage the CAV-DLs for improving the system performance, especially in low PR cases.

5.3.3 CAV-DLs Utilization Rate Analysis

In the dynamic right-of-way allocation strategy, when the green utilization rate is lower than 0.6, the lane was supposed to be not fully utilized and the HDVs will be allowed to the CAV-DLs. To forecast the utilization rate on the CAV-DLs, the traffic flow during green was predicted by the Kalman Filter-based method. The prediction time interval varies for different lanes, which is determined by the cycle length of the downstream intersections, and the traffic flow was predicted for each CAV-DL during every cycle. Fig. 5.5 illustrates the prediction accuracy and relative errors using a selected lane as an example. The number of vehicles departing during green was predicted and compared with the simulated results, and the relative prediction errors are within 20%. It can also be noticed that most of the errors are within 10%.

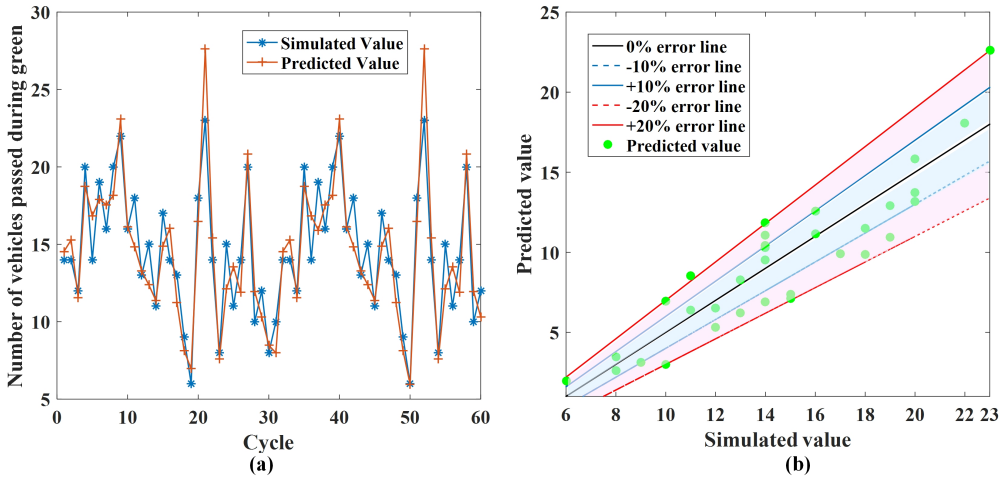

Figure 5.5: Example of traffic flow prediction (a)Traffic flow value (b)Relative errors

Based on the predicted traffic flow, we can determine for each dedicated lane whether the HDVs were allowed to use it during each cycle. Fig. 5.6 displays the effective green utilization rate of the CAV-DL under different PR cases in the peak hour. The x-axis represents the cycle, and the y-axis

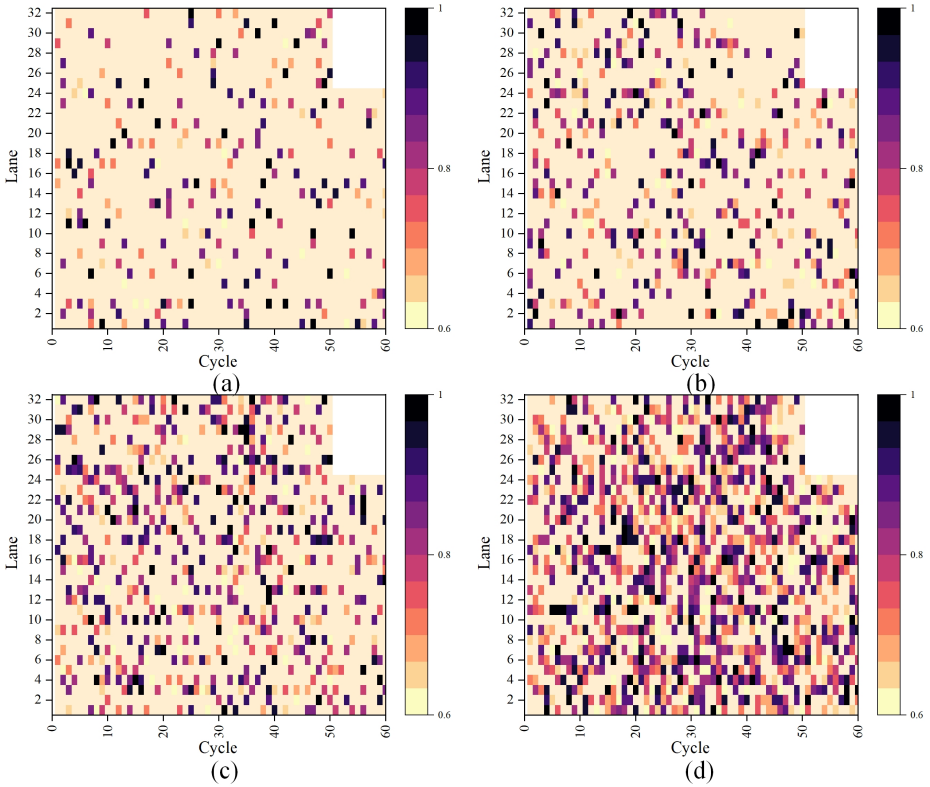

Figure 5.6: Effective green utilization rate (a)0.2 PR (b) 0.4 PR (c)0.6 PR (d) 0.8 PR

represents each dedicated lane. The light orange color is defined to represent the case when the green utilization rate is lower than 0.6, which means the CAV-DL can be converted to GL and HDVs are allowed to use it. For those with a value greater than 0.6, the darker the color, the larger the value. Based on the figure, it can be concluded that a greater number of lanes are being converted to GLs in lower PR cases. (e.g., there are more than 70% of lanes that allow HDVs in the 0.2 PR case).

5.3.4 Tolling Strategy Analysis

Fig. 5.7 demonstrates the ATT and travel time difference between CAV-DL and GL on a link with a length of 100 meters under different PR. In low PR cases, the traffic condition on the CAV-DL is free flow and the travel time is low no matter in peak or non-peak hours. However, the GL is very congested with much higher travel time, which lasts until the PR reaches 0.8 in peak

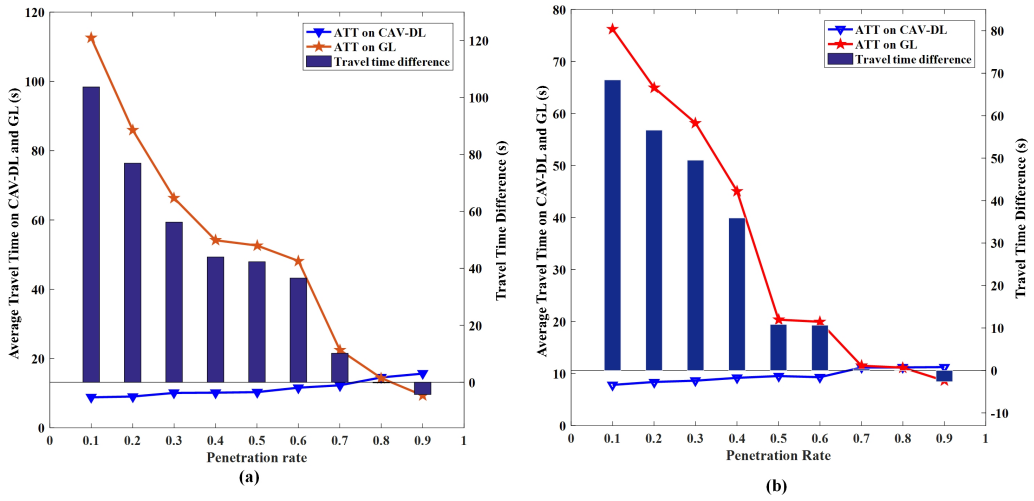

Figure 5.7: ATT and travel time difference on CAV-DL and GL (a) Peak hour (b) non-peak hour

$$\tau_{\overline{a},\widetilde{v}}(n) = \begin{cases} \$0.1\ CAD, & t_{\widetilde{a}}(n) - t_{\overline{a}}(n+1) < 10s \\ \$0.0089\ CAD * [t_{\widetilde{a}}(n) - t_{\overline{a}}(n+1)], & 10s \leq t_{\widetilde{a}}(n) - t_{\overline{a}}(n+1) < 180s \\ \$1.6\ CAD, & t_{\widetilde{a}}(n) - t_{\overline{a}}(n+1) \geq 180s \end{cases} \tag{5.22}$$

hour and 0.7 in non-peak hour. In other words, the ATT on the CAV-DL is consistently lower than GL, and HDVs can change to the dedicated lane to reduce the travel time by paying a toll. In higher PR cases, the travel time on CAV-DL will exceed the GL, and HDVs don't have to change lanes.

According to the Canadian Income Survey released by Statistics Canada, the Canadian average after-tax income was $66,800 CAD in 2020 [190]. With the assumption of working time to be 260 days per year and 8 hours per day, the VOT for people in Canada is approximately $32.12 CAD/hr (i.e., $0.0089 CAD/s). According to the defined value of VOT, the toll was determined as shown in Eq. (5.22). The minimum toll for HDVs using the CAV-DLs is $0.1 CAD when the travel time difference between the CAV-DL and the GL is less than 10 seconds (i.e., the Lower limit for the toll). When the travel time difference is larger than or equal to 10 seconds but less than 180 seconds, the charge will maintain a linear relationship with the travel time difference, and an extra $0.0089 CAD will be charged for every one seconds' increase. Then, for a travel time difference larger than 180 seconds, the charge will be $1.6

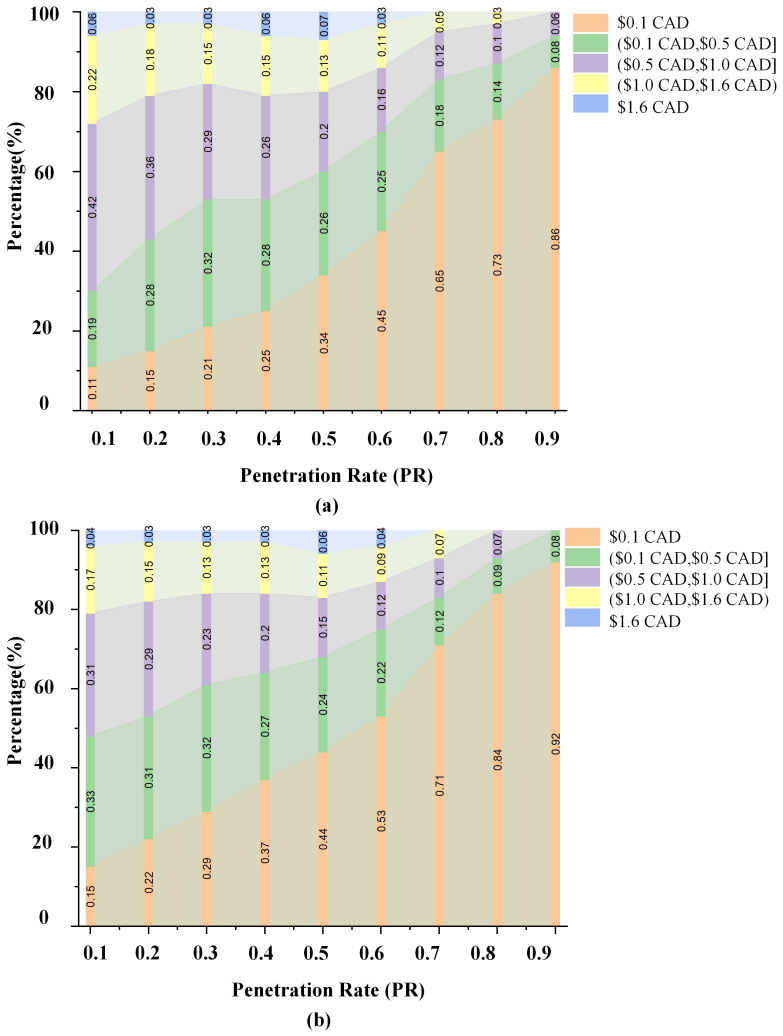

Figure 5.8: Example of toll rate distribution in different PR cases (a)Peak hour (b)Non-peak hour

CAD (i.e., the Upper limit for the toll).

Based on the tolling rule, Fig. 5.8 indicates the distribution of the toll for all lanes in a certain time step for both peak and non-peak hours. In low PR cases, for example, when PR=0.1, the travel time on the GL is much longer than the CAV-DL. As a result, a majority of HDVs can change their travel lane from the GL to the CAV-DL. However, in the meanwhile, due to the significant difference between the travel time of GL and CAV-DL, the toll with a higher value will take a larger proportion. On the contrary, in higher PR cases, since the CAV-DL is much more congested than the GL, the travel

time on the CAV-DL is higher than the GL. Consequently, only a very small proportion of CAV-DLs will allow HDVs to use with a much lower toll value. This is the reason why over 85% of CAV-DLs in peak hour and over 90% in non-peak hour have a toll of less than \$0.1 CAD in 0.9 PR cases.

Table 5.3 further presented the average toll that an HDV needs to pay when traveling within the network under different PR cases. When PR=0.1, in the non-peak hour, HDVs pay \$3.63 CAD on average to travel on the dedicated lane for reducing travel time during their whole trip, while the CAV-DLs charge more on HDVs in the peak hour than in non-peak hour due to the higher demand, with a toll to be \$5.55 CAD. Nevertheless, along with the increase in PR, the toll will decrease. When the PR reaches 0.6, the toll for the non-peak hour is only \$0.57 CAD, and in higher PR cases, since the volume of CAVs is high enough to sufficiently utilize the dedicated lane, the toll strategy is not applicable anymore.

Table 5.3: Average toll for HDVs traveling within the network.

PR		**0.1**	**0.2**	**0.3**	**0.4**	**0.5**	**0.6**	**0.7**	**0.8**	**0.9**
Toll	Non-peak	3.63	3.04	2.68	1.82	0.68	0.57	N/A	N/A	N/A
(\$CAD)	Peak	5.55	4.11	2.99	2.35	2.24	1.98	0.59	N/A	N/A

5.3.5 Overall Performance of Different Control Methods

Lastly, the overall effectiveness of the proposed two methods [*a). The dynamic right-of-way allocation, b). Tolling*] was compared with the two benchmarks [*c). Without CAV-DLs, d). With CAV-DLs*].

In the non-peak hour, the ATT of the two proposed control methods presents a similar value, with the *tolling* slightly better than the *dynamic right-of-way allocation*, and both notably outperformed the *With CAV-DLs*. Along with the increase of the PR, deploying the CAV-DLs started express strength in terms of reduced travel time. When PR>= 0.4, the *With CAV-DLs* displayed a remarkable reduction in ATT compared to the *Without CAV-DLs* condition. At the same time, the ATT resulted from the *dynamic right-of-way*

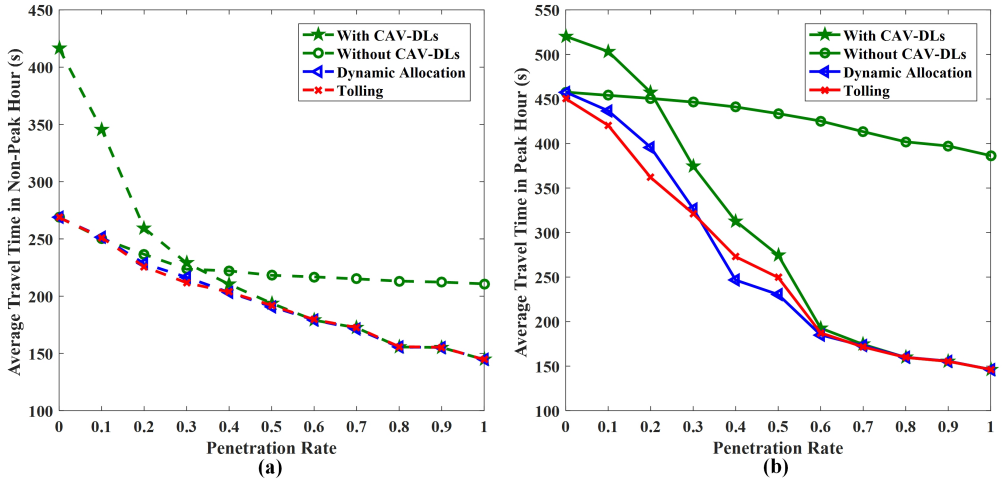

Figure 5.9: Performance comparison of different strategies (a) Non-peak hour (b) Peak hour

allocation and *tolling* also outperformed the *Without CAV-DLs* strategy (Fig. 5.9(a)).

Similar results can be observed in peak hour, with the effectiveness of different strategies being noticed more clearly (Fig. 5.9(b)). In low PR cases (<= 0.3), *tolling* is the best strategy with the lowest ATT value, and both *tolling* and *dynamic right-of-way allocation* were better than the other two strategies. For 0.3<PR<=0.6, the ATT of *tolling* surpassed the *dynamic right-of-way allocation*, with the *dynamic right-of-way allocation* being the best among the four schemes. When PR>=0.7, deploying the CAV-DLs has good potency, and the proposed two methods also show comparable effectiveness.

In general, when the PR of CAVs is high enough, network efficiency can be significantly improved by deploying the CAV-DLs, and no additional lane management measures are required. In Low PR cases, *tolling* is the best approach in reducing travel time because the strategy allows more HDVs to use the CAV-DLs. From the users' point of view, when the PR is higher, the toll will be lower. Therefore, applying such a strategy to promote the adoption of CAVs can also benefit HDVs. However, in practical cases, to ensure the feasibility of the tolling policy, further investigation into the exact money to charge and drivers' willingness to pay is necessary. The *dynamic right-of-way allocation* is more flexible in operation with relatively good effectiveness.

However, it relies on the accurate prediction of effective lane utilization rate. Overall, the two proposed strategies are both suitable to be implemented in either low PR or high PR cases, and they are feasible to be applied in other traffic networks.

5.4 Conclusions

This chapter proposed two innovative approaches for CAV-DL management to promote the CAVs and improve traffic efficiency. The two goals were realized by dynamically allocating the right-of-way for CAV-DLs or tolling. Based on the prediction of the effective green utilization rate on the CAV-DL, the first strategy allows HDVs to use the lanes when they are predicted to be relatively vacant, and the second approach gives HDVs access to the CAV-DLs whenever essential by charging a fee.

The strategies were evaluated through a case study based on the Edmonton downtown area. Principally, both methods were efficacious in reducing travel time, and the results indicated that both dynamic right-of-way allocation and tolling outperformed the two benchmarks in low PR cases and had similar control effectiveness with implementing CAV-DLs in higher PR cases. What's more, the toll value that HDVs should pay in different PR cases was also given. They pay less in high PR cases, which may potentially stimulate more HDVs to shift to CAVs. The feasibility of implementing the proposed methods has also been compared and discussed. In general, tolling is slightly better in reducing travel time, while the dynamic right-of-way allocation is more flexible without the potential trepidation of drivers' compliance. Overall, the study in this chapter reveals the possibility of enhancing network efficiency through appropriate lane management strategies in the mixed traffic environment, which can bring some inspiration to policymakers and practitioners.

Chapter 6

Achieving Energy-Efficient and Travel Time-Optimized Trajectory and Signal Control for Future CAEVs

6.1 Introduction

EVs are on the horizon due to their potential benefits in reducing travel costs and emissions. However, despite the potential benefits of EVs, there are still significant segments of the population who are reluctant to embrace them. In certain countries, the market penetration rate for EVs remains relatively low, even if several types of subsidies and privileges were given by the government to stimulate the purchase of EVs, especially in cities with extreme weather conditions (e.g., Edmonton, Canada where the average winter temperature drops to -20 degrees Celsius). In such harsh climates, the energy consumption of EVs increases significantly, and the range of EVs can decrease by up to 30% in freezing temperatures [191]. In such a circumstance, two primary concerns, namely charge anxiety (i.e., the worry about the accessibility of charging infrastructure) and range anxiety (i.e., the fear of running out of electricity before reaching a charging station) [192], [193] have impeded the widespread EV adoption.

On one hand, the limitations of current battery technology have resulted in low battery efficiency [194]. On the other hand, the lack of adequate charging

infrastructure can lead to longer waiting times or the need to travel greater distances in search of a charging station. To address these technical challenges, electrical engineers are dedicating their efforts to improving motor efficiency for better conversion of electrical energy into kinetic energy [195]–[197], while others are focused on advancing fast charging technologies [196], [198]. From the perspective of traffic engineers, their efforts can be categorized into three types. The first type involves assessing and developing relevant traffic policies for the electrification of vehicles, both in the short and long term [14], [199]–[201]. The second type focuses on the deployment of charging infrastructure, including optimizing the location and allocation of EV charging stations [202], [203], while the last type seeks better traffic management and control strategies to save energy [204]–[206]. The majority of current EV-related research has primarily concentrated on the first two categories, with limited attention given to the third type.

In this context, this chapter focuses on studying EV energy-saving problems from the perspective of traffic control, addressing the third type of investigation. As shown in Fig. 6.1, He and Wu [207] compared the fuel economy of a conventional gasoline passenger car with that of the Tesla Roadster.

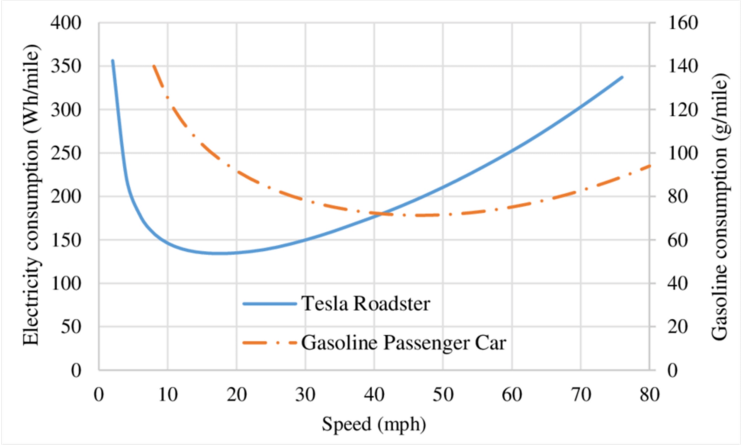

Figure 6.1: Vehicle energy economy at different speeds ([207]).

The results indicate that the gasoline car achieves its highest fuel efficiency at around 45 mph (72.42 km/h). However, the Tesla Roadster demonstrates its optimal energy consumption at a relatively low speed of 15 mph (24.14

km/h). Similar findings have been observed in other studies as well [208], [209]. These results suggest that, unlike traditional gasoline-powered vehicles, EVs tend to exhibit better energy efficiency when driving at lower speeds. While lower driving speeds may reduce energy consumption, they also result in longer travel time. Additionally, the use of vehicle accessories such as the air conditioning system can contribute to increased energy consumption as travel time prolongs. However, travel time is the most important concern for most commuters [210] as the primary objective of travel is to reach the destination as soon as possible. Therefore, it is essential to consider the trade-off between energy consumption and total travel time to realize both traffic and energy efficiency. In the limited research concerning EV controls, the objectives were generally either aimed at enhancing traffic efficiency or reducing energy consumption, but seldom did these approaches integrate both goals. Furthermore, the data used for controlling EV trajectories primarily relied on static loop detectors or video cameras which offered limited accuracy and low updating frequency. Consequently, the generated control strategies could not be promptly applied, compromising their effectiveness.

It was not until the advent of CAV technology that these challenges began to be effectively addressed. Being able to communicate with each other as well as all connected entities in the traffic environment through V2V and V2I in real-time, abundant traffic information will be available on both the vehicle and infrastructure side. Moreover, onboard or edge computing devices enable simple data processing and algorithm solving, empowering vehicles to receive immediate action plans based on the most up-to-date traffic information [162]. The speed and acceleration rate of EVs can be dynamically adjusted according to the signal timing parameters, and the signal timing plan can also be optimized based on the updated EV trajectories. The EVs can also communicate and cooperate with each other to form platoons which will further generate smoother trajectories. The combined CAV and EV technology provides the possibility to realize the goal of effectively balancing energy consumption and total travel time by signal control and trajectory optimization. With the increasing need to enhance both travel and energy efficiency, it is not difficult to

see that connected and automated electrical vehicles will secure a substantial market share in future traffic systems [211], [212].

Leveraging the advantages of CAV technology, a substantial body of literature has delved into the realms of signal control and trajectory optimization, encompassing both traditional gasoline-based vehicles and EVs [213]–[217]. Table 6.1 offers a comprehensive summary of these seminal studies, shedding light on the methodologies employed and providing insights into their effectiveness and limitations. Within this array of research, the primary objectives are enhancing traffic efficiency, minimizing energy consumption, mitigating safety issues, and optimizing the synergy between energy and traffic efficiency. In general, all the listed studies utilized the feature of CAVs for communication to obtain the most up-to-date traffic information to optimize the related variables. The Cooperative Adaptive Cruise Control (CACC) strategy along with signal control and speed guidance, has been pivotal in the pursuit of energy reduction and throughput improvement. These studies employ a spectrum of techniques, encompassing both AI-driven approaches [218] and analytical-model-based techniques [204], [217]. Based on the Table, it's apparent that although different control goals are achieved with the pros and cons of the methods, the common issue was the lack of discussion for the models' capability of being applied to real-time cases which is critical in the context of CAVs.

Table 6.1: Representative studies of signal control and trajectory optimization

Control Objective	**Vehicle Type**	**Control Strategy**				**Methodology**	**Effectiveness(E)and Drawback(D)**	**Reference**
		S.C.	T.C.	S.G.	P.C.			
Improve traffic efficiency	GB-CACC	✓			✓	Simple Rule-based Optimization	(E). Able to reduce delay, stops, emission and fuel consumption of vehicles. (D). Too simple scenarios designed without generalization.	Malakorn et al. [218]
Reduce energy consumption	GB-CACC			✓	✓	Multi-stage Control	(E). Considers using the latest traffic information; Significantly reduced the stop time and delay. (D). Availability to expand on larger network is questionable.	Wang et al. [219]
	GB-CACC		✓	✓		Traffic flow model-based optimization	(E). Specifically considering the queuing impact, Save up to 40% fuel. (D). Did not count for other performance metrics.	Yang et al. [220]
	CEVs				✓	Rule-based Control	(E). Outperforms IDM, CACC in energy consumption. (D). Different congestion levels were not tested.	Lu et al. [216]
Addressing both safety and energy concerns	CEVs		✓		✓	Deep-reinforcement Learning	(E). Model-free, off-policy with less execution time and capable of real-time application. (D). Dependent on the data for training.	Moghaddam et al. [221]
	CEVs		✓		✓	Two-stage Control	(E). Better robustness than learning-based methods. (D). Tested on a limited number of vehicles; Rely on the EV efficiency map.	Zhang et al. [214]
Improve both traffic and energy efficiency	GB-CACC	✓	✓		✓	Binary Optimization	(E). Maximizes throughput and increases average speed; Optimizes green time based on platoon rather than individual vehicles' arrival. (D). The applicability in real-time was not discussed.	Liu et al. [222]
	CEVs	✓	✓			Discrete Optimization	((E). Designed a feedback control-based system which has effective control ability. (D). Complex model and limited to a very small network; Can not be solved in real-time.	Li et al. [204]
	CEVs	✓		✓		Bi objective Multi-stage Optimization	(E). Incorporated traffic flow modeling and estimated link level energy consumption accurately. (D). Complex model and limited to a very small network; Can not be solved in real-time.	Pace et al. [217]
Trade-off between energy consumption and travel time	CAEVs	✓	✓			Discrete Optimization	(E). Effective feedback-based closed-loop control; Simplified controlling process enables real-time application. (D). Constant acceleration and decceleration rate.	The proposed method

Note: GB-CACC: Gasoline-based CACC Vehicles; CEVs: Connected Electric Vehicles; S.C.: Signal Control; T.C.: Trajectory Control; S.G.: Speed Guidance; P.C.: Platoon Control

For estimating the energy consumption, various approaches that have evolved over the decades, conveniently categorized in Table 6.2. These approaches fall into distinct classes: Forward models, Powertrain-based models, Backward models, Data-based models, and rule-based models. Data-based models are typically reliant on empirical data without generalization. Rule-based models, while straightforward, face challenges when extending their applicability to macroscopic scales and integrating them into traffic control systems. Forward models, such as ADVISOR [223], are computationally intensive since they model more detailed vehicle components (e.g., engines, transmissions, and wheels). Moreover, these models use drivers' commands as input, making it challenging to integrate them with traffic simulations [224]. What's worse, some of the models rely heavily on the efficiency map, which is often undisclosed and unavailable. In contrast, backward models utilize vehicle speed, acceleration, and some other relevant parameters as input, making them more suitable for coupling with traffic simulations. Representative backward energy consumption estimation models include VT-CPPM (Virginia Tech Comprehensive Power-based PHEV Model) [225] and VT-CPEM (Virginia Tech comprehensive Power-based Electric Vehicle Energy Consumption Model) [226], [227]. Among these models, VT-CPEM stands out as a highly-resolved power-based model that has demonstrated superior accuracy compared to other models [228].

Table 6.2: Summary of state-of-the-art energy consumption estimation models

Category	**Representative Model**	**Input Variables**	**Performance Metrics**				**Pros (P) and cons (C)**	**Reference**
Forward Model	ADVISOR	Vehicle features, Drive cycle	✓	✓			(P). Highly parameterized models;Validated and widely adopted. (C). Complex and long execution time. Difficult to implement in traffic simulation.	Markel, et al. [223]
	AUTONOMIE	Efficiency map			✓	✓	(P). Realistic evaluation (C). Relying on efficiency map;Limited flexibility of adoption	Kim et al. [229]
Powertrain-based model	ALPHA	State of Engines; Batteries; Transmission	✓	✓			(P). Capable of estimating effects of off-cycle technologies (e.g.,) on GHG emissions. (C). Hard to integrate with traffic simulation	Lee et al. [230]
Backward Model	VT-CPEM	Vehicle speed profile	✓		✓	✓	(P). More accurate and flexible. Simple to incorporate with microscopic traffic simulation. (C). No detailed description for vehicle parameters.	Fiori et al. [226]
	VT-CPPM	Vehicle speed profile				✓	(P). Validated using real data. Simple and fast to compute. (C). Does not consider the impact of cold engine start.	Fiori et al. [227]
Data-based Model	Wu's Model	Power train; Vehicle dynamic	✓			✓	(P). Computationally cheap after model training. (C). Result being dataset dependent.	Wu et al. [231]
Rule-based Model	Genikomsakis's Model	Motor, battery and transmission characteristics	✓	✓			(P). Accurate and computational efficient (C). Challenging to extent to macroscopic level and incorporate with traffic control.	Genikomsakis et al. [232]

Note: A-Accuracy; C.T.-Computation Time; F-Flexibility; G.A.-Generalization Ability

Among the above discussed literatures, Zhang et al. [214] developed a two-stage decision-making framework. This framework relied on an efficiency map of EVs, enabling the determination of a safety region in the initial stage, followed by the search for optimal energy efficiency within that region during the second stage. Despite that, the approach heavily relies on the availability of the efficiency map, which is typically undisclosed and kept confidential by automakers. To circumvent the reliance on the efficiency map, Pace et al. [217] employed the widely used VT-CPEM model [226], which calculates energy consumption at the link level while accurately considering the regenerative braking. A cell transmission model (CTM) was incorporated to capture traffic flow propagation, enabling the determination of total travel time across the entire network. Both total travel time and energy consumption were optimized as objectives in their study, but the method is limited to a very small and simple network due to the complexity and numerous variables involved in the CTM flow model. Li et al. [204] also conducted a study on the eco-driving system in the vehicle-to-everything (V2X) environment considering the mixed traffic of connected EVs (CEVs) and non-connected EVs (Non-CEVs). They constructed an optimization model that regulated vehicle speeds and signal timing plans at intersections, resulting in improved mobility and reduced energy. The study also examined network performance at various CEV penetration rates. However, the proposed non-linear and complex mathematical model was solved using heuristic algorithms, which incurred significant computation time and did not cater to real-time conditions.

Based on the discussion above, this chapter makes the following key contributions:

I. A thorough comparison of energy and traffic efficiency metrics has been conducted between human-driving electric vehicles (HDEVs) and CAEVs. This analysis provides readers with a comprehensive understanding of the performance differences of EVs with and without connectivity and automation.

II. An integrated energy consumption and total travel time optimization model was proposed to find a trade-off between the two parts. The objectives are achieved through the optimization of CAEVs' trajectories as well as the sig-

nal timing plans. The CAEVs are equipped with a CACC car-following model, which enhances traffic efficiency by regulating the traffic stream. Moreover, an accurate energy consumption computation method was employed, utilizing meticulously calibrated parameters derived from the work of Pace et al. [217].

III. Based on this optimization model, a simplified control method was further derived that eliminates the need for complex heuristic algorithms, ensuring a more efficient and effective solution. The computation time of the proposed method was verified to be applicable to real-time conditions.

6.2 Methodology

The study aims to achieve a trade-off between the energy consumption and total travel time of EVs by controlling vehicles' trajectory and intersection signal timing plans. Accordingly, this section will first present an accurate energy consumption estimation model, then introduce the formulated optimization problem and the simplified control strategies for both EVs and intersection signal controllers. All the notations used in this chapter can be found in Table 6.3.

The assumptions adopted in this study include the following:

1. The CAEVs in the study are 100% connected so that they can talk with each other as well as with the infrastructure (i.e., 100% valid V2V and V2I communication).

2. The communication was considered accurate and timely. i.e., the communication delay and mechanical reaction time were not considered.

3. For the different testing scenarios, the control variable method was adopted in computing the energy consumption of EVs. i.e., The various factors such as driving behavior, road smoothness, weather conditions, tire pressure, vehicle shape, and aerodynamic resistance of the exterior are assumed to be the same in different testing scenarios. Only the trajectory and speed profile were set as control variables.

4. The value of acceleration and deceleration rate were assumed to be constant with the value coming from literature.

Table 6.3: Notations

I	Set of all lanes
t_a	Time of arrival
V_a	Speed of arrival
a	Acceleration rate
a	Decceleration rate
V_{d1}	Desired speed for the first stage
V_{d2}	Desired speed for the second stage
T_i	Travel time on lane i
t_1	The start time of trajectory control
t_{i^d}	Departure time of the vehicle on lane i
t_{i^a}	Arrival time of the vehicle on lane i
$d_{\min}$	Minimum decceleration rate
$d_{\max}$	Maximum decceleration rate
$a_{\min}$	Minimum acceleration rate
$a_{\max}$	Maximum acceleration rate
$V_{\min}$	Minimum speed
V_f	Maximum speed/Free flow speed
t_0	The time at which the vehicle trajectories start to be controlled
L	The distance from the next intersection when the vehicle trajectories start to be controlled
V_0	Initial speed of the targeted vehicle
τ	Reaction time
N_i	Number of vehicles in front of the target vehicle
h	Headway
k	Control gain or feedback gain, distinguished by the subscripts
$a_{i,k}$	Acceleration rate for the i_th vehicle at time step k
$e_{i,k}$	Gap error for the i_th vehicle at time step k
${G_{p_i}}^k$	Green time for phase $p_i$during the k_th cycle
${G_{p_i^{\min}}}^k$	Required minimum green for each phase
t_e	Green extension
${N_{p_i}}^k$	Vehicle number to serve for phase $p_i$during the k_th cycle
${G_{p_i^{\max}}}^k$	Required maximum green for each phase

6.2.1 Energy Consumption Estimation Model

The VT-CPEM model was utilized for estimating the energy consumption in this Chapter. It enables the estimation of instantaneous power, energy consumption, and the state of charge (SOC) of the battery given the value of speed, acceleration, and various road characteristics. Initially, the power at the wheels $P_w(t)$ is computed using Eq. (6.1), where $v(t)$ represents the speed of vehicles and $a(t) = dv(t)/dt$ is the acceleration rate of the vehicle. For a better understanding, please refer to Table 6.4 for an explanation of the parameters used. The values of these parameters were obtained from [217], [226] based on the 2011 Nissan leaf as a reference.

Table 6.4: Parameter explanation and value based on the 2011 Nissan Leaf

Parameter	**Description**	**Value**	**Unit**
m	Vehicle mass	1521	$[kg]$
g	The gravitational acceleration	9.8066	$[m/s^2]$
θ	Road grade	0	
C_r	Rolling resistance parameters based on different road surface types	1.75	
c_1	Rolling resistance parameters based on different road conditions	0.0328	
c_2	Rolling resistance parameters based on vehicle tire types	4.575	
ρ_{Air}	Air mass density	1.2256	$[kg/m^3]$
A_f	The frontal area of the vehicle	2.3316	$[m^2]$
C_D	The aerodynamic drag coefficient of the vehicle	0.28	
η_{DL}	Driveline efficiency	0.969	
η_{EM}	The efficiency of the electric motor	0.979	
η_{BAT}	Battery efficiency	0.955	
$\eta_{RB}(t)$	Regenerative braking energy efficiency (the value is computed by Eq. (3))		
α	A parameter in the exponential relationship	0.079	

$$P_w(t) = [ma(t) + mg \cdot \cos(\theta) \cdot \tfrac{C_r}{1000}(c_1 v(t) + c_2) + \tfrac{1}{2}\rho_{Air} A_f C_D v^2(t) + mg \cdot \sin(\theta)] \cdot v(t) \tag{6.1}$$

Once the power at the wheels $P_w(t)$ is obtained, the power at the electric motor $P_T(t)$ can be computed using Eq. (6.2), considering the driveline effi-

ciency η_{DL} , the efficiency of the electric motor η_{EM} , and the efficiency of the battery η_{BAT}. When the EV is in traction mode, the energy flows from the motor to the wheels, and the power at the wheel is assumed to be positive ($P_W(t) \geq 0$). Conversely, in the regenerative braking mode, the energy flows from the wheels to the motor, causing the power at the wheels to be negative ($P_W(t) < 0$). In this scenario, the regenerative braking efficiency $\eta_{RB}(t)$ should be considered. The calculation of $\eta_{RB}(t)$ can be performed using Eq. (6.3), where α is a parameter that can be calibrated using real EV driving data.

$$P_T(t) = \begin{cases} \frac{P_W(t)}{\eta_{DL} \cdot \eta_{EM} \cdot \eta_{BAT}}, if\ P_W(t) \geq 0 \\ \\ P_W(t) \cdot (\eta_{DL} \cdot \eta_{EM} \cdot \eta_{BAT}) \cdot \eta_{RB}(t), \\ if\ P_W(t) < 0 \end{cases} \tag{6.2}$$

$$\eta_{RB}(t) = \begin{cases} e^{-\frac{\alpha}{|a(t)|}}, if\ a(t) < 0 \\ 0, if\ a(t) \geq 0 \end{cases} \tag{6.3}$$

Given the value of the above parameters, it is possible to compute energy consumption [kWh/km] by Eq. (6.4). Here x is the distance traveled in [km].

$$EC\left[\frac{\text{kW} \cdot \text{h}}{\text{km}}\right] = \frac{1}{3600 \cdot 1000} \int_0^t P_T(t)dt \cdot \frac{1}{x} \tag{6.4}$$

6.2.2 Energy and Travel Time Optimization Model

Utilizing the calibrated VT-CPEM model, the energy consumption of vehicles can be accurately estimated. Different from the HDEVs, CAEVs have the advantage of real-time trajectory and signal timing data availability which allows for dynamic adjustment of their speed and acceleration rates. As illustrated in Fig. 6.2, HDEVs (Fig. 6.2(a)) typically come to a complete stop, forming queues during the red signal, and then dissipate once the signal turns green. This stop-and-go behavior creates shockwaves and results in increased energy and travel time loss due to abrupt acceleration and deceleration. In this context, a smoother trajectory should be designed to reduce the number of stops by taking advantage of connectivity and automation (Fig. 6.2(b)).

In time instant t_a, when a CAEV approaches the intersection at a speed of V_a and encounters a red signal, trajectory control will be conducted. The goal is to minimize energy consumption and total travel time which is shown

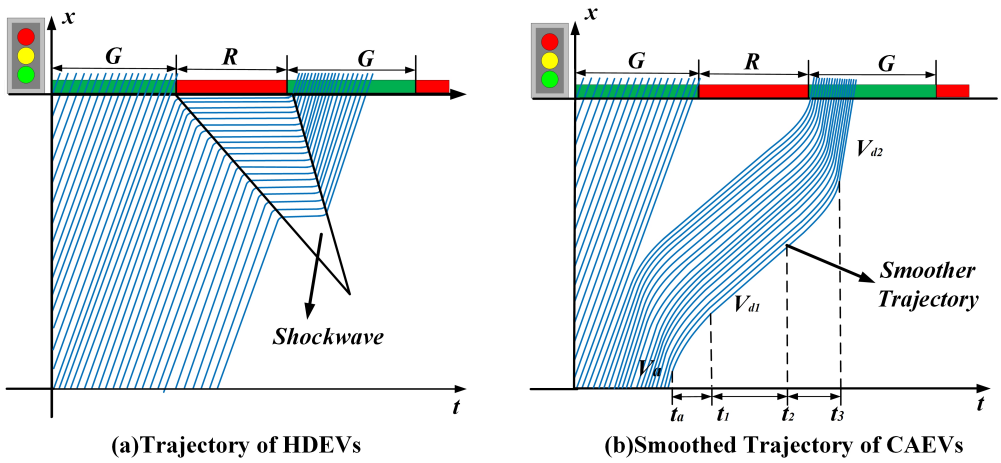

Figure 6.2: Space-time diagram. (a) The trajectory of HDEVs (b) Smoothed trajectory of CAEVs.

in Eq. (6.5). The calculation of energy consumption will be divided into three stages. In the first stage, the CAEV decelerates at a rate of d to reach the desired speed V_{d1}, then during the second stage, it maintains a constant speed from t_1 to t_2. In the third stage, it accelerates at a rate of a to reach V_{d2} from t_2 to t_3. In the first and third stages, the control variables include speed, deceleration/acceleration rate, and time duration, while in the second stage, the only variable is time duration, with the acceleration rate set to zero and the speed maintained at a stable level. The total travel time for a CAEV on all lanes is computed by $\sum_{i \in I} T_i$ ($i \in I$ represents the lane index) with T_i given by Eq. (6.6), where the t_i^d and t_i^a are the departure and arrival times of the vehicle on lane i.

To ensure feasibility and safety, for CAEV driving on a specific lane, several constraints need to be considered, as outlined in Eq. (6.7) to Eq. (6.14). These constraints include physical time constraints (Eq. (6.7)), minimum and maximum acceleration/deceleration limits (Eq. (6.8) to Eq. (6.9)), minimum and maximum speed limits (Eq. (6.10) to Eq. (6.11)), and kinematic constraints (Eq. (6.12) to Eq. (6.13)). In Eq. (6.5) and Eq. (6.14), V_f is the free flow speed and x represents the distance from the vehicle being controlled until it leaves the intersection.

$$
\begin{aligned}
&\min\{EC, TTT\} \\
&= \min\left\{\int_0^t P_T(t)dt \cdot \tfrac{1}{x}, \sum_{i\in I} T_i\right\} \\
&= \min\left\{\begin{array}{l} \left[\begin{array}{l} \int_{t_a}^{t_1} P_T(V(d,t),d)dt + \\ \int_{t_1}^{t_2} P_T(V_{d1},0)dt + \int_{t_2}^{t_3} P_T(V(a,t),a)dt \end{array}\right] \cdot \tfrac{1}{x}, \\ \sum_{i\in I} T_i \end{array}\right\}
\end{aligned} \tag{6.5}
$$

$$T_i = t_i^d - t_i^a \tag{6.6}$$

$$t_a \le t_1 \le t_2 \le t_3 \tag{6.7}$$

$$d_{\min} \le d \le d_{\max} \tag{6.8}$$

$$a_{\min} \le a \le a_{\max} \tag{6.9}$$

$$0 \le V_{d1} \le V_f \tag{6.10}$$

$$0 \le V_{d2} \le V_f \tag{6.11}$$

$$V_a + d(t_1 - t_a) = V_{d1} \tag{6.12}$$

$$V_{d1} + a(t_3 - t_2) = V_{d2} \tag{6.13}$$

$$V_a t_a + \frac{1}{2}d(t_1 - t_a)^2 + V_{d1}(t_2 - t_1) + V_{d1}t_2 + \frac{1}{2}a(t_3 - t_2)^2 = x \tag{6.14}$$

By solving the optimization model, the value of the control variables (e.g., speed, acceleration/deceleration rate) can be obtained. However, this approach is non-trivial since the model optimizes for a single vehicle only. For a network with high demand, the requirement for computation hardware will be high and it is time-consuming to obtain the solution for all vehicles simultaneously. Even when using vectors to represent the variables, generating timely solutions becomes unfeasible and thus impractical for applying the optimization technique in real-time. To overcome these limitations while maintaining the same objective, the optimization model was simplified, which is introduced in the subsequent section.

6.2.3 Simplified Trajectory Control

As depicted in Fig. 6.3, two main scenarios, "arrive on red" and "arrive on green," are typically encountered when a vehicle approaches an intersection [233]. The two scenarios were discussed separately. In the first scenario, vehicles that arrive on red are advised to decelerate to save energy, and they will keep a constant speed until the next green starts (Fig. 6.3 (a)). However, for those arriving on the green, the vehicle will be guided to accelerate within the remaining green time to avoid stopping (Fig. 6.3 (b)).

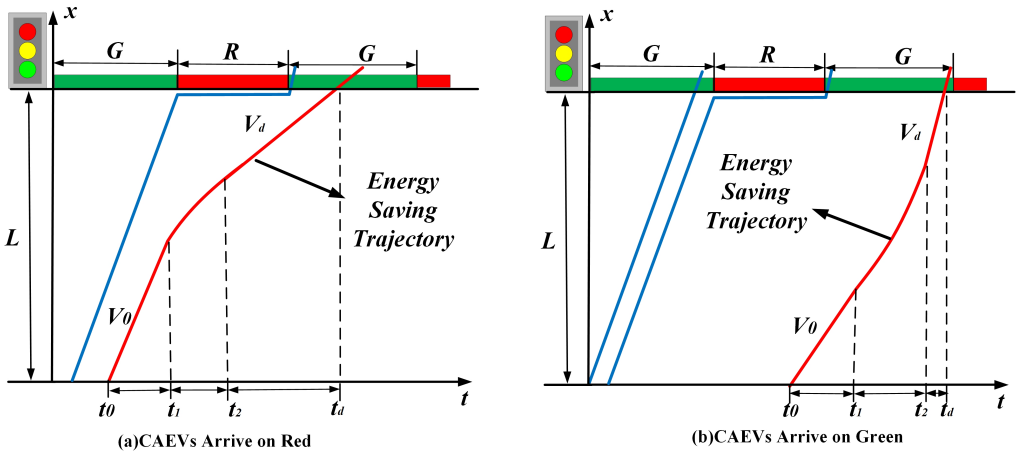

Figure 6.3: Illustration on trajectory control (a)Arrive on red (b)Arrive on green.

In Fig. 6.3, t_0 is the time at which the vehicle trajectories start to be controlled. At this point, the CAEVs have an initial speed of V_0 and are positioned L meters away from the next intersection. $t_1 - t_0 = \tau$ represents the reaction time. After which, from t_1 to t_2, the vehicles will either decelerate or accelerate to the desired speed V_d and they will leave the intersection at the time t_d.

Through the mathematical process, the relationships between these time instants were established in Eq. (6.15). Additionally, Eq. (6.16) serves as a criterion to determine whether it is necessary for the vehicle trajectory to be controlled, while Eq. (6.17) represents the kinematic formulation. Eq. (6.18) plays a critical role in ensuring that the departure time of the target vehicle is larger than the queue dissipating time. To estimate the dissipation time, it is assumed that the first vehicle in the queue can exit the intersection at

the start of the green signal in the next cycle. Utilizing CAV technology, the number of vehicles in front of the target vehicle, denoted as N_i, can be easily determined. By multiplying N_i by the headway h, the time it takes for the front vehicles to leave the intersection can be estimated (Eq. (6.19)). Finally, Eq. (6.20) was derived to determine the desired speed.

$$t_d - t_2 = t_d - t_0 - \tau - (t_2 - t_1) \tag{6.15}$$

$$V_0 > \frac{L}{t_d - t_0} \tag{6.16}$$

$$t_2 - t_1 = (V_0 - V_d^{'})/d \tag{6.17}$$

$$t_d - t_0 \geq t_{dissipation} \tag{6.18}$$

$$t_{dissipation} = t_{remain,red}^{\varphi_c} + N_i \cdot h \tag{6.19}$$

$$\begin{aligned} V_d^{'} = & d[(\tfrac{V_0}{d} + t_0 + \tau - t_d) + \\ & \sqrt{(\tfrac{V_0}{d} + t_0 + \tau - t_d)^2 - \tfrac{{V_0}^2}{d^2} + \tfrac{2}{d}(L - V_0\tau)}] \end{aligned} \tag{6.20}$$

Similar to the decelerating scenario, vehicles arriving on the green are suggested to accelerate. To determine the desired speed in this situation, formulations were derived from Eq. (6.21) to Eq. (6.24). However, it is important to note that the desired speed cannot exceed the free flow speed for both decelerating and accelerating cases. This restriction is established in Eq. (6.25) to ensure that the desired speed remains within a realistic and safe range.

$$V_0 \leq \frac{L}{t_d - t_0} \tag{6.21}$$

$$t_2 - t_1 = (V_d^{'} - V_0)/a \tag{6.22}$$

$$t_d - t_0 \geq t_{remain,green}^{\varphi_c} \tag{6.23}$$

$$\begin{aligned} V_d^{'} = & a[(\tfrac{V_0}{a} + t_d - t_0 - \tau) + \\ & \sqrt{(\tfrac{V_0}{a} + t_d - t_0 - \tau)^2 - \tfrac{{V_0}^2}{a^2} + \tfrac{2}{a}(L - V_0\tau)}] \end{aligned} \tag{6.24}$$

$$V_d = \min\{V_f,\ V_d^{'}\} \tag{6.25}$$

In the decelerating scenario, the trajectory control strategy can be applied to all CAEVs entering the intersection, as decelerating is not constrained by the leading vehicle. On the contrary, for the accelerating scenario, the behavior of the following vehicle will be confined by the leading vehicle. In this

case, the accelerating strategy is applied exclusively to the leading vehicle, while a Cooperative Adaptive Cruise Control (CACC) strategy is employed for the following vehicles. This approach ensures coordinated and cooperative movement among the vehicles, with the leading vehicle setting the pace and the following vehicles adjusting their speeds accordingly.

The CACC car-following model been adopted in this chapter is built upon the research of Milanés et al. and Xiao et al. [234]–[236]. The model is categorized into three distinct modes: (i) cruising control mode, (ii) gap control mode, and (iii) gap-closing control mode. The cruising mode aims to eliminate the deviation between the vehicle speed and the desired speed which is given as Eq. (6.26). In this equation, k is the control gain to determine the rate of speed error for $a_{i,k}$ which is the acceleration rate for the ith vehicle at time step k. v_{des} is the desired speed and $v_{i,k-1}$ indicates the speed of the ith vehicle at time step $k-1$. In the gap control mode, the acceleration $a_{i,k}$ is modelled as a second-order transfer function as given by Eq. (6.27). $e_{i,k}$ is the gap error for vehicle i at time step k. k_1, k_2 are feedback gains, and $v_{i-1,k-1} - v_{i,k-1}$ represents a speed difference with the preceding vehicle. As for the gap-closing mode, it is derived by tuning the parameters of the gap-control mode. In Eq. (6.28), $\dot{e}_{i,k-1}$ is the derivative of the gap deviation ($e_{i,k-1}$) which is used to modify the gap error. The detailed model explanation, as well as the specific values of the controlling and feedback gains (i.e., k, k_1, k_2, k_p, k_d) can be found in [235].

The CACC allows vehicles to form platoons by maintaining small inter-vehicle gaps and operating at a consistent speed and enabling smooth and coordinated acceleration and deceleration among vehicles in a platoon. This cooperative behavior helps to minimize unnecessary speed changes and harsh braking, which potentially reduces energy consumption and total travel time.

$$a_{i,k} = k \cdot (v_{des} - v_{i,k-1}) \tag{6.26}$$

$$a_{i,k} = k_1 \cdot e_{i,k} + k_2 \cdot (v_{i-1,k-1} - v_{i,k-1}) \tag{6.27}$$

$$v_{i,k} = v_{i,k-1} + k_p \cdot e_{i,k-1} + k_d \cdot \dot{e}_{i,k-1} \tag{6.28}$$

After determining the desired speed, deceleration/acceleration rate, and time duration, the corresponding energy consumption can be computed using Eq. (6.29).

$$\begin{aligned} EC &= \int_0^t P_T(t)dt \cdot \tfrac{1}{L} \\ &= \left[\begin{array}{l} \int_{t_0}^{t_1} P_T(V_0, 0)dt + \\ \int_{t_1}^{t_2} P_T(V(d,0), d)dt + \int_{t_2}^{t_d} P_T(V_d, 0)dt \end{array} \right] \cdot \tfrac{1}{L} \end{aligned} \tag{6.29}$$

6.2.4 Signal Timing Control

To achieve the objective of reducing energy consumption and total travel time, the signal timing plan will be controlled in a more intelligent way rather than utilizing a fixed-time control strategy. It will follow an actuated control principle leveraging the capabilities of CAVs. The following Fig. 6.4 illustrates the closed-loop control framework for the proposed trajectory and signal control strategy. As shown in the figure, with the initial traffic parameters as input, the traffic can be simulated, then the vehicle trajectories can be optimized based on the signal timing plan (by V2I communication). Additionally, vehicles will form platoons using CACC (based on V2V). After the trajectory control being applied to all vehicles, their traveling speed will be changed which results in a new traffic flow pattern within each cycle. Based on the updated flow distribution, the signal timing plan was again optimized utilizing the aggregate traffic volume in each approach.

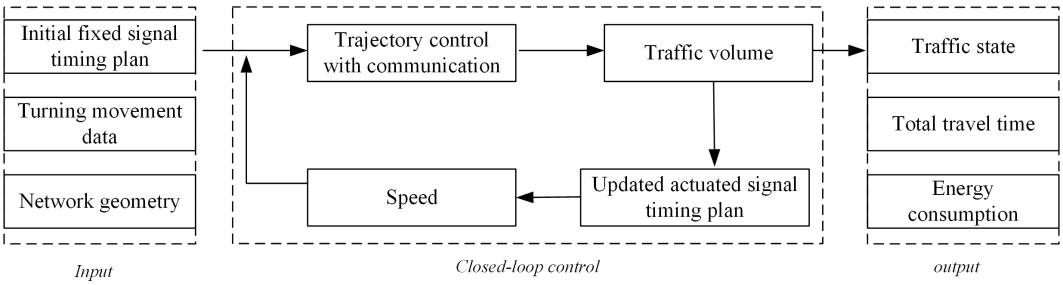

Figure 6.4: The closed-loop trajectory and signal control framework

Eq. (6.30) gives the way to calculate the green time, where ${G_{p_i^{\min}}}^k$ is the required minimum green for each phase (set to be 5s in this study), t_e is the green extension (set to be 3s in this study), and ${N_{p_i}}^k$ is the vehicle number

to be served for phase p_i during the k_{th} controlling cycle. The green for each phase is constrained to the minimum and maximum green as shown in Eq. (6.31). The simplified trajectory and signal control strategy can be generated quickly to sufficiently meet the requirement of real-time control.

$$G_{p_i}{}^k = G_{p_i^{\min}}{}^k + t_e \cdot N_{p_i}{}^k \tag{6.30}$$

$$G_{p_i^{\min}}{}^k \leq G_{p_i}{}^k \leq G_{p_i^{\max}}{}^k \tag{6.31}$$

6.3 Case Study

6.3.1 Simulation Settings

In this section, a corridor comprising eight intersections along Jasper Avenue in the downtown area of the City of Edmonton, Canada (Fig. 6.5) was selected to test the proposed method. The selected site begins at the intersection of 112 Street @ Jasper Avenue and extends to 105 Street @ Jasper Avenue. The corridor is approximately 850 meters long, with a speed limit of 50 km/h, which is also considered the free-flow speed for this study. The corridor's geometry and the number of lanes were accurately represented in the simulation, based on real-world field information.

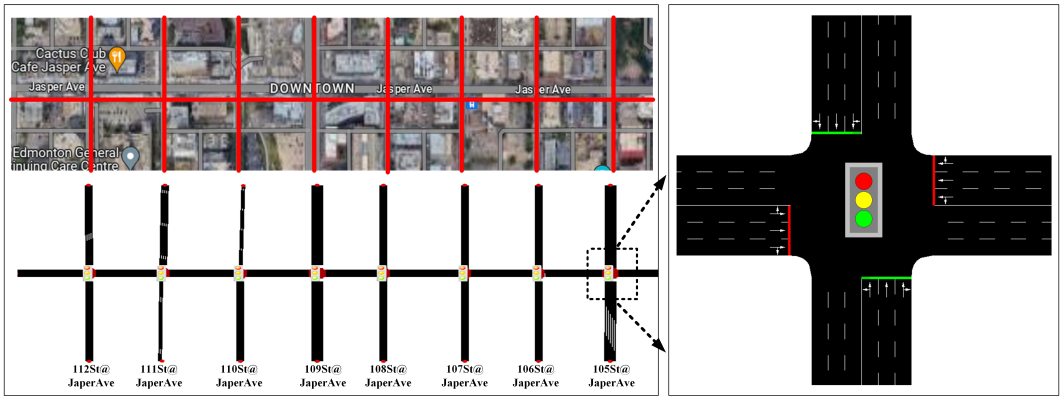

Figure 6.5: Testing corridor: Jasper Avenue.

Both peak and non-peak hour traffic demands were tested, with the traffic movement data of each intersection obtained from the City of Edmonton. The initial fixed signal timing plans were also obtained from the field, with the

cycle length of some intersections being 90 seconds and the others being 110 seconds. The intersection layout is shown in Fig. 6.5 where the permitted left-turn phase was adopted and there is no exclusive left-turn lane designed to maximize the road capacity utilization.

According to previous studies, the reaction time of individual drivers typically falls within the range of 1.0 to 2.0 seconds, with a probability of 99.5%. To ensure both safety and comfort, it is reasonable to assume an average acceleration rate of 1.4 m/s^2 and a deceleration rate of -2.0 m/s^2 [233]. Additionally, a reaction time of 1.0 seconds was assumed for the CAEVs, aligning with the lower end of the typical range observed in driver behavior. The simulation was conducted with a time step of one second, and the overall simulation duration was set to 5,400 seconds for the peak hour and 4,200 seconds for the non-peak hour. These time durations ensure that all vehicles within the simulation complete their trips and exit the simulation successfully. In the case study, three different scenarios were tested and compared:

(i) All vehicles are HDEVs without any trajectory control, and the intersection timing plans were fixed. For the HDEVs, the embedded car-following model is the Intelligent Driver Model (IDM) [237];

(ii) All vehicles are CAEVs, and the embedded car-following model is CACC where vehicles will communicate and cooperate to maintain a smaller inter-vehicle gap and achieve a more stable traffic flow. At the same time, the signal timing plan will be in an actuated controlling mode.

(iii) All vehicles are CAEVs with CACC and the proposed trajectory control. Real-time communication between vehicles and infrastructure allowed for the exchange of information. The vehicle trajectories were actively controlled every 10 seconds, and the signal timing plan was updated based on the latest traffic information. For all three scenarios, the energy and traffic efficiency-based metrics will be calculated.

6.3.2 Overall Performance Comparison

This section presents the findings of the case study conducted in various scenarios to evaluate the efficacy of the proposed method in enhancing overall system

performance and balancing traffic and energy efficiency. Table 6.5 showcases the values of the overall performance indicators which are calculated based on the parameters of a 2011 Nissan Leaf.

Table 6.5: Performance indicators for different scenarios

	Control Method	**TTT (s)**	**AWT (s)**	**AS (km/h)**	**TEC (kWh)**	**AEC (kWh/ 100km)**	**Summary**
Peak	HDEVs	982,125.76	65.60	24.41	901.96	19.52	Min EC
(TVN=9,076)	CAEVs_SC	583,360.81	10.96	31.57	1,122.11	24.29	Min TTT
(ATL=509.27)	CAEVs_SC_TC	601,553.65	17.40	30.24	962.76	20.84	**Trade-off**
Non-Peak	HDEVs	405,477.92	17.52	30.74	604.71	20.13	Min EC
(TVN=5,927)	CAEVs_SC	339,199.84	5.72	34.34	721.07	23.80	Min TTT
(ATL=506.95)	CAEVs_SC_TC	345,250.71	11.53	33.48	614.63	20.63	**Trade-off**

*TVN: Total Vehicle Number(veh); ATL: Average Travel Length(m); TTT: Total Travel Time(s); AWT: Average Waiting Time(s); AS: Average Speed (m/s); TEC: Total Energy Consumption (kWh); AEC: Average Energy Consumption per Vehicle per 100km (kWh/100km).

As shown in the Table, regardless of peak or non-peak hours, the first scenario where all vehicles are HDEVs exhibits significantly higher TTT and AWT compared to the other two scenarios with CAEVs. However, the TEC and AEC of the network are lower. Referring to Fig. 6.1 in the introduction, the optimal speed for achieving the lowest energy consumption is approximately 24.14 km/h, which explains why the first scenario exhibits the highest total travel time while generating the lowest energy consumption.

In the second scenario, the CACC car-following model was implemented for all CAEVs, enabling vehicles to form platoons with reduced inter-vehicle distances and reaction time. This tight coupling among CAEVs significantly enhances the capacity of the roadway. Additionally, the green time dynamically adjusts based on the number of approaching vehicles, providing greater flexibility with reduced total travel time and improved average speed. However, the increase in average speed leads to a higher energy consumption, and the energy consumption increment resulting from the speed increase outweighs the energy consumption reduction due to reduced travel time. Consequently, the TEC and AEC is higher than in the first scenario.

In the third scenario, to achieve a balance between energy consumption and total travel time, additional trajectory control is implemented on the base of the second scenario. This control aims to ensure a smoother trajectory

while reducing travel time. By incorporating this control logic, the third scenario reaches a compromise between energy consumption and total travel time, resulting in lower energy consumption compared to the second scenario and lower total travel time compared to the first scenario.

Fig. 6.6 further analyzes the value of TTT and AEC in the three scenarios, and the study particularly focus on the second and third scenarios, where the impact of the proposed trajectory control on the performance of CAEVs can be explicitly investigated. In comparison to the second scenario, where all vehicles are CAEVs without trajectory control (CAEVs_SC), the third scenario, which incorporates the proposed trajectory control (CAEVs_SC_TC), shows a noteworthy decrease of 14.20% in AEC (Fig. 6.6 (a)), despite a slight increase of 3.12% in TTT. Similarly, Fig. 6.6 (b) confirms this trend, despite the non-peak hour case shows a slightly smaller magnitude of increase and decrease compared to the peak hour condition.

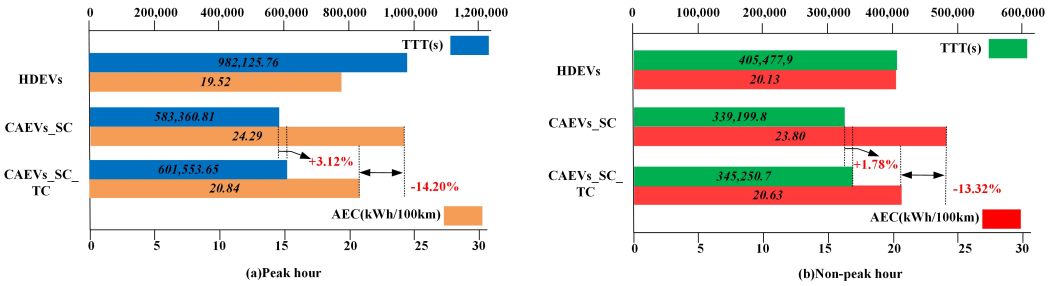

Figure 6.6: TTT and AEC comparison in different scenarios (a)Peak hour (b)Non-peak hour.

These findings further support the conclusion that the application of the proposed trajectory control method can achieve a balance between energy and travel efficiency, resulting in reduced energy consumption without significantly sacrificing travel time, during both peak and non-peak hours.

6.3.3 Number of Stops Analysis

Fig. 6.7 presents the frequency distribution histogram depicting the number of stops for vehicles. The index, comprising maximum, minimum, average, and median values, was calculated to further analyze the data. Notably, the median remains consistent across all scenarios, with a value of 1.0. However, there are

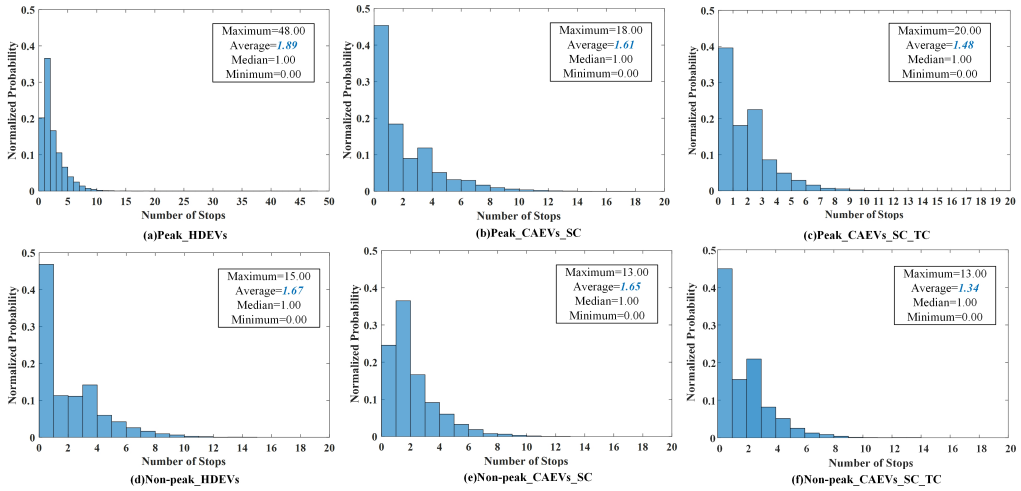

Figure 6.7: Number of stops in different scenarios (a)Peak-HDEVs (b)Peak-CAEVs-SC (c)Peak_CAEVs_SC-TC (d)Non-peak-HDEVs (e)Non-peak-CAEVs-SC (f)Non-peak-CAEVs-SC-TC.

variations in the average values observed under different circumstances. The proposed control method yields significant reductions in the number of stops for vehicles. In peak hour conditions, the average number of stops decreases to 1.48, while during non-peak hours, it decreases to 1.34.

Moreover, the proposed method (i.e., CAEVs-SC-TC) results in a distribution that is predominantly concentrated in the region characterized by smaller values. This indicates that the combined approach of trajectory and signal control effectively reduces the occurrence of frequent stops, leading to smoother vehicle movements and less start-up loss.

6.3.4 Trajectory Analysis

The time-space diagram presented in Fig. 6.8 illustrates the trajectories of vehicles heading eastbound during the peak hour.

In Fig. 6.8(a), a prominent observation is the occurrence of a shockwave, resulting in the blockage of numerous vehicles at intersections, particularly at 110 St @ Jasper Ave, 109 St @ Jasper Ave, and 108 St @ Jasper Ave. This congestion leads to long queues and extended waiting times for vehicles. However, a notable improvement can be observed in Fig. 6.8(b) when HDEVs are replaced with CAEVs. Due to the applied CACC car-following model and

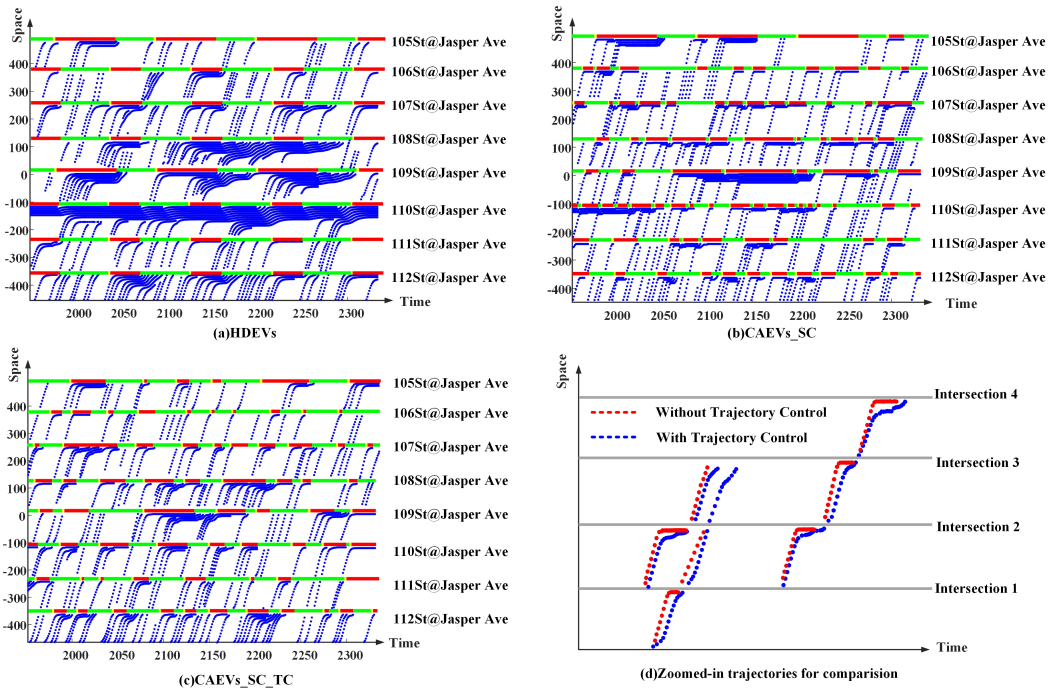

Figure 6.8: Eastbound vehicle trajectories in different scenarios (a)HDEVs (b)CAEVs-SC (c)CAEVs-SC-TC (d)Zoomed-in trajectories for comparison.

actuated signal control, the traffic stream is more stable and there are fewer queues. Nevertheless, it is important to note that in Fig. 6.8(b), the deceleration and acceleration rates change sharply because of the reduced reaction time and headway between the CAEVs. In Fig. 6.8(c), similar to Fig. 6.8(b), the queues dissipate efficiently. Furthermore, benefiting from the proposed trajectory control, most vehicles can go through the intersection during the green time. To provide a more detailed analysis of the trajectories, Fig. 6.8(d) offers zoomed-in images for a clearer view. In these images, the red lines depict trajectories without control while the blue lines represent trajectories with control. It is evident from the figure that the blue lines effectively avoid unnecessary stops, showcasing a considerably smooth pattern which is crucial in reducing energy consumption.

Overall, the comparison between the different scenarios in Fig. 6.8 highlights the advantages of employing the CAEVs-SC-TC control strategy, as it leads to faster queue dissipation and smoother trajectories.

6.3.5 Signal Timing Plans

In Fig. 6.9, the signal timing plans for each intersection in different scenarios were presented. In the first scenario, where all vehicles are HDEVs, a fixed signal timing plan is employed. Six intersections have a cycle length of 90 seconds, while two intersections have a cycle length of 110 seconds. The duration of the green time is indicated in the figure. However, in the other two scenarios, the signal timing adapts dynamically to real-time traffic conditions. The green duration adjusts based on the changing number of vehicles in each lane. This flexible and actuated control approach increases the opportunity for vehicles to pass through intersections during the green phase. As a result, it significantly enhances traffic efficiency and allows for improved traffic flow.

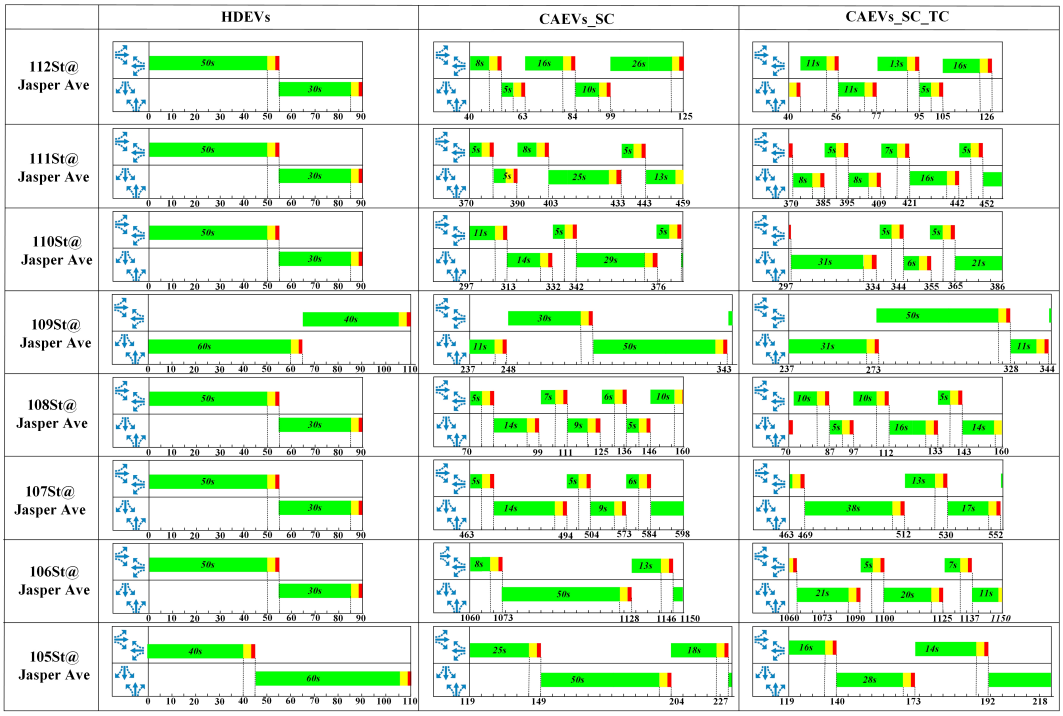

Figure 6.9: Signal timing plans in different scenarios.

6.3.6 Capability for real-time application

Typically, problems related to signal control and traffic optimization were solved by heuristic algorithms, such as the Genetic algorithm (GA) [126] and particle swarm optimization (PSO) algorithm [238]. To obtain a more robust

solution, Li et al. [204] further combined both GA and PSO. However, GA and PSO typically express the following drawbacks:

Computational Complexity: Both GA and PSO can be computationally intensive. The selection, crossover, and mutation operations for GA can require a substantial number of computational resources. Similarly, the PSO requires several rounds of iterations before finding the optimal solution.

Parameter Tuning: The performance of GA and PSO is sensitive to the choice of parameters. GA often requires careful tuning of parameters such as population size, mutation rate, and crossover rate to achieve good performance. This tuning process can be time-consuming and may not guarantee optimal results for all problem domains. Finding the right parameter values for PSO for a specific problem can also be challenging.

Scalability Issues: Both GA and PSO may struggle to handle high-dimensional search spaces efficiently, as the probability of finding good solutions decreases with increasing dimensionality.

Table 6.6 displays the computation time of the proposed method which is significantly lower than those GA and PSO-based methods in solving similar optimization problems. According to the recommendations from some key organizations, such as ETSI and 5GAA, most of the use cases (e.g., green light optimized speed advisory (GLOSA)) in the CAV environment requires an end-to-end delay that is lower than 100ms, which includes both communication and computation time [239], [240]. To conclude from the Table, it's apparent that the computation time for those utilizing a heuristic algorithm is too long compared to the required millisecond scale, which cannot fulfill the requirement of dynamic control in a CAV environment. Furthermore, the solving time increases significantly with the increased intersection numbers, vehicle numbers, and network scale. It's hard to get the optimal solution, let alone a real-time application.

In contrast, the proposed method does not rely on any heuristic solving algorithm and only requires simple numerical operations which can save a lot of computational effort. In addition, the proposed method can be solved in a distributed framework, which enables generating the solution for all vehicles

Table 6.6: Summary of state-of-the-art energy consumption estimation models

Problem	**Method**	**Network Scale**	**Computational CPU Time**	**Remark**	**Can be used in Real-time?**	**Reference**
Route and Signal Timing Optimization	GA	10 intersections	10s/vehicle	Time increases with vehicle and network scale.	NO	Sun et al. [126]
Signal Timing Optimization	PSO	20 intersections	3.18s/vehicle	Time increases with vehicle and network scale.	NO	Garcia-Nieto et al. [238]
Trajectory and Signal Timing Optimization	The proposed method	8 intersections	**12ms/vehicle**	The solution for all individuals can be obtained simultaneously. Computation time does not increase with number of vehicle	**YES**	This dissertation

simultaneously. Therefore, the solving time will not increase along with the increase of network scale and demand level.

6.4 Conclusions

This chapter presents a novel trajectory and signal control method that aims to strike a balance between reducing energy consumption and minimizing total travel time with the future existence of CAEVs. Initially, the VT-CPEM model was utilized to compute the energy consumption to achieve a more accurate estimation. Then, a CACC algorithm was employed for CAEVs to simulate their car-following behavior and regulate the traffic. By implementing CACC, the total travel time was significantly reduced, and the average speed increased substantially. However, it was observed that the increased speed resulted in higher energy consumption, which outweighed the energy saved from reduced total travel time.

To address this issue, a trajectory control method was further imposed on CAEVs when they entered the intersections. They are suggested to either decelerate during the remaining red time or accelerate in the remaining green, and the desired speed was calculated based on the signal timing information. Moreover, an actuated signal control strategy was incorporated to dynamically

update the signal timing plan based on the latest trajectories. By carefully avoiding abrupt stops and ensuring a continuous flow, the proposed method provides a smoother trajectory while saving travel time.

The effectiveness of the proposed method was thoroughly assessed through a comprehensive case study conducted on a corridor located in Edmonton, Canada. Utilizing the simulation techniques, both peak and non-peak hour demands were tested. The analysis of key performance indicators, including TEC, AEC, TTT, ATT and the number of stops, unequivocally demonstrated the ability of the proposed method to enhance traffic efficiency while concurrently reducing energy consumption. Compared with existing complex optimization-based approaches, the proposed method is of practical real-time applicability and the findings of this study suggest the potential of achieving a greener and more efficient traffic curriculum, particularly with the anticipated emergence of CAEVs.

However, it is important to note that in this study, certain assumptions were made regarding the deceleration and acceleration rates, which may not always align with real-world scenarios. As part of the ongoing research, it is necessary to consider the deceleration and acceleration rates as variables to explore optimal values that better reflect real-world driving conditions.

Chapter 7

Conclusions and Future Extensions

As urban cities worldwide grapple with burgeoning populations, traffic congestion, and environmental concerns, the integration of CAV and EV technology within the framework of a Smart City offers a beacon of hope for sustainable urban development. These interconnected elements promise not only to shape the way we commute but also to address critical issues of energy efficiency, reduced emissions, and enhanced mobility within our urban environments. In this exploration, the dissertation delves into the intricate interplay between CAVs, EVs, and the Smart City concept, illuminating the pathways by which these technologies are reshaping our urban ecosystems.

This research predominantly tackles challenges in urban arterial traffic demand management and control, with a specific focus on enhancing traffic efficiency through the incorporation of CAV technology. The dissertation introduces innovative models and algorithms pertaining to vehicle routing, signal timing optimization, CAV-DL management, and vehicle trajectory control. Fig. 7.1 succinctly recaps the research content of the core chapters in this dissertation as well as their interconnectedness.

(1) Firstly, the dissertation centered on the integration of adaptive signal control mechanisms with dynamic routing. By describing the traffic dynamics with CAVs, the proposed framework captured the interaction between traffic control and demand management using a closed-loop control framework which can realize a UO or SO traffic state.

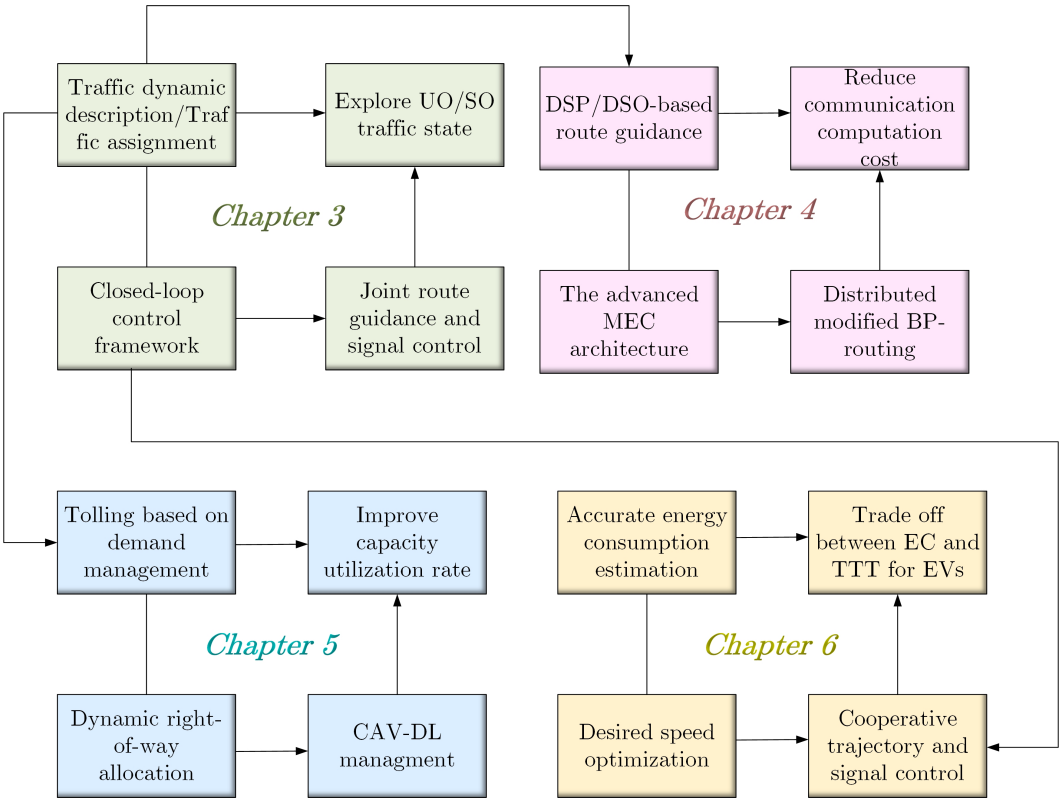

Figure 7.1: Recap of the core chapters in this dissertation.

(2) Secondly, the dissertation explored the implementation of a distributed routing control structure, designed to seamlessly mesh with MEC and 5G infrastructure, providing a more holistic solution for CAV traffic management. The proposed backpressure-based routing algorithm can not only improve traffic efficiency but also reduce communication and computation time when compared with the DSP and DSO control.

(3) Thirdly, in pursuit of advancing CAV adoption, the dissertation extended its efforts to encompass the design and implementation policies for CAV-DLs. Two methods, namely dynamic right-of-way allocation and tolling were presented and these methods enhanced the utilization of urban roadway capacities.

(4) Lastly, in response to the evolving landscape of EVs and the imperative to cultivate green and intelligent cities, the dissertation proposed a novel trajectory and signal control method combining the features of CAVs and EVs. The proposed method successfully reached a trade-off between energy

consumption and total travel time of EVs.

7.1 Dissertation Contribution

Each chapter of the dissertation, although centered on distinct research content, enriched the existing literature by introducing innovative ideas, methodologies, and problem-solving algorithms. The control and management strategies derived from this research can offer valuable guidance and shed some light on the practical implementation of CAV technologies. The detailed contributions of the four main tasks in this dissertation can be encapsulated as follows.

The first task focused on joint routing and signal control (chapter 3): This chapter proposed a DRG-SC model to improve traffic efficiency. Initially, it charted the design of a comprehensive data processing, information communication, and transmission protocol for executing DRG-SC within the context of the MEC-enabled CAV environment. A detailed description of the roles of vehicles, infrastructure, and the MEC was presented which can help practitioners to test the algorithm in corresponding use cases. Subsequently, this chapter formulated a DRG-SC model to capture the interaction between routing and signal control. Diverging from traditional approaches that frame the DRG-SC issue as a mathematical optimization problem, the approach decentralized the route strategy, empowering individual vehicles to select either UO or SO route. The model also incorporated the critical impact of intersection delay, a facet often overlooked even by the most popular route planners such as Google Maps. Lastly, this chapter specifically discussed computation time, probing the efficiency of the proposed method across varying core configurations through the lens of parallel computing techniques. The result advances the quantitative understanding of a distributed framework in ameliorating computation efficiency.

The second task focused on the distributed DRC problem (chapter 4): This chapter discussed the limitations of two widely used algorithms, namely DSP and DSO, employed for addressing the DRC problem. Both DSP and DSO necessitate complete information about the entire traffic network to

generate a routing solution, incurring significant communication costs. Furthermore, DSO is usually complex to solve and may not offer timely solutions in a CAV environment. In response to this challenge, firstly, a distributed backpressure-based routing algorithm was proposed, and the backpressure routing was designed to provide scalable DRC strategies utilizing only local information. Then, the backpressure mechanism in the proposed strategy was defined as the difference in the squared ratio of link density and jam density between two adjacent links which avoids the unrealistic point queue assumption in the original backpressure routing algorithm. Lastly, the performance of the proposed method was rigorously evaluated by conducting a comparative analysis against the DSP and DSO control. This evaluation encompasses a comprehensive exploration of control effectiveness, algorithmic complexity, and computation time. The performance of the proposed method is better than the DSP and can even compute with the DSO, while the communication and computation time is far below the DSP and the DSO. As such, the proposed method can be appropriately applied to the MEC-enabled CAVs.

The third task focused on CAV-DLs management (chapter 5): This chapter explored the way to better manage road capacity and promote CAVs, considering the existence of CAV-DLs. Firstly, two approaches are proposed to reach the goal, including dynamic right-of-way allocation and tolling. The dynamic right-of-way allocation was achieved by monitoring the capacity utilization rate of the CAV-DLs. The CAV occupancy on the dedicated lane was predicted using the Kalman Filter method, and the CAV-DLs can be used as GLs when they are vacant. In the second approach, a dynamic tolling approach has been designed to allow HDVs to use the CAV-DLs. Different from existing tolling strategies, the toll rate is calculated in real time and changes with the travel time difference between the CAV-DLs and the GLs. Then, the strengths and weaknesses of the two lane management strategies were compared and analyzed. Lastly, suggestions were given from both the technical and policy implementation points of view. The contents presented in this chapter can benefit both traffic policymakers and practitioners in designing and making the regulations for the utilization of CAV-DLs.

The fourth task focused on the trajectory and signal control for CAEVs (chapter 6): Considering the great possibility of CAEVs being applied in the future, this chapter explored the benefits of CAVs on EVs. Firstly, this chapter conducted a thorough comparison of energy and traffic efficiency metrics between HDEVs and CAEVs. This analysis provides readers with a comprehensive understanding of the performance differences of EVs with and without connectivity and automation. Secondly, a mathematical model designed to minimize energy consumption and total travel time through the optimization of CAEVs' trajectories was proposed. The model employs a more accurate energy consumption computation method, utilizing meticulously calibrated parameters. Based on this optimization model, a simplified control method that eliminates the need for complex heuristic algorithms was further derived, ensuring a more efficient and effective solution. Lastly, the chapter strikes a balance between reducing energy consumption and optimizing travel time. The work in this chapter provides insight into how to exploit CAV technology to promote and benefit EVs.

7.2 Limitations and Future Extensions

Although the research made some valuable contributions to the body of knowledge, there are some limitations and possibilities for future extensions. In general, the research within this dissertation, in its current form, lacks consideration for pedestrians and other traffic modes, leaving out crucial elements of real-world traffic dynamics. Furthermore, the validation process primarily relies on traffic simulations, which, although valuable, may not faithfully replicate the complexities of real-world conditions. To bolster the credibility of the findings, the integration of field tests is strongly recommended in future work. These on-road assessments could offer a more precise gauge of how the proposed method functions in practical, real-world scenarios. To look at specifically on each chapter, the limitations and future work were summarized below:

(1) For solving the DRG-SC problem, the study operated under the as-

sumption of 100% accurate communication without incorporating any communication latency. In future work, an essential component to be considered is to integrate the network simulator (e.g. OMNET++) to simulate communication in a CAV network. It enables the assignment of different weights for the latency of data transmission at different communication levels (local or networkwide), facilitating a quantitative assessment of the impact of latency on control strategies.

(2) In future work, a valuable extension for the route guidance would be to provide customized navigation services to CAVs according to their preferences. Other route properties will be considered in addition to the travel time. For example, the toll status, the road types (freeway or arterial), and the number of turns (left turn and U-turn) can be included as new metrics when designing the routing strategy. This type of personalized routing service would be more attractive for highly intelligent CAVs. What's more, the collectors and local roads were not considered in the route guidance problem, which connects directly from traveler's home to the main roads. It's necessary to incorporate them in the route planning and try to deliver "door to door" route service to the road users.

(3) In the CAV-DL management, a more detailed investigation on the value of headway for CAVs and HDVs should be conducted, since it is the key factor determining the capacity utilization rate at the intersections. Although the qualitative analysis results will be similar, distinct headway values will result in different quantitative control effectiveness. In addition, the travelers' income level may impact their acceptance of the toll rate and thus influence the enforceability of the tolling policy. Therefore, a valuable extension for this study may focus on the classification of the value of VOT for different income groups and designate different toll rates for different groups.

(4) In the trajectory and signal control for CAEVs, it is necessary to calibrate the energy consumption estimation model for EVs using realistic field-collected data, especially considering the weather impacts. By incorporating actual data into the model, the precision can be improved, and its validity in practical applications will be ensured. In the signal control, although the

actuated control strategy was utilized to dynamically change the timing plan, the signal coordination was not included. The optimization for the offset of the intersections along the corridor can further improve traffic efficiency, and a novel signal control strategy designed especially for CACC vehicles would be beneficial.

References

[1] S. J. Palmisano, "A smarter planet: The next leadership agenda," *IBM. November*, vol. 6, pp. 1–8, 2008.

[2] D. L. Greene, H. H. Baker Jr, and S. E. Plotkin, "Reducing greenhouse gas emissions from us transportation," 2010.

[3] A. Eskandarian, C. Wu, and C. Sun, "Research advances and challenges of autonomous and connected ground vehicles," *IEEE Transactions on Intelligent Transportation Systems*, vol. 22, no. 2, pp. 683–711, 2019.

[4] Z. Xu, X. Li, X. Zhao, M. H. Zhang, Z. Wang, *et al.*, "Dsrc versus 4g-lte for connected vehicle applications: A study on field experiments of vehicular communication performance," *Journal of advanced transportation*, vol. 2017, 2017.

[5] S.-Y. Lien, D.-J. Deng, C.-C. Lin, *et al.*, "3gpp nr sidelink transmissions toward 5g v2x," *IEEE Access*, vol. 8, pp. 35 368–35 382, 2020.

[6] S Standard, "J3016b: Taxonomy and definitions for terms related to driving automation systems for on-road motor vehicles-sae international," 2018.

[7] E. Shi, T. M. Gasser, A. Seeck, and R. Auerswald, "The principles of operation framework: A comprehensive classification concept for automated driving functions," *SAE International Journal of Connected and Automated Vehicles*, vol. 3, no. 12-03-01-0003, pp. 27–37, 2020.

[8] M. M. Rana and K. Hossain, "Connected and autonomous vehicles and infrastructures: A literature review," *International Journal of Pavement Research and Technology*, vol. 16, no. 2, pp. 264–284, 2023.

[9] A. Biswas and H.-C. Wang, "Autonomous vehicles enabled by the integration of iot, edge intelligence, 5g, and blockchain," *Sensors*, vol. 23, no. 4, p. 1963, 2023.

[10] S. Kekki, W. Featherstone, Y. Fang, *et al.*, "Mec in 5g networks," *ETSI white paper*, vol. 28, no. 2018, pp. 1–28, 2018.

[11] L. Liu, C. Chen, Q. Pei, S. Maharjan, and Y. Zhang, "Vehicular edge computing and networking: A survey," *Mobile networks and applications*, vol. 26, pp. 1145–1168, 2021.

[12] J. Y. Yong, V. K. Ramachandaramurthy, K. M. Tan, and N. Mithulananthan, "A review on the state-of-the-art technologies of electric vehicle, its impacts and prospects," *Renewable and sustainable energy reviews*, vol. 49, pp. 365–385, 2015.

[13] J. Hagman, S. Ritzén, J. J. Stier, and Y. Susilo, "Total cost of ownership and its potential implications for battery electric vehicle diffusion," *Research in Transportation Business & Management*, vol. 18, pp. 11–17, 2016.

[14] C. Hagem, S. Kverndokk, E. Nævdal, and K. E. Rosendahl, "Policies for electrification of cars in the short and long run," *Transportation Research Part D: Transport and Environment*, vol. 117, p. 103 606, 2023.

[15] H. Chai, H. M. Zhang, D. Ghosal, and C.-N. Chuah, "Dynamic traffic routing in a network with adaptive signal control," *Transportation Research Part C: Emerging Technologies*, vol. 85, pp. 64–85, 2017.

[16] Y.-C. Chiu, J. Bottom, M. Mahut, *et al.*, "Dynamic traffic assignment: A primer (transportation research circular e-c153)," 2011.

[17] H. Mahmassani and R. Herman, "Dynamic user equilibrium departure time and route choice on idealized traffic arterials," *Transportation Science*, vol. 18, no. 4, pp. 362–384, 1984.

[18] D. Watling and T. Van Vuren, "The modelling of dynamic route guidance systems," *Transportation Research Part C: Emerging Technologies*, vol. 1, no. 2, pp. 159–182, 1993.

[19] Y. M. Nie and X. Wu, "Shortest path problem considering on-time arrival probability," *Transportation Research Part B: Methodological*, vol. 43, no. 6, pp. 597–613, 2009.

[20] M. Yildirimoglu, M. Ramezani, and N. Geroliminis, "Equilibrium analysis and route guidance in large-scale networks with mfd dynamics," *Transportation Research Procedia*, vol. 9, pp. 185–204, 2015.

[21] M. Papageorgiou, "Dynamic modeling, assignment, and route guidance in traffic networks," *Transportation Research Part B: Methodological*, vol. 24, no. 6, pp. 471–495, 1990.

[22] M. Papgeorgiou and A. Messmer, "Dynamic network traffic assignment and route guidance via feedback regulation," *Transportation Research Record*, vol. 1306, pp. 49–58, 1991.

[23] K. Kim, M. Kwon, J. Park, Y. Eun, *et al.*, "Dynamic vehicular route guidance using traffic prediction information," *Mobile Information Systems*, vol. 2016, 2016.

[24] P. Li, X. Wang, H. Gao, X. Xu, M. Iqbal, and K. Dahal, "A dynamic and scalable user-centric route planning algorithm based on polychromatic sets theory," *IEEE transactions on intelligent transportation systems*, vol. 23, no. 3, pp. 2762–2772, 2021.

[25] D. Delling, A. V. Goldberg, T. Pajor, and R. F. Werneck, "Customizable route planning," in *Experimental Algorithms: 10th International Symposium, SEA 2011, Kolimpari, Chania, Crete, Greece, May 5-7, 2011. Proceedings 10*, Springer, 2011, pp. 376–387.

[26] G. Cui, J. Luo, and X. Wang, "Personalized travel route recommendation using collaborative filtering based on gps trajectories," *International journal of digital earth*, vol. 11, no. 3, pp. 284–307, 2018.

[27] Z. Li, I. Kolmanovsky, E. Atkins, J. Lu, D. P. Filev, and J. Michelini, "Road risk modeling and cloud-aided safety-based route planning," *IEEE transactions on cybernetics*, vol. 46, no. 11, pp. 2473–2483, 2015.

[28] A. Abdelrahman, A. S. El-Wakeel, A. Noureldin, and H. S. Hassanein, "Crowdsensing-based personalized dynamic route planning for smart vehicles," *Ieee Network*, vol. 34, no. 3, pp. 216–223, 2020.

[29] J. G. Wardrop, "Road paper. some theoretical aspects of road traffic research.," *Proceedings of the institution of civil engineers*, vol. 1, no. 3, pp. 325–362, 1952.

[30] D. K. Merchant and G. L. Nemhauser, "A model and an algorithm for the dynamic traffic assignment problems," *Transportation science*, vol. 12, no. 3, pp. 183–199, 1978.

[31] W. Szeto and S. Wong, "Dynamic traffic assignment: Model classifications and recent advances in travel choice principles," *Central European Journal of Engineering*, vol. 2, pp. 1–18, 2012.

[32] E. Cascetta and G. E. Cantarella, "Modelling dynamics in transportation networks: State of the art and future developments," *Simulation practice and theory*, vol. 1, no. 2, pp. 65–91, 1993.

[33] S. Peeta and A. K. Ziliaskopoulos, "Foundations of dynamic traffic assignment: The past, the present and the future," *Networks and spatial economics*, vol. 1, pp. 233–265, 2001.

[34] B. Ran and D. Boyce, *Modeling dynamic transportation networks: an intelligent transportation system oriented approach*. Springer Science & Business Media, 2012.

[35] D. Boyce, D.-H. Lee, and B. Ran, "Analytical models of the dynamic traffic assignment problem," *Networks and spatial economics*, vol. 1, pp. 377–390, 2001.

[36] W. Szeto and H. K. Lo, "Dynamic traffic assignment: Review and future research directions," *Journal of Transportation Systems Engineering and Information Technology*, vol. 5, no. 5, p. 85, 2005.

[37] W. Y. SZETO and H. K. LO, "Properties of dynamic traffic assignment with physical queues," *Journal of the Eastern Asia Society for Transportation Studies*, vol. 6, pp. 2108–2123, 2005.

[38] J.-S. Mun, "Traffic performance models for dynamic traffic assignment: An assessment of existing models," *Transport reviews*, vol. 27, no. 2, pp. 231–249, 2007.

[39] K. M. Fisher, "Transims is coming!" *Public Roads*, vol. 63, no. 5, pp. 49–51, 2000.

[40] G. D. Cameron and G. I. Duncan, "Paramics—parallel microscopic simulation of road traffic," *The Journal of Supercomputing*, vol. 10, pp. 25–53, 1996.

[41] H. Mahmassani, "Dynamic traffic assignment and simulation for advanced network informatics (dynasmart)," in *the 2nd International Seminar on Urban Traffic Networks, 1992*, 1992.

[42] M. Ben-Akiva, M. Bierlaire, H. Koutsopoulos, and R. Mishalani, "Dynamit: A simulation-based system for traffic prediction," in *DACCORD short term forecasting workshop*, Delft The Netherlands, vol. 12, 1998.

[43] D. Leonard, J. Tough, and P. Baguley, "Contram: A traffic assignment model for predicting flows and queues during peak periods," Tech. Rep., 1978.

[44] S. Yagar, "Dyanmic traffic assignment by individual path minimization and queueing," *Transportation Research/UK/*, vol. 5, no. 3, 1971.

[45] W. Y. Szeto and H. K. Lo, "A cell-based simultaneous route and departure time choice model with elastic demand," *Transportation Research Part B: Methodological*, vol. 38, no. 7, pp. 593–612, 2004.

[46] H. K. Lo and W. Y. Szeto, "A cell-based dynamic traffic assignment model: Formulation and properties," *Mathematical and computer modelling*, vol. 35, no. 7-8, pp. 849–865, 2002.

[47] J. Long, W. Szeto, Z. Gao, H.-J. Huang, and Q. Shi, "The nonlinear equation system approach to solving dynamic user optimal simultaneous route and departure time choice problems," *Transportation Research Part B: Methodological*, vol. 83, pp. 179–206, 2016.

[48] S. Peeta and H. S. Mahmassani, "System optimal and user equilibrium time-dependent traffic assignment in congested networks," *Annals of Operations Research*, vol. 60, no. 1, pp. 81–113, 1995.

[49] C. Tong and S. Wong, "A predictive dynamic traffic assignment model in congested capacity-constrained road networks," *Transportation Research Part B: Methodological*, vol. 34, no. 8, pp. 625–644, 2000.

[50] W. Y. Szeto, "Enhanced lagged cell-transmission model for dynamic traffic assignment," *Transportation Research Record*, vol. 2085, no. 1, pp. 76–85, 2008.

[51] M. Ben-Akiva, D. Cuneo, M. Hasan, M. Jha, and Q. Yang, "Evaluation of freeway control using a microscopic simulation laboratory," *Transportation research Part C: emerging technologies*, vol. 11, no. 1, pp. 29–50, 2003.

[52] R. E. Allsop, "Some possibilities for using traffic control to influence trip distribution and route choice," in *Transportation and traffic theory, proceedings*, vol. 6, 1974.

[53] R. Allsop and J. Charlesworth, "Traffic in a signal-controlled road network: An example of different signal timings including different routeing," *Traffic Engineering & Control*, vol. 18, no. Analytic, 1977.

[54] T. van Vuren, M. J. Smith, and D. Van Vliet, *The interaction between signal-setting optimization and reassignment: background and preliminary results*, 1142. 1987.

[55] H. Yang and S. Yagar, "Traffic assignment and signal control in saturated road networks," *Transportation Research Part A: Policy and Practice*, vol. 29, no. 2, pp. 125–139, 1995.

[56] N. H. Gartner and C. Stamatiadis, "Arterial-based control of traffic flow in urban grid networks," *Mathematical and computer modelling*, vol. 35, no. 5-6, pp. 657–671, 2002.

[57] P. Li, P. Mirchandani, and X. Zhou, "Solving simultaneous route guidance and traffic signal optimization problem using space-phase-time hypernetwork," *Transportation Research Part B: Methodological*, vol. 81, pp. 103–130, 2015.

[58] H. Zhang, Y. Nie, and Z. Qian, "Modelling network flow with and without link interactions: The cases of point queue, spatial queue and cell transmission model," *Transportmetrica B: Transport Dynamics*, vol. 1, no. 1, pp. 33–51, 2013.

[59] W. Shen and H. Zhang, "What do different traffic flow models mean for system-optimal dynamic traffic assignment in a many-to-one network?" *Transportation research record*, vol. 2088, no. 1, pp. 157–166, 2008.

[60] C. F. Daganzo, "The cell transmission model: A dynamic representation of highway traffic consistent with the hydrodynamic theory," *Transportation research part B: methodological*, vol. 28, no. 4, pp. 269–287, 1994.

[61] ——, "The cell transmission model, part ii: Network traffic," *Transportation Research Part B: Methodological*, vol. 29, no. 2, pp. 79–93, 1995.

[62] A. K. Ziliaskopoulos, "A linear programming model for the single destination system optimum dynamic traffic assignment problem," *Transportation science*, vol. 34, no. 1, pp. 37–49, 2000.

[63] H. K. Lo, E. Chang, and Y. C. Chan, "Dynamic network traffic control," *Transportation Research Part A: Policy and Practice*, vol. 35, no. 8, pp. 721–744, 2001.

[64] H. K. Lo, "A cell-based traffic control formulation: Strategies and benefits of dynamic timing plans," *Transportation Science*, vol. 35, no. 2, pp. 148–164, 2001.

[65] H. K. Lo and W. Y. Szeto, "A cell-based variational inequality formulation of the dynamic user optimal assignment problem," *Transportation Research Part B: Methodological*, vol. 36, no. 5, pp. 421–443, 2002.

[66] W.-H. Lin and C. Wang, "An enhanced 0-1 mixed-integer lp formulation for traffic signal control," *IEEE Transactions on Intelligent transportation systems*, vol. 5, no. 4, pp. 238–245, 2004.

[67] F. Wu, *Routes and trajectories based dynamic models for traffic prediction and control*. The University of Arizona, 2008.

[68] J. L. Adler and V. J. Blue, "A cooperative multi-agent transportation management and route guidance system," *Transportation Research Part C: Emerging Technologies*, vol. 10, no. 5-6, pp. 433–454, 2002.

[69] J. L. Adler, G. Satapathy, V. Manikonda, B. Bowles, and V. J. Blue, "A multi-agent approach to cooperative traffic management and route guidance," *Transportation Research Part B: Methodological*, vol. 39, no. 4, pp. 297–318, 2005.

[70] Z. Cao, H. Guo, J. Zhang, and U. Fastenrath, "Multiagent-based route guidance for increasing the chance of arrival on time," in *Proceedings of the AAAI Conference on Artificial Intelligence*, vol. 30, 2016.

[71] R. Claes, T. Holvoet, and D. Weyns, "A decentralized approach for anticipatory vehicle routing using delegate multiagent systems," *IEEE Transactions on Intelligent Transportation Systems*, vol. 12, no. 2, pp. 364–373, 2011.

[72] H. F. Wedde and S. Senge, "Beejama: A distributed, self-adaptive vehicle routing guidance approach," *IEEE Transactions on Intelligent Transportation Systems*, vol. 14, no. 4, pp. 1882–1895, 2013.

[73] R. K. Guha and W. Chen, "A distributed traffic navigation system using vehicular communication," in *2009 IEEE Vehicular Networking Conference (VNC)*, IEEE, 2009, pp. 1–8.

[74] K. Faez and M. Khanjary, "Utospf: A distributed dynamic route guidance system based on wireless sensor networks and open shortest path first protocol," in *2008 IEEE International Symposium on Wireless Communication Systems*, IEEE, 2008, pp. 558–562.

[75] J. Pan, I. S. Popa, and C. Borcea, "Divert: A distributed vehicular traffic re-routing system for congestion avoidance," *IEEE Transactions on Mobile Computing*, vol. 16, no. 1, pp. 58–72, 2016.

[76] L. Tassiulas and A. Ephremides, "Stability properties of constrained queueing systems and scheduling policies for maximum throughput in multihop radio networks," in *29th IEEE Conference on Decision and Control*, IEEE, 1990, pp. 2130–2132.

[77] E. Athanasopoulou, L. X. Bui, T. Ji, R Srikant, and A. Stolyar, "Back-pressure-based packet-by-packet adaptive routing in communication networks," *IEEE/ACM transactions on networking*, vol. 21, no. 1, pp. 244–257, 2012.

[78] M. J. Neely and R. Urgaonkar, "Optimal backpressure routing for wireless networks with multi-receiver diversity," *Ad Hoc Networks*, vol. 7, no. 5, pp. 862–881, 2009.

[79] L. Tassiulas, "Adaptive back-pressure congestion control based on local information," *IEEE Transactions on Automatic Control*, vol. 40, no. 2, pp. 236–250, 1995.

[80] P. Varaiya, "Max pressure control of a network of signalized intersections," *Transportation Research Part C: Emerging Technologies*, vol. 36, pp. 177–195, 2013.

[81] ——, "The max-pressure controller for arbitrary networks of signalized intersections," in *Advances in dynamic network modeling in complex transportation systems*, Springer, 2013, pp. 27–66.

[82] P. Grandinetti, C. Canudas-de Wit, and F. Garin, "Distributed optimal traffic lights design for large-scale urban networks," *IEEE Transactions on Control Systems Technology*, vol. 27, no. 3, pp. 950–963, 2018.

[83] A. Kouvelas, J. Lioris, S. A. Fayazi, and P. Varaiya, "Maximum pressure controller for stabilizing queues in signalized arterial networks," *Transportation Research Record*, vol. 2421, no. 1, pp. 133–141, 2014.

[84] X. Sun and Y. Yin, "A simulation study on max pressure control of signalized intersections," *Transportation research record*, vol. 2672, no. 18, pp. 117–127, 2018.

[85] H. Wei, C. Chen, G. Zheng, *et al.*, "Presslight: Learning max pressure control to coordinate traffic signals in arterial network," in *Proceedings of the 25th ACM SIGKDD international conference on knowledge discovery & data mining*, 2019, pp. 1290–1298.

[86] A. A. Zaidi, B. Kulcsár, and H. Wymeersch, "Back-pressure traffic signal control with fixed and adaptive routing for urban vehicular networks," *IEEE Transactions on Intelligent Transportation Systems*, vol. 17, no. 8, pp. 2134–2143, 2016.

[87] R. Zhang, Z. Li, C. Feng, and S. Jiang, "Traffic routing guidance algorithm based on backpressure with a trade-off between user satisfaction and traffic load," in *2012 ieee vehicular technology conference (vtc fall)*, IEEE, 2012, pp. 1–5.

[88] H. Taale, J. van Kampen, and S. Hoogendoorn, "Integrated signal control and route guidance based on back-pressure principles," *Transportation Research Procedia*, vol. 10, pp. 226–235, 2015.

[89] J. Van Kampen, "Route guidance and signal control based on the back-pressure algorithm," *Delft University of Technology*, 2015.

[90] W.-L. Jin, X. Wang, and Y. Lou, "Stable dynamic pricing scheme independent of lane-choice models for high-occupancy-toll lanes," *Transportation Research Part B: Methodological*, vol. 140, pp. 64–78, 2020.

[91] S. E. Seilabi, M. T. Tabesh, A. Davatgari, M. Miralinaghi, and S. Labi, "Promoting autonomous vehicles using travel demand and lane management strategies," *Frontiers in Built Environment*, vol. 6, p. 560 116, 2020.

[92] B. Madadi, R. van Nes, M. Snelder, and B. van Arem, "A bi-level model to optimize road networks for a mixture of manual and automated driving: An evolutionary local search algorithm," *Computer-Aided Civil and Infrastructure Engineering*, vol. 35, no. 1, pp. 80–96, 2020.

[93] S. R. Rad, H. Farah, H. Taale, B. van Arem, and S. P. Hoogendoorn, "Design and operation of dedicated lanes for connected and automated vehicles on motorways: A conceptual framework and research agenda," *Transportation research part C: emerging technologies*, vol. 117, p. 102 664, 2020.

[94] Z. Chen, F. He, L. Zhang, and Y. Yin, "Optimal deployment of autonomous vehicle lanes with endogenous market penetration," *Transportation Research Part C: Emerging Technologies*, vol. 72, pp. 143–156, 2016.

[95] Y. Ye and H. Wang, "Optimal design of transportation networks with automated vehicle links and congestion pricing," *Journal of Advanced Transportation*, vol. 2018, 2018.

[96] Z. Chen, F. He, Y. Yin, and Y. Du, "Optimal design of autonomous vehicle zones in transportation networks," *Transportation Research Part B: Methodological*, vol. 99, pp. 44–61, 2017.

[97] B. Madadi, R. Van Nes, M. Snelder, and B. Van Arem, "Optimizing road networks for automated vehicles with dedicated links, dedicated lanes, and mixed-traffic subnetworks," *Journal of Advanced Transportation*, vol. 2021, pp. 1–17, 2021.

[98] K. Hamad and A. R. Alozi, "Shared vs. dedicated lanes for automated vehicle deployment: A simulation-based assessment," *International journal of transportation science and technology*, vol. 11, no. 2, pp. 205–215, 2022.

[99] S. R. Rad, H. Farah, H. Taale, B. van Arem, and S. P. Hoogendoorn, "The impact of a dedicated lane for connected and automated vehicles on the behaviour of drivers of manual vehicles," *Transportation research part F: traffic psychology and behaviour*, vol. 82, pp. 141–153, 2021.

[100] I. Stamos, G. Kitis, S. Basbas, and I. Tzevelekis, "Evaluation of a high occupancy vehicle lane in central business district thessaloniki," *Procedia-Social and Behavioral Sciences*, vol. 48, pp. 1088–1096, 2012.

[101] N. D. Chan and S. A. Shaheen, "Ridesharing in north america: Past, present, and future," *Transport reviews*, vol. 32, no. 1, pp. 93–112, 2012.

[102] J. Viegas and B. Lu, "The intermittent bus lane signals setting within an area," *Transportation Research Part C: Emerging Technologies*, vol. 12, no. 6, pp. 453–469, 2004.

[103] M. Eichler and C. F. Daganzo, "Bus lanes with intermittent priority: Strategy formulae and an evaluation," *Transportation Research Part B: Methodological*, vol. 40, no. 9, pp. 731–744, 2006.

[104] H. Yang and X. Wang, "Managing network mobility with tradable credits," *Transportation Research Part B: Methodological*, vol. 45, no. 3, pp. 580–594, 2011.

[105] A. De Palma and R. Lindsey, "Traffic congestion pricing methodologies and technologies," *Transportation Research Part C: Emerging Technologies*, vol. 19, no. 6, pp. 1377–1399, 2011.

[106] M. Mansourianfar, Z. Gu, S. T. Waller, and M. Saberi, "Joint routing and pricing control of autonomous vehicles in mixed equilibrium simulation-based dynamic traffic assignment," *arXiv preprint arXiv:2009.10907*, 2020.

[107] Z. Gu and M. Saberi, "A simulation-based optimization framework for urban congestion pricing considering travelers' departure time rescheduling," in *2019 IEEE Intelligent Transportation Systems Conference (ITSC)*, IEEE, 2019, pp. 2557–2562.

[108] X. Wang, H. Yang, and D. Han, "Traffic rationing and short-term and long-term equilibrium," *Transportation research record*, vol. 2196, no. 1, pp. 131–141, 2010.

[109] D. Han, H. Yang, and X. Wang, "Efficiency of the plate-number-based traffic rationing in general networks," *Transportation Research Part E: Logistics and Transportation Review*, vol. 46, no. 6, pp. 1095–1110, 2010.

[110] L. W. Davis, "The effect of driving restrictions on air quality in mexico city," *Journal of Political Economy*, vol. 116, no. 1, pp. 38–81, 2008.

[111] W. Fan, F. Xiao, *et al.*, "Managing bottleneck congestion with tradable credits under asymmetric transaction cost," *Transportation Research Part E: Logistics and Transportation Review*, vol. 158, p. 102 600, 2022.

[112] L. Krabbenborg, N. Mouter, E. Molin, J. A. Annema, and B. van Wee, "Exploring public perceptions of tradable credits for congestion management in urban areas," *Cities*, vol. 107, p. 102 877, 2020.

[113] Y. M. Nie, "Transaction costs and tradable mobility credits," *Transportation Research Part B: Methodological*, vol. 46, no. 1, pp. 189–203, 2012.

[114] S. Grant-Muller and M. Xu, "The role of tradable credit schemes in road traffic congestion management," *Transport Reviews*, vol. 34, no. 2, pp. 128–149, 2014.

[115] J. A. Sanguesa, V. Torres-Sanz, P. Garrido, F. J. Martinez, and J. M. Marquez-Barja, "A review on electric vehicles: Technologies and challenges," *Smart Cities*, vol. 4, no. 1, pp. 372–404, 2021.

[116] P. Penmetsa, S. Dhondia, E. K. Adanu, C. Harper, S. Nambisan, and S. Jones, "Incentives to encourage the adoption of connected and automated vehicles: Lessons learned from hybrid-electric vehicle incentive programs," *Future Transportation*, vol. 3, no. 3, pp. 986–995, 2023.

[117] S. Yang, C. Deng, T. Tang, and Y. Qian, "Electric vehicle's energy consumption of car-following models," *Nonlinear Dynamics*, vol. 71, pp. 323–329, 2013.

[118] S. E. Li, R. Li, J. Wang, X. Hu, B. Cheng, and K. Li, "Stabilizing periodic control of automated vehicle platoon with minimized fuel consumption," *IEEE Transactions on Transportation Electrification*, vol. 3, no. 1, pp. 259–271, 2016.

[119] S. E. Li, H. Peng, K. Li, and J. Wang, "Minimum fuel control strategy in automated car-following scenarios," *IEEE Transactions on Vehicular Technology*, vol. 61, no. 3, pp. 998–1007, 2012.

[120] G. Wang, K. Makino, A. Harmandayan, and X. Wu, "Eco-driving behaviors of electric vehicle users: A survey study," *Transportation research part D: transport and environment*, vol. 78, p. 102 188, 2020.

[121] S. Agrawal, H. Zheng, S. Peeta, and A. Kumar, "Routing aspects of electric vehicle drivers and their effects on network performance," *Transportation Research Part D: Transport and Environment*, vol. 46, pp. 246–266, 2016.

[122] A. Karoonsoontawong and S. T. Waller, "Integrated network capacity expansion and traffic signal optimization problem: Robust bi-level dynamic formulation," *Networks and Spatial Economics*, vol. 10, pp. 525–550, 2010.

[123] L.-W. Chen and T.-Y. Hu, "Flow equilibrium under dynamic traffic assignment and signal control—an illustration of pretimed and actuated signal control policies," *IEEE Transactions on intelligent transportation systems*, vol. 13, no. 3, pp. 1266–1276, 2012.

[124] H. Ceylan and M. G. Bell, "Traffic signal timing optimisation based on genetic algorithm approach, including drivers' routing," *Transportation Research Part B: Methodological*, vol. 38, no. 4, pp. 329–342, 2004.

[125] F. Teklu, A. Sumalee, and D. Watling, "A genetic algorithm approach for optimizing traffic control signals considering routing," *Computer-Aided Civil and Infrastructure Engineering*, vol. 22, no. 1, pp. 31–43, 2007.

[126] D. Sun, R. F. Benekohal, and S. T. Waller, "Bi-level programming formulation and heuristic solution approach for dynamic traffic signal optimization," *Computer-Aided Civil and Infrastructure Engineering*, vol. 21, no. 5, pp. 321–333, 2006.

[127] R. Liu and M. Smith, "Route choice and traffic signal control: A study of the stability and instability of a new dynamical model of route choice and traffic signal control," *Transportation Research Part B: Methodological*, vol. 77, pp. 123–145, 2015.

[128] C. Priemer and B. Friedrich, "A decentralized adaptive traffic signal control using v2i communication data," in *2009 12th international ieee conference on intelligent transportation systems*, IEEE, 2009, pp. 1–6.

[129] J. Lee, B. Park, and I. Yun, "Cumulative travel-time responsive real-time intersection control algorithm in the connected vehicle environment," *Journal of Transportation Engineering*, vol. 139, no. 10, pp. 1020–1029, 2013.

[130] S. B. Al Islam and A. Hajbabaie, "Distributed coordinated signal timing optimization in connected transportation networks," *Transportation Research Part C: Emerging Technologies*, vol. 80, pp. 272–285, 2017.

[131] T. Wongpiromsarn, T. Uthaicharoenpong, Y. Wang, E. Frazzoli, and D. Wang, "Distributed traffic signal control for maximum network throughput," in *2012 15th international IEEE conference on intelligent transportation systems*, IEEE, 2012, pp. 588–595.

[132] L. Du, L. Han, and S. Chen, "Coordinated online in-vehicle routing balancing user optimality and system optimality through information perturbation," *Transportation Research Part B: Methodological*, vol. 79, pp. 121–133, 2015.

[133] J. Wang and H. Niu, "A distributed dynamic route guidance approach based on short-term forecasts in cooperative infrastructure-vehicle systems," *Transportation Research Part D: Transport and Environment*, vol. 66, pp. 23–34, 2019.

[134] H. Yu, P. Liu, R. Ma, and L. Bai, "Performance evaluation of integrated strategy of vehicle route guidance and traffic signal control using traffic simulation," *IET Intelligent Transport Systems*, vol. 12, no. 7, pp. 696–702, 2018.

[135] P. A. Lopez, M. Behrisch, L. Bieker-Walz, *et al.*, "Microscopic traffic simulation using sumo," in *2018 21st international conference on intelligent transportation systems (ITSC)*, IEEE, 2018, pp. 2575–2582.

[136] A. Varga, "Omnet++," in *Modeling and tools for network simulation*, Springer, 2010, pp. 35–59.

[137] P. Li, P. Mirchandani, and X. Zhou, "Solving simultaneous route guidance and traffic signal optimization problem using space-phase-time hypernetwork," *Transportation Research Part B: Methodological*, vol. 81, pp. 103–130, 2015.

[138] H. Fu, A. J. Pel, and S. P. Hoogendoorn, "Optimization of evacuation traffic management with intersection control constraints," *IEEE Transactions on Intelligent Transportation Systems*, vol. 16, no. 1, pp. 376–386, 2014.

[139] C. Kun and Y. Lei, "Microscopic traffic-emission simulation and case study for evaluation of traffic control strategies," *Journal of Transportation Systems Engineering and Information Technology*, vol. 7, no. 1, pp. 93–99, 2007.

[140] K. Ozbay and B. Bartin, "Estimation of economic impact of vms route guidance using microsimulation," *Research in transportation economics*, vol. 8, pp. 215–241, 2004.

[141] S.-R. Yang, Y.-J. Su, Y.-Y. Chang, and H.-N. Hung, "Short-term traffic prediction for edge computing-enhanced autonomous and connected cars," *IEEE Transactions on Vehicular Technology*, vol. 68, no. 4, pp. 3140–3153, 2019.

[142] E. W. Dijkstra, "A note on two problems in connexion with graphs," in *Edsger Wybe Dijkstra: His Life, Work, and Legacy*, 2022, pp. 287–290.

[143] J. Kiefer, "Sequential minimax search for a maximum," *Proceedings of the American mathematical society*, vol. 4, no. 3, pp. 502–506, 1953.

[144] L. Adacher and M. Tiriolo, "Performance analysis of decentralized vs centralized control for the traffic signal synchronization problem," *Journal of Advanced Transportation*, vol. 2020, pp. 1–19, 2020.

[145] M. Mehrabipour and A. Hajbabaie, "A cell-based distributed-coordinated approach for network-level signal timing optimization," *Computer-Aided Civil and Infrastructure Engineering*, vol. 32, no. 7, pp. 599–616, 2017.

[146] A. H. Chow, R. Sha, and S. Li, "Centralised and decentralised signal timing optimisation approaches for network traffic control," *Transportation Research Part C: Emerging Technologies*, vol. 113, pp. 108–123, 2020.

[147] B. Chen, Z. Ding, Y. Wu, J. Zhou, and Y. Chen, "An optimal global algorithm for route guidance in advanced traveler information systems," *Information Sciences*, vol. 555, pp. 33–45, 2021.

[148] L. Du, S. Chen, and L. Han, "Coordinated online in-vehicle navigation guidance based on routing game theory," *Transportation Research Record*, vol. 2497, no. 1, pp. 106–116, 2015.

[149] N. Mahajan, A. Hegyi, S. P. Hoogendoorn, and B. van Arem, "Design analysis of a decentralized equilibrium-routing strategy for intelligent vehicles," *Transportation Research Part C: Emerging Technologies*, vol. 103, pp. 308–327, 2019.

[150] S. A. Bagloee, M. Sarvi, M. Patriksson, and A. Rajabifard, "A mixed user-equilibrium and system-optimal traffic flow for connected vehicles stated as a complementarity problem," *Computer-Aided Civil and Infrastructure Engineering*, vol. 32, no. 7, pp. 562–580, 2017.

[151] Z. Chen, X. Lin, Y. Yin, and M. Li, "Path controlling of automated vehicles for system optimum on transportation networks with heterogeneous traffic stream," *Transportation Research Part C: Emerging Technologies*, vol. 110, pp. 312–329, 2020.

[152] I. Klein and E. Ben-Elia, "Emergence of cooperative route-choice: A model and experiment of compliance with system-optimal atis," *Transportation research part F: traffic psychology and behaviour*, vol. 59, pp. 348–364, 2018.

[153] W. Lu and W. Lee, "Vehicular edge computing and networking: A survey," *Mobile Networks and Applications*, vol. 5, no. 2, pp. 101–102, 2000.

[154] Y. Yu, "Mobile edge computing towards 5g: Vision, recent progress, and open challenges," *China Communications*, vol. 13, no. Supplement2, pp. 89–99, 2016.

[155] L. Ying, S. Shakkottai, A. Reddy, and S. Liu, "On combining shortest-path and back-pressure routing over multihop wireless networks," *IEEE/ACM Transactions on Networking*, vol. 19, no. 3, pp. 841–854, 2010.

[156] J. Gao, Y. Shen, M. Ito, and N. Shiratori, "Multi-agent q-learning aided backpressure routing algorithm for delay reduction," *arXiv preprint arXiv:1708.06926*, 2017.

[157] L. Li, V. Okoth, and S. E. Jabari, "Backpressure control with estimated queue lengths for urban network traffic," *IET Intelligent Transport Systems*, vol. 15, no. 2, pp. 320–330, 2021.

[158] P. Mercader, W. Uwayid, and J. Haddad, "Max-pressure traffic controller based on travel times: An experimental analysis," *Transportation Research Part C: Emerging Technologies*, vol. 110, pp. 275–290, 2020.

[159] C. F. Daganzo, "Urban gridlock: Macroscopic modeling and mitigation approaches," *Transportation Research Part B: Methodological*, vol. 41, no. 1, pp. 49–62, 2007.

[160] M. D. Simoni, A. J. Pel, R. A. Waraich, and S. P. Hoogendoorn, "Marginal cost congestion pricing based on the network fundamental diagram," *Transportation Research Part C: Emerging Technologies*, vol. 56, pp. 221–238, 2015.

[161] C. F. Daganzo, V. V. Gayah, and E. J. Gonzales, "Macroscopic relations of urban traffic variables: Bifurcations, multivaluedness and instability," *Transportation Research Part B: Methodological*, vol. 45, no. 1, pp. 278–288, 2011.

[162] R. Hussain and S. Zeadally, "Autonomous cars: Research results, issues, and future challenges," *IEEE Communications Surveys & Tutorials*, vol. 21, no. 2, pp. 1275–1313, 2018.

[163] Z. Liu and Z. Song, "Strategic planning of dedicated autonomous vehicle lanes and autonomous vehicle/toll lanes in transportation networks," *Transportation Research Part C: Emerging Technologies*, vol. 106, pp. 381–403, 2019.

[164] M. W. Levin and S. D. Boyles, "Effects of autonomous vehicle ownership on trip, mode, and route choice," *Transportation Research Record*, vol. 2493, no. 1, pp. 29–38, 2015.

[165] V. A. Van den Berg and E. T. Verhoef, "Autonomous cars and dynamic bottleneck congestion: The effects on capacity, value of time and preference heterogeneity," *Transportation Research Part B: Methodological*, vol. 94, pp. 43–60, 2016.

[166] M. W. Levin and S. D. Boyles, "A multiclass cell transmission model for shared human and autonomous vehicle roads," *Transportation Research Part C: Emerging Technologies*, vol. 62, pp. 103–116, 2016.

[167] Q. Guo, X. J. Ban, and H. A. Aziz, "Mixed traffic flow of human driven vehicles and automated vehicles on dynamic transportation networks," *Transportation research part C: emerging technologies*, vol. 128, p. 103 159, 2021.

[168] X. Jiang and Q. Shang, "A dynamic cav-dedicated lane allocation method with the joint optimization of signal timing parameters and smooth trajectory in a mixed traffic environment," *IEEE Transactions on Intelligent Transportation Systems*, 2022.

[169] Y. Shao, J. Sun, Y. Kan, and Y. Tian, "Operation of dedicated lanes with intermittent priority on highways: Conceptual development and simulation validation," *Journal of Intelligent Transportation Systems*, pp. 1–15, 2022.

[170] A. A. Walters, "The theory and measurement of private and social cost of highway congestion," *Econometrica: Journal of the Econometric Society*, pp. 676–699, 1961.

[171] S. Dafermos and F. T. Sparrow, "Optimal resource allocation and toll patterns in user-optimised transport networks," *Journal of Transport Economics and Policy*, pp. 184–200, 1971.

[172] Y. Chen, Y. Zhang, and Z. Gu, "Differential congestion pricing strategies for heterogeneous users in the mixed traffic condition," *Journal of Advanced Transportation*, vol. 2022, pp. 1–14, 2022.

[173] P. Ferrari, "Road pricing and network equilibrium," *Transportation Research Part B: Methodological*, vol. 29, no. 5, pp. 357–372, 1995.

[174] H. Yang and W. H. Lam, "Optimal road tolls under conditions of queueing and congestion," *Transportation Research Part A: Policy and Practice*, vol. 30, no. 5, pp. 319–332, 1996.

[175] Z. Song, Y. Yin, and S. Lawphongpanich, "Optimal deployment of managed lanes in general networks," *International Journal of Sustainable Transportation*, vol. 9, no. 6, pp. 431–441, 2015.

[176] J. Dahlgren, "High-occupancy/toll lanes: Where should they be implemented?" *Transportation Research Part A: Policy and Practice*, vol. 36, no. 3, pp. 239–255, 2002.

[177] Y. Lou, Y. Yin, and J. A. Laval, "Optimal dynamic pricing strategies for high-occupancy/toll lanes," *Transportation Research Part C: Emerging Technologies*, vol. 19, no. 1, pp. 64–74, 2011.

[178] J. Wang, L. Lu, S. Peeta, and Z. He, "Optimal toll design problems under mixed traffic flow of human-driven vehicles and connected and autonomous vehicles," *Transportation Research Part C: Emerging Technologies*, vol. 125, p. 102 952, 2021.

[179] A. Emami, M. Sarvi, and S. Asadi Bagloee, "Using kalman filter algorithm for short-term traffic flow prediction in a connected vehicle environment," *Journal of Modern Transportation*, vol. 27, pp. 222–232, 2019.

[180] Y. Wang, Z. Yao, Y. Cheng, Y. Jiang, and B. Ran, "Kalman filtering method for real-time queue length estimation in a connected vehicle environment," *Transportation Research Record*, vol. 2675, no. 10, pp. 578–589, 2021.

[181] C. P. Van Hinsbergen, T. Schreiter, F. S. Zuurbier, J. Van Lint, and H. J. Van Zuylen, "Localized extended kalman filter for scalable real-time traffic state estimation," *IEEE transactions on intelligent transportation systems*, vol. 13, no. 1, pp. 385–394, 2011.

[182] F. Dion, H. Rakha, and Y.-S. Kang, "Comparison of delay estimates at under-saturated and over-saturated pre-timed signalized intersections," *Transportation Research Part B: Methodological*, vol. 38, no. 2, pp. 99–122, 2004.

[183] L. Chu, S Oh, and W. Recker, "Adaptive kalman filter based freeway travel time estimation," in *84th TRB Annual Meeting, Washington DC*, 2005.

[184] B. Chen, L. Dang, N. Zheng, and J. C. Principe, "Kalman filtering," in *Kalman Filtering Under Information Theoretic Criteria*, Springer, 2023, pp. 11–51.

[185] K. Ogata, *Discrete-time control systems*. Prentice-Hall, Inc., 1995.

[186] T. Toledo and D. Zohar, "Modeling duration of lane changes," *Transportation Research Record*, vol. 1999, no. 1, pp. 71–78, 2007.

[187] R. Niroumand, M. Tajalli, L. Hajibabai, and A. Hajbabaie, "Joint optimization of vehicle-group trajectory and signal timing: Introducing the white phase for mixed-autonomy traffic stream," *Transportation research part C: emerging technologies*, vol. 116, p. 102 659, 2020.

[188] H. Yao and X. Li, "Decentralized control of connected automated vehicle trajectories in mixed traffic at an isolated signalized intersection," *Transportation research part C: emerging technologies*, vol. 121, p. 102 846, 2020.

[189] H. Chen, F. Wu, K. Hou, and T. Z. Qiu, "Backpressure-based distributed dynamic route control for connected and automated vehicles," *IEEE Transactions on Intelligent Transportation Systems*, vol. 23, no. 11, pp. 20 953–20 964, 2022.

[190] S. C. G. of Canada. " The Daily — Canadian Income Survey, 2020 kernel description." (2022), [Online]. Available: `https://www150.statcan.gc.ca/n1/daily-quotidien/220323/dq220323a-eng.htm` (visited on 01/03/2023).

[191] M. Steinstraeter, T. Heinrich, and M. Lienkamp, "Effect of low temperature on electric vehicle range," *World Electric Vehicle Journal*, vol. 12, no. 3, p. 115, 2021.

[192] N. Rauh, T. Franke, and J. F. Krems, "Understanding the impact of electric vehicle driving experience on range anxiety," *Human factors*, vol. 57, no. 1, pp. 177–187, 2015.

[193] D. Pevec, J. Babic, A. Carvalho, Y. Ghiassi-Farrokhfal, W. Ketter, and V. Podobnik, "A survey-based assessment of how existing and potential electric vehicle owners perceive range anxiety," *Journal of Cleaner Production*, vol. 276, p. 122 779, 2020.

[194] O. Egbue and S. Long, "Barriers to widespread adoption of electric vehicles: An analysis of consumer attitudes and perceptions," *Energy policy*, vol. 48, pp. 717–729, 2012.

[195] X. Men, Y. Guo, G. Wu, S. Chen, and C. Shi, "Implementation of an improved motor control for electric vehicles," *Energies*, vol. 15, no. 13, p. 4833, 2022.

[196] H. Tu, H. Feng, S. Srdic, and S. Lukic, "Extreme fast charging of electric vehicles: A technology overview," *IEEE Transactions on Transportation Electrification*, vol. 5, no. 4, pp. 861–878, 2019.

[197] Y. Yang, Q. He, C. Fu, S. Liao, and P. Tan, "Efficiency improvement of permanent magnet synchronous motor for electric vehicles," *Energy*, vol. 213, p. 118 859, 2020.

[198] T. Gnann, S. Funke, N. Jakobsson, P. Plötz, F. Sprei, and A. Bennehag, "Fast charging infrastructure for electric vehicles: Today's situation and future needs," *Transportation Research Part D: Transport and Environment*, vol. 62, pp. 314–329, 2018.

[199] M. Contestabile, M. Alajaji, and B. Almubarak, "Will current electric vehicle policy lead to cost-effective electrification of passenger car transport?" *Energy Policy*, vol. 110, pp. 20–30, 2017.

[200] T. Pardi, "Prospects and contradictions of the electrification of the european automotive industry: The role of european union policy," *International Journal of Automotive Technology and Management*, vol. 21, no. 3, pp. 162–179, 2021.

[201] M. Weiss, M. K. Patel, M. Junginger, A. Perujo, P. Bonnel, and G. van Grootveld, "On the electrification of road transport-learning rates and price forecasts for hybrid-electric and battery-electric vehicles," *Energy Policy*, vol. 48, pp. 374–393, 2012.

[202] F. Baouche, R. Billot, R. Trigui, and N.-E. El Faouzi, "Efficient allocation of electric vehicles charging stations: Optimization model and application to a dense urban network," *IEEE Intelligent transportation systems magazine*, vol. 6, no. 3, pp. 33–43, 2014.

[203] X. Xi, R. Sioshansi, and V. Marano, "Simulation–optimization model for location of a public electric vehicle charging infrastructure," *Transportation Research Part D: Transport and Environment*, vol. 22, pp. 60–69, 2013.

[204] M. Li, X. Wu, X. He, G. Yu, and Y. Wang, "An eco-driving system for electric vehicles with signal control under v2x environment," *Transportation Research Part C: Emerging Technologies*, vol. 93, pp. 335–350, 2018.

[205] S. Qiu, L. Qiu, L. Qian, Z. Abdollahi, and P. Pisu, "Closed-loop hierarchical control strategies for connected and autonomous hybrid electric vehicles with random errors," *IET Intelligent Transport Systems*, vol. 12, no. 10, pp. 1378–1385, 2018.

[206] H. Zhang, J. Peng, H. Dong, H. Tan, and F. Ding, "Hierarchical reinforcement learning based energy management strategy of plug-in hybrid electric vehicle for ecological car-following process," *Applied Energy*, vol. 333, p. 120 599, 2023.

[207] X. He and X. Wu, "Eco-driving advisory strategies for a platoon of mixed gasoline and electric vehicles in a connected vehicle system," *Transportation Research Part D: Transport and Environment*, vol. 63, pp. 907–922, 2018.

[208] F. Grée, V. Laznikova, B. Kim, G. Garcia, T. Kigezi, and B. Gao, "Cloud-based big data platform for vehicle-to-grid (v2g)," *World Electric Vehicle Journal*, vol. 11, no. 2, p. 30, 2020.

[209] Y. Kim, I. Lee, and S. Kang, "Eco assist techniques through real-time monitoring of bev energy usage efficiency," *Sensors*, vol. 15, no. 7, pp. 14 946–14 959, 2015.

[210] A. De Palma and D. Rochat, "Understanding individual travel decisions: Results from a commuters survey in geneva," *Transportation*, vol. 26, pp. 263–281, 1999.

[211] Z. P. Cano, D. Banham, S. Ye, *et al.*, "Batteries and fuel cells for emerging electric vehicle markets," *Nature energy*, vol. 3, no. 4, pp. 279–289, 2018.

[212] M. Li, M. Feng, D. Luo, and Z. Chen, "Fast charging li-ion batteries for a new era of electric vehicles," *Cell Reports Physical Science*, vol. 1, no. 10, 2020.

[213] X. Qu, L. Zhong, Z. Zeng, H. Tu, and X. Li, "Automation and connectivity of electric vehicles: Energy boon or bane?" *Cell Reports Physical Science*, vol. 3, no. 8, 2022.

[214] Y. Zhang, T. You, J. Chen, C. Du, Z. Ai, and X. Qu, "Safe and energy-saving vehicle-following driving decision-making framework of autonomous vehicles," *IEEE Transactions on Industrial Electronics*, vol. 69, no. 12, pp. 13 859–13 871, 2021.

[215] Y. Shao, Y. Zheng, and Z. Sun, "Machine learning enabled traffic prediction for speed optimization of connected and autonomous electric vehicles," in *2021 American Control Conference (ACC)*, IEEE, 2021, pp. 172–177.

[216] C. Lu, J. Dong, and L. Hu, "Energy-efficient adaptive cruise control for electric connected and autonomous vehicles," *IEEE Intelligent Transportation Systems Magazine*, vol. 11, no. 3, pp. 42–55, 2019.

[217] R. Di Pace, C. Fiori, F. Storani, S. de Luca, C. Liberto, and G. Valenti, "Unified network traffic management framework for fully connected and electric vehicles energy consumption optimization (urano)," *Transportation Research Part C: Emerging Technologies*, vol. 144, p. 103 860, 2022.

[218] K. J. Malakorn and B. Park, "Assessment of mobility, energy, and environment impacts of intellidrive-based cooperative adaptive cruise control and intelligent traffic signal control," in *Proceedings of the 2010 IEEE International Symposium on Sustainable Systems and Technology*, IEEE, 2010, pp. 1–6.

[219] P. Wang, Y. Jiang, L. Xiao, Y. Zhao, and Y. Li, "A joint control model for connected vehicle platoon and arterial signal coordination," *Journal of Intelligent Transportation Systems*, vol. 24, no. 1, pp. 81–92, 2020.

[220] H. Yang, H. Rakha, and M. V. Ala, "Eco-cooperative adaptive cruise control at signalized intersections considering queue effects," *IEEE Transactions on Intelligent Transportation Systems*, vol. 18, no. 6, pp. 1575–1585, 2016.

[221] I. T.-z. Moghaddam, M. Ayati, and A. Taghavipour, "Cooperative adaptive cruise control system for electric vehicles through a predictive deep reinforcement learning approach," *Proceedings of the Institution of Mechanical Engineers, Part D: Journal of Automobile Engineering*, p. 09 544 070 231 160 304, 2023.

[222] H. Liu, X.-Y. Lu, and S. E. Shladover, "Traffic signal control by leveraging cooperative adaptive cruise control (cacc) vehicle platooning capabilities," *Transportation research part C: emerging technologies*, vol. 104, pp. 390–407, 2019.

[223] T. Markel, A. Brooker, T. Hendricks, *et al.*, "Advisor: A systems analysis tool for advanced vehicle modeling," *Journal of power sources*, vol. 110, no. 2, pp. 255–266, 2002.

[224] B. Luin, S. Petelin, and F. Al-Mansour, "Microsimulation of electric vehicle energy consumption," *Energy*, vol. 174, pp. 24–32, 2019.

[225] H. Zhai, H. C. Frey, and N. M. Rouphail, "A vehicle-specific power approach to speed-and facility-specific emissions estimates for diesel transit buses," *Environmental science & technology*, vol. 42, no. 21, pp. 7985–7991, 2008.

[226] C. Fiori, K. Ahn, and H. A. Rakha, "Power-based electric vehicle energy consumption model: Model development and validation," *Applied Energy*, vol. 168, pp. 257–268, 2016.

[227] ——, "Microscopic series plug-in hybrid electric vehicle energy consumption model: Model development and validation," *Transportation Research Part D: Transport and Environment*, vol. 63, pp. 175–185, 2018.

[228] I. Sagaama, A. Kchiche, W. Trojet, and F. Kamoun, "Evaluation of the energy consumption model performance for electric vehicles in sumo," in *2019 IEEE/ACM 23rd International Symposium on Distributed Simulation and Real Time Applications (DS-RT)*, IEEE, 2019, pp. 1–8.

[229] N. Kim, A. Rousseau, and E. Rask, "Autonomie model validation with test data for 2010 toyota prius," SAE Technical Paper, Tech. Rep., 2012.

[230] B. Lee, S. Lee, J. Cherry, A. Neam, J. Sanchez, and E. Nam, "Development of advanced light-duty powertrain and hybrid analysis tool," SAE Technical Paper, Tech. Rep., 2013.

[231] X. Wu, D. Freese, A. Cabrera, and W. A. Kitch, "Electric vehicles' energy consumption measurement and estimation," *Transportation Research Part D: Transport and Environment*, vol. 34, pp. 52–67, 2015.

[232] K. N. Genikomsakis and G. Mitrentsis, "A computationally efficient simulation model for estimating energy consumption of electric vehicles in the context of route planning applications," *Transportation Research Part D: Transport and Environment*, vol. 50, pp. 98–118, 2017.

[233] X. Liang, S. I. Guler, and V. V. Gayah, "Joint optimization of signal phasing and timing and vehicle speed guidance in a connected and autonomous vehicle environment," *Transportation research record*, vol. 2673, no. 4, pp. 70–83, 2019.

[234] V. Milanés and S. E. Shladover, "Modeling cooperative and autonomous adaptive cruise control dynamic responses using experimental data," *Transportation Research Part C: Emerging Technologies*, vol. 48, pp. 285–300, 2014.

[235] L. Xiao, M. Wang, and B. Van Arem, "Realistic car-following models for microscopic simulation of adaptive and cooperative adaptive cruise control vehicles," *Transportation Research Record*, vol. 2623, no. 1, pp. 1–9, 2017.

[236] L. Xiao, M. Wang, W. Schakel, and B. van Arem, "Unravelling effects of cooperative adaptive cruise control deactivation on traffic flow characteristics at merging bottlenecks," *Transportation research part C: emerging technologies*, vol. 96, pp. 380–397, 2018.

[237] A. Kesting, M. Treiber, and D. Helbing, "Enhanced intelligent driver model to access the impact of driving strategies on traffic capacity," *Philosophical Transactions of the Royal Society A: Mathematical, Physical and Engineering Sciences*, vol. 368, no. 1928, pp. 4585–4605, 2010.

[238] J. Garcia-Nieto, A. C. Olivera, and E. Alba, "Optimal cycle program of traffic lights with particle swarm optimization," *IEEE Transactions on Evolutionary Computation*, vol. 17, no. 6, pp. 823–839, 2013.

[239] 5GAA, "White paper on c-v2x use cases: Methodology, examples and service level requirements," 2019.

[240] ETSI, "Technical report 102 638 v1.1.1 intelligent transport systems (its)," 2009.